Calvet el al. (2015), www.soil-discuss.net/2/737/2015/

Impact of gravels and organic matter on the thermal properties of grassland soils in southern France

New title: Deriving pedotransfer functions for soil quartz fraction in southern France from reverse modelling

10 November 2016.

Dear Prof. Artemio Cerdà,

Please find enclosed a point by point response to the reviewers' comments, together with changes in the revised version of our work. In response to the reviewers' comments, we did our best to improve the quality of Figures. In order to improve the focus of the paper, we moved some material to the Supplement. We completed the description of the soils we considered and of the experimental / modelling protocol. We changed the titles of Sections 4.1 and 4.2. We completed the reference list.
The Title and Abstract were rewritten.

Sincerely,

Jean-Christophe Calvet and co-authors

Calvet el al. (2015), www.soil-discuss.net/2/737/2015/

Impact of gravels and organic matter on the thermal properties of grassland soils in southern France

New title: Deriving pedotransfer functions for soil quartz fraction in southern France from reverse modelling

Response to Reviewer #1

The authors thank referee 1 for their review of the manuscript and for the fruitful comments.

1.1 [**This manuscript is a revised version. I notice and appreciate authors have spent much efforts, per the request/recommendation of first-round reviewers, to reanalyze the data, expand the comparative evaluation, add extensive discussion of pedotransfer functions and rewrite to do better job in presentation. Authors' serious efforts have significantly improved this manuscript in terms of both scientific and presentation quality. However, presentation is somewhat lacking focus. The objective seems to investigative relationship between thermal properties reverse-modeled quartz fraction and soil textures including gravels and SOM via pedotransfer function. I would like to see a better focused presentation.**]

RESPONSE 1.1

Many thanks for these positive comments. In order to remove the lack of focus of the presentation, we have revised the title of the paper and we moved three Figures to the Supplement (see below).

1.2 [**Lines 310-323. I believe this section of modeled λsat (λsatMOD) serves alternative way to evaluate the quartz pedotransfer function. Reword to make better clarification.**]

RESPONSE 1.2

Yes. The following sentence was introduced in the text: "An alternative way to evaluate the quartz pedotransfer functions is to compare the simulated λsat with the retrieved values presented in Table 2."

1.3 [**Discussion on pedotransfer function assessment. The Lu et al (2007) dataset was included here to intentionally "assess the applicability of the pedotransfer function for quartz obtained in this study" (Line 404), which turn out to highlight the need of using different predictors (explanatory variables) and/or different parameters in pedotransfer function to model quartz fraction for different soil types. Such a result with across-soil-type assessment is something one would expect. This additional pedotransfer function development for another independent dataset could be made concise (merge or remove related figures) since it does not constitute the true test phase of the French soil types used in this study. I see authors have used bootstrap method as model test.**]

RESPONSE 1.3

We introduced this analysis in order to address a comment of Reviewer 2, asking to verify the consistency of our results against another thermal conductivity measurement type. We think this new material adds value to our work. In order to improve the focus of the presentation, we moved former Figs. 10 and 12 to Supplement 4 (new Figs. S4.1 and S4.2). We left only one Figure including results from Chinese soils in the paper, former Fig. 11 (new Fig. 10), as this figure, together with Table 6, is useful for the evaluation of our results.

1.4 [**Title. Given the current work, the title should be changed. To me, current title would imply how variation of measured quartz content lead to associated change of soil thermal properties. This is not really what this study is about.**]

RESPONSE 1.4

Yes. New title is: "Deriving pedotransfer functions for soil quartz fraction in southern France from reverse modelling".

1.5 [**Fig 9. Dispensable and can be removed.**]

RESPONSE 1.5

Yes. Former Fig. 9 was moved to Supplement 3.

1.6 [**Some figures may need consistent/better resolution. List the empirical models in the figures would help.**]

RESPONSE 1.6

We agree. We did our best to improve the quality of the original Figures.

=======================END =======================

Calvet el al. (2015), www.soil-discuss.net/2/737/2015/

Impact of gravels and organic matter on the thermal properties of grassland soils in southern France

New title: Deriving pedotransfer functions for soil quartz fraction in southern France from reverse modelling

Response to Reviewer #3

The authors thank referee 3 for his/her review of the manuscript and for the fruitful comments.

3.1 [**This paper shows great efforts by the authors to analyse soil temperature and thermal conductivity affected by quartz contents and a high variation of the climatic conditions during the year. In this paper, a topic related to soil and climate sciences are worked in France (21 meteorological stations). However, the introduction is very short with not actual and relevant bibliography, the methods did not present clear concepts or tools about soil properties in this land degraded area (it suppose that it is degraded or this topic is important), the study area was not good explained and, therefore in my opinion, it is impossible to do a discussion (without any cites!) of the results. Without clear information about the methods, how can I good interpret the data? The results are not clears to support the interpretation and conclusions, because it seems a recompilation of climate and pedological data and directly exposed in the text, with parametric models (also without citations). The authors should work more in the discussion and to clear the applied methods. The description of the methods (soil collected samples, soil analysis, data collecting are not clear for me, because they are not described in the text).**

Firstly, I suggest general comments and finally, attached in the pdf, authors can observe some appreciations to improve and to reach, in my opinion, a greater scientific level of

this research. Sorry for the review, but I must be clear and objective with my perception. I hope the author can follow and understand the suggestions (if you considerer)..]

RESPONSE 3.1

The authors would like to acknowledge the thorough review of their work by Referee 3. Many thanks for these comments, which helped us improving the description of the objectives of this work. First of all, we acknowledge that the Title and the Abstract of the paper could be misleading. The new title ("Deriving pedotransfer functions for soil quartz fraction in southern France from reverse modelling") is more in line with the real content of this work. We did our best to improve the Introduction, giving more details on the soil types. Also, details about soil properties' observations are available in Tables 1, 2, and Supplement 1. We added material to Supplement 1. It must be noted that the recent open literature dealing with λsat models usable in practical applications such as meteorological models of climate models has not been that flourishing during the last years. As we emphasised in the Introduction, most of current land surface models follow the approach of Peters-Lidard et al. (1998). We believe that this work is a key contribution in that field. In response to your comments, we added more recent references in the Introduction. Also, we completed the Data and Methods section as much as possible. We made clear that we use our own data. We made these data available to the research community on the web (see Sect. 2.1). This study is not a recompilation of data acquired by others, except for the Lu et al. (2007) data, which are only used in the Discussion section. We moved part of the latter material in the Supplement in order to improve the focus of the presentation (in response to Reviewer 1). We also addressed your detailed comments (see below).

3.2 [**Title: I find the title very clear and precise. But any information about the applied models.**]

RESPONSE 3.2

Yes. We changed the title to: "Deriving pedotransfer functions for soil quartz fraction in southern France from reverse modelling". See also the responses to Reviewer 1.

3.3 [**Abstract: It needs a couple of sentences about the general focus of the topic. There aren´t any explanation about where is developed the work and the aims. The English is not too correct (sentences too longs… also in the rest).**]

RESPONSE 3.3

We agree. We added three sentences (and deleted one) in the Abstract and split the long sentences. Some sentences were rephrased following your recommendations. We tried to shorten sentences as much as possible. New abstract is:

" **The quartz fraction in soils is a key parameter of soil thermal conductivity models. Because it is difficult to measure the quartz fraction in soils, this information is usually unavailable. This source of uncertainty impacts the simulation of sensible heat flux, evapotranspiration, and land surface temperature in numerical simulations of the Earth system. Improving the estimation of soil quartz fraction is needed for practical applications in meteorology, hydrology, and climate modelling. This paper investigates the use of long time series of routine ground observations made in weather stations to retrieve the soil quartz fraction. Profile soil temperature and water content were monitored at 21 weather stations in southern France. Soil thermal diffusivity was derived from the temperature profiles. Using observations of bulk density, soil texture, and fractions of gravel and soil organic matter, soil heat capacity and thermal conductivity were estimated. The quartz fraction was inversely estimated using an empirical geometric mean thermal conductivity model. Several pedotransfer functions for estimating quartz content from gravimetric or volumetric fractions of soil particles (e.g. sand) were analysed. The soil volumetric fraction of quartz (f_q) was systematically better correlated to soil characteristics than the gravimetric fraction of quartz. More than 60 % of the variance of f_q could be explained using indicators based on the sand fraction. It was shown that soil organic matter and (or) gravels may have a marked impact on thermal conductivity values depending on which predictor of f_q is used. For the grassland soils examined in this study, the ratio of sand to soil organic matter fractions was the best predictor of f_q, followed by the gravimetric fraction of sand. An error propagation analysis and a comparison with independent data from other tested models showed that the gravimetric fraction of sand is the best predictor of f_q when a larger variety of soil types is considered**."

3.4 [**Introduction: Please, the authors must include more actual bibliography. Almost all literature is old and there are a lot of affirmation without citations… cite please! This action will make your paper more interesting and relevant. Actually, the scientific language in English is not correct for me. The most important lack of the introduction is the information related to the grass, the importance of these measurements in your region. This kind of soils are specific from your region (?) and the readers need some pictures (soil profiles, general chemical and physical properties...), information and actual problematic (grass, agriculture, urbanisation...)… Finally, the aims of this work aren´t clear, please, make a concrete paragraph only with the goals: i)…; ii)…; iii)….**]

RESPONSE 3.4

Yes. We tried to improve the English. The copy editing phase could improve the English further.

We added six new references in Section 1 (Sourbeer and Loheide, 2015; Subin et al., 2013; Lawrence and Slater, 2008; Decharme et al. 2016; Farouki, 1986; Zakharova et al., 2012).

We added information on the goals of the study, on the weather stations and on the SMOSMANIA network in Section 1 and in Supplement 1.

- Section 1:

" The main goals of this study are to (1) assess the feasibility of using routine automatic soil temperature profile sub-hourly measurements (one observation every 12 minutes) to retrieve instantaneous soil thermal diffusivity values at a depth of 0.10 m; (2) retrieve instantaneous λ values from the soil thermal diffusivity estimates, accounting for the impact of soil vertical heterogeneities; (3) obtain, from reverse modelling, the quartz fraction together with soil thermal conductivity at saturation (λ_{sat}); (4) assess the impact of gravels and SOM on λ_{sat}; (5) derive pedotransfer functions for the soil quartz fraction."

"The soil temperature and the soil moisture probes are buried in the enclosure around each weather station. Most of these stations are located in agricultural areas. However, the vegetation cover in the enclosure around the stations consist of grass. Along the Atlantic-Mediterranean transect formed by the SMOSMANIA network (Fig. 1), the grass land cover fraction ranges between 10 % and 40 % (Zakharova et al., 2012). Various mineral soil types can be found along this transect, ranging from sand to clay and silt loam (see Supplement 1).

During the installation of the probes, we collected soil samples which were used to determine soil characteristics: soil texture, soil gravel content, soil organic matter, and bulk density."

- Supplement 1: we added C/N ration and total nitrogen in Table S1.1; we included the names of the USDA soil classes in Fig. S1.1; we added a map with stations' names (Fig. S1.3) together with a short text describing the landscapes surrounding the stations; we added a photograph of one of the stations (Fig. S1.4), together with photographs of the soil for the four stations of Fig. 3 and for BRN (Figs. S1.5 to S1.9); we added a photograph of a gravimetric soil sample (Fig. S1.10).

New references:

Decharme, B., Brun, E., Boone, A., Delire, C., Le Moigne, P., and Morin, S.: Impacts of snow and organic soils parameterization on northern Eurasian soil temperature profiles simulated by the ISBA land surface model, The Cryosphere, 10, 853–877, doi:10.5194/tc-10-853-2016, 2016.

Farouki, O. T.: Thermal properties of soils, Series on Rock and Soil Mechanics, 11, Trans. Tech. Pub., Rockport, MA, USA, 136 pp., 1986.

Lawrence, D. M., and Slater, A. G.: Incorporating organic soil into a global climate model, Clim. Dyn., 30, 145-160, doi:10.1007/s00382-007-0278-1, 2008.

Sourbeer, J. J., and Loheide II, S. P.: Obstacles to long-term soil moisture monitoring with heated distributed temperature sensing, Hydrol. Process., 30, 7, 1017-1035, 2015.

Subin, Z. M., Koven, C. D., Riley, W. J., Torn, M. S., Lawrence, D. M., and Swenson, S. C.: Effects of soil moisture on the responses of soil temperatures to climate change in cold regions, J. Clim., doi:10.1175/JCLI-D-12-00305.1, 26, 3139-3158, 2013.

Zakharova, E., Calvet, J.-C., Lafont, S., Albergel, C., Wigneron, J.-P., Pardé, M., Kerr, Y., Zribi, M. : Spatial and temporal variability of biophysical variables in southwestern France from airborne L-band radiometry, Hydrol. Earth Syst. Sci., 16, 1725-1743, doi:10.5194/hess-16-1725-2012, 2012.

3.5 [**Methods: Methods, study areas, climatic analysis… they are exposed really confuse. There are a lot of equation (and more in supplementary materials!). Maybe you can reduce this part. Any equation, any model had citation… all is new? If yes, please explain it. The description of the study area is difficult to understand. Better, I recommend: Study area: 1) first group with some areas 2) second group with some areas 3) third group with some areas … with soil properties, land uses, geology and climatic patterns. Now, a lot of information is repeated and has any correct order. Why do you put only one graphic about one station? Please, attach more information about the study area in your map and tables. When you classify the soils where your study areas are**

situated, you can use actual and international "soil classifications", which all authors around the world can understand: USDA (2010) or FAO-WRB (2014).]

RESPONSE 3.5

Equations (1)-(6) are quite basic but they are needed to properly define the quantities and the symbols we use.

We added two references in response to your comment. For Eq. (5), we added the Crank and Nicolson (1996) reference. For Eq. (8), we added the Kersten (1949) reference. The Laanaia et al. (2016) reference was added to describe the purpose of the soil moisture/temperature network.

We reorganized Sections 2.1 and 2.2 and included more material to Supplement 1 (see Fig. S1.3 and text on page 5 of the Supplement).

We included the names of the USDA soil classes in Fig. S1.1.

We added the following sentences in Sections 2.1 and 2.2:

"The 21 stations cover a very large range of soil texture characteristics. For example, SBR is located on a sandy soil, PRD on a clay loam, and MNT on a silt loam (Table 1 and Supplement 1). "

"Table 1 shows that 12 soils present a volumetric gravel content (f_{gravel}) larger than 15 %. Among these, 3 soils (at PRD, BRN, and MJN) have f_{gravel} values larger than 30 %."

"Figure 2 shows soil temperature time series in wet conditions at various soil depths, for a station presenting an intermediate value of λsat (Table 2) and of soil texture (see Fig. S1.1 in Supplement 1). "

We added the following sentence in Sect. 2.5:

"Various approaches can be used to simulate thermal conductivity of unsaturated soils (Dong et al., 2015). In this study, we use an empirical approach based on thermal conductivity values in dry conditions and at saturation."

New references:

Dong, Y., McCartney, J. S., and Lu, N.: Critical review of thermal conductivity models for unsaturated soils, Geotech. Geol. Eng., 33,2,207-221, doi:10.1007/s10706-015-9843-2, 2015.

Kersten, M. S.: Thermal properties of soils, University of Minnesota Engineering Experiment Station Bulletin, 28, 227 pp. [Available from University of Minnesota Agricultural Experiment Station, St. Paul, MN 55108], 1969.

Laanaia, N., Carrer, D., Calvet, J.-C., and Pagé, C.: How will climate change affect the vegetation cycle over France? A generic modeling approach, Climate Risk Management, 13, 31-42, doi:10.1016/j.crm.2016.06.001, 2016.

3.6 [**Results: Please, the tables are too big and there is a lot of information without explanations (the same for the graphics). Figures have all different types of letters, colours… the resolution is really low (I cannot increase the zoom to read one part of the graphic). Maybe, authors should be considered the possibility to cut some graphics. I´m sure that the authors have really amazing information and they can show the scientific community of soil sciences with only concrete numbers, graphics and some statistical analysis your results.**]

RESPONSE 3.6

We agree. We did our best to improve the quality of Figures and to complete the captions of Tables and Figures. Note that some Figures were moved to the Supplement.

3.7 [**Discussion: Please, put more attention in the author guidelines with the information about what is it a discussion. You should make a comparison between your results and others from different authors, and discuss methods, results and ideas. You need bibliography.**]

RESPONSE 3.7

We agree. Nine references from various authors are used in Sect. 4. We added the Churchman and Lowe (2012) reference. We reorganized Sections 4.3 and 4.4. In order to improve the focus of the presentation, we moved former Figs. 10 and 12 to Supplement 4 (new Figs. S4.1 and S4.2). We left only one Figure including results from Chinese soils in the paper, former Fig. 11 (new Fig. 9), as this figure, together with Table 6, is useful for the evaluation of our results.

New reference:

Churchman, G. J. and Lowe, D. J.: Alteration, formation, and occurrence of minerals in soils, in Huang, P. M., Li, C., Summer, M. E. (eds.), Handbook of soil sciences: properties and processes, Chapter 20, 40-42, isbn:978-1-4398-0306-6, CRC Press, Boca Raton (FL), 2012.

3.8 [**Reviewer's annotations**]

RESPONSE 3.8

Your editorial comments were accounted for.

=======================END =======================

Deriving pedotransfer functions for soil quartz fraction in southern France from reverse modelling~~Impact of quartz on the thermal properties of grassland soils in southern France~~

Jean-Christophe Calvet, Noureddine Fritz,
Christine Berne, Bruno Piguet, William Maurel, and Catherine Meurey

CNRM, UMR 3589 (Météo-France, CNRS), Toulouse, France

~~12 January~~ 27 October 2016

Abstract

The quartz fraction in soils is a key parameter of soil thermal conductivity models. Because it is difficult to measure the quartz fraction in soils, this information is usually unavailable. ~~The information on quartz fraction in soils is usually unavailable but has a major effect on the accuracy of soil thermal conductivity models and on their~~This source of uncertainty impacts the simulation of sensible heat flux, evapotranspiration, and land surface temperature in numerical simulations of the Earth system. Improving the estimation of soil quartz fraction is needed for practical applications in meteorology, hydrology, and climate modelling~~land surface models~~. This paper investigates the use of long time series of routine ground observations made in weather stations to retrieve the soil quartz fraction. ~~influence of quartz fraction, soil organic matter (SOM) and gravels on soil thermal conductivity. Field~~ Profile ~~observations of~~ soil temperature and water content were monitored at ~~from~~ 21 weather stations in southern France.~~,~~ Soil thermal diffusivity was derived from the temperature profiles. ~~along with the information on~~ Using observations of bulk density, soil texture, and fractions of gravel and soil organic matter, ~~and bulk density, are used to estimate~~ soil ~~thermal diffusivity and~~ heat capacity~~,~~ and ~~then~~ thermal conductivity were

estimated. The quartz fraction wa~~i~~s inversely estimated using an empirical geometric mean thermal conductivity model. Several pedotransfer functions for estimating quartz content from gravimetric or volumetric fractions of soil particles (e.g. sand) ~~texture information~~ we~~a~~re analysed. ~~It is found that t~~The soil volumetric fraction of quartz (f_q) ~~i~~was systematically better correlated to soil characteristics than the gravimetric fraction of quartz. More than 60 % of the variance of f_q could~~an~~ be explained using indicators based on the sand fraction. It ~~i~~was shown that soil organic matter ~~SOM~~ and (or) gravels may have a marked impact on thermal conductivity values depending on which predictor of f_q is used. For the grassland soils examined in this study, the ratio of sand to soil organic matter ~~SOM~~ fractions ~~i~~was the best predictor of f_q~~.~~, followed by the gravimetric fraction of sand. An error propagation analysis and a comparison with independent data from ~~Lu et al. (2007)~~ other tested models showed that the gravimetric fraction of sand is ~~a better~~the best predictor of f_q when a larger variety of soil types is considered.

1. Introduction

Soil moisture is the main driver of temporal changes in values of the soil thermal conductivity (Sourbeer and Loheide, 2015). The latter is a key variable in land surface models (LSMs) used in hydrometeorology or in climate models, for the simulation of the vertical profile of soil temperature in relation to soil moisture (Subin et al., 2013). Shortcomings in soil thermal conductivity models tend to limit the impact of improving the simulation of soil moisture and snowpack in LSMs (Lawrence and Slater, 2008; Decharme et al. 2016). Models of the thermal conductivity of soils are affected by uncertainties, especially in the representation of the impact of soil properties such as the volumetric fraction of quartz (f_q), soil organic matter, and gravels (Farouki, 1986; Chen et al., 2012). As soil organic matter (SOM) and gravels are often neglected in LSMs, the soil thermal conductivity models used in most LSMs represent the mineral fine earth, only. ~~Today~~Nowadays, f_q estimates are not given in global digital soil maps and it is often assumed that this quantity is equal to the fraction of sand (Peters-Lidard et al., 1998). Soil thermal properties are characterized by two key variables: the soil volumetric heat capacity (C_h), and the soil thermal conductivity (λ), in $Jm^{-3}K^{-1}$ and $Wm^{-1}K^{-1}$, respectively. Provided the volumetric fractions of moisture, minerals and organic matter are known, C_h can be calculated easily. ~~On the other hand, t~~The estimation of λ relies on empirical models and is affected by uncertainties (Peters-Lidard et al., 1998~~–~~; Tarnawski et al., 2012). The construction and the verification of the λ models is not easy. ~~as~~The λ values of undisturbed soils are difficult to directly observe. They are~~is~~ often measured in the lab on perturbed soil samples (Abu-Hamdeh et al., 2000; Lu et al., 2007). Although recent advances in line-source probe and heat pulse methods have made it easier to monitor soil thermal conductivity in the field (Bristow et al., 1994; Zhang et al., 2014), such measurements are currently not made in operational meteorological networks. Moreover, for given soil moisture conditions, λ depends to a large extent on the fraction of soil minerals presenting high thermal conductivities such as quartz, hematite, dolomite or pyrite (Côté and Conrad, 2005). In~~At~~ mid-latitude~~s~~ regions of the world, quartz is the main driver of λ. The information on quartz fraction in a soil is usually unavailable as it can only be measured using X-ray diffraction (XRD) or X-ray fluorescence (XRF) techniques.~~,~~ ~~which~~ These techniques are difficult to implement because the sensitivity to quartz is low. In practise, using XRD and XRF together is needed to improve the accuracy of the measurements (Schönenberger et al., 2012).

This lack of observations has a major effect on the accuracy of thermal conductivity models and their applications (Bristow, 1998).

Most of the Land Surface Models (LSMs) currently used ~~Today, most of the Land Surface Models (LSMs) used~~ in meteorology and hydrometeorology simulate λ following the approach proposed by Peters-Lidard et al. (1998). This approach consists of an updated version of the Johansen (1975) model, and assumes that the gravimetric fraction of quartz (Q) is equal to the gravimetric fraction of sand within mineral fine earth. This is a strong assumption, as some sandy soils (e.g. calcareous sands) may contain little quartz, and as quartz may be found in the silt and clay fractions of the soil minerals (Schönenberger et al., 2012). Moreover, ~~soil organic matter (SOM) and gravels are often neglected in LSMs, and~~ the λ models used in most LSMs represent only the mineral fine earth~~, only~~. Yang et al. (2005) and Chen et al. (2012) have shown the importance of accounting for SOM and gravels in λ models for organic top soil layers of grasslands of the Tibetan plateau.

The main goals of this study are to (1) assess the feasibility of ~~In this study, an attempt is made to~~ usinge routine automatic soil temperature profile sub-hourly measurements (one observation every 12 minutes) to retrieve instantaneous soil thermal diffusivity values at a depth of 0.10 m; (2) -retrieve instantaneous λ values from the soil thermal diffusivity estimates, accounting for the impact of soil vertical heterogeneities; (3) obtain, from reverse modelling, the quartz fraction together with soil thermal conductivity at saturation (λ_{sat}); (4) assess the impact of gravels and SOM on λ_{sat}; (5) derive pedotransfer functions for the soil quartz fraction.

For this purpose, we use the data from~~at~~ 21 weather stations of the Soil Moisture Observing System – Meteorological Automatic Network Integrated Application (SMOSMANIA) network (Calvet et al., 2007) in southern France~~, at a depth of 0.10 m~~. The soil temperature and the soil moisture probes are buried in the enclosure around each weather station. Most of these stations are located in agricultural areas. However, the vegetation cover in the enclosure around the stations consists of grass. Along the Atlantic-Mediterranean transect formed by the SMOSMANIA network (Fig. 1), the grass land cover fraction ranges between 10 % and 40 % (Zakharova et al., 2012). Various mineral soil types can be found along this transect, ranging from sand to clay and silt loam (see Supplement 1). During the installation of the probes, we collected soil samples which were used to determine soil characteristics: Using information on soil moisture, soil texture, soil gravel content, soil organic matter, and bulk density. Using this information together with soil moisture, λ values are derived from soil thermal diffusivity and heat capacity. The response of λ to soil moisture is investigated. and tThe feasibility of modelling the λ value at saturation (λ_{sat}) with or without using SOM and gravel fraction observations is assessed using aan geometric mean empirical thermal conductivity model based on Lu et al. (2007). The volumetric fraction of quartz, f_q, is retrieved by reverse modelling together with *Q*. Pedotransfer functions are further proposed for estimating quartz content from soil texture information.

The field data and the method to retrieve λ values are presented in Sect. 2. The λ and f_q retrievals are presented in Sect. 3 together with a sensitivity analysis of λ_{sat} to SOM and gravel fractions. Finally, the results are discussed in Sect. 4, and the main conclusions are summarized in Sect. 5. Technical details are given in Supplements.

2. Data and methods

2.1. The SMOSMANIA data

The SMOSMANIA soil moisture network was developed by Calvet et al. (2007) in southern France. The main purposes of SMOSMANIA in order are to (1) validate satellite-derived soil moisture products (Parrens et al., 2012);, (2) assess land surface models used in hydrological models (Draper et al., 2011) and in meteorological models (Albergel et al., 2010);, and (3) monitor the impact of climate change on water resources and droughts (Laanaia et al., 2016). The station network forms a transect between the Atlantic coast and the Mediterranean sea (Fig. 1). It consists of pre-existing automatic weather stations operated by Meteo-France, upgraded with four soil moisture probes at four depths: 0.05 m, 0.10 m, 0.20 m, and 0.30 m. Twelve SMOSMANIA stations were activated in 2006 in southwestern France. In 2008, nine more stations were installed along the Mediterranean coast, and the whole network (21 stations) was gradually equipped with temperature sensors at the same depths as soil moisture probes. The soil moisture and soil temperature probes consisted of Thetaprobe ML2X and PT100 sensors, respectively. Soil moisture and soil temperature observations were made every 12 minutes at four depths. The soil temperature observations were recorded with a resolution of 0.1 °C.

In this study, the sub-hourly measurements of soil temperature and soil moisture at a depth of 0.10 m were used, together with soil temperature measurements at 0.05 m and 0.20 m, from 1 January 2008 to 30 September 2015.

In general, the stations are located on former cultivated fields and consist of grasslands. Soil properties were measured at each stations using soil samples collected during the installation of the probes. The 21 stations cover a very large range of soil texture characteristics (see Supplement 1). Other properties such as the gravimetric fraction of the Soil Organic Matter (SOM) and of gravels were determined from the soil samples. In addition, we measured the bulk dry density of the soil (ρ_d) was measured using unperturbed undisturbed oven-dried soil samples we collected using metal cylinders of known volume (about 7×10^{-4} m^3), see Fig. S1.10 in the Supplement).

Twelve SMOSMANIA stations were activated in 2006 in southwestern France. In 2008, nine more stations were installed along the Mediterranean coast, and the whole network (21 stations) was gradually equipped with temperature sensors at the same depths as soil moisture probes. The soil moisture and soil temperature probes consisted of Thetaprobe ML2X and PT100 sensors, respectively.

The ThetaProbe soil moisture sensors provide a voltage signal in units of (V). In order to convert the voltage signal into volumetric soil moisture content (m^3 m^{-3}), site-specific calibration curves were developed using in situ gravimetric soil samples for all stations, and for all depths (Albergel et al., 2008). We revised the calibration In this study, the calibration was revised in order to avoid spurious high soil moisture values during intense precipitation events. Logistics curves were used (see Supplement 1) instead of exponential curves in the previous version of the data set.

The soil temperature observations are recorded with a resolution of 0.1 °C.

The observations from the 48 soil moisture (48) probes and from the 48 temperature (48) probes are automatically recorded every 12 minutes. The data are available to the research community through the International Soil Moisture Network web site (https://ismn.geo.tuwien.ac.at/).

Figure 2 shows soil temperature time series in wet conditions at various soil depths, for a station presenting an intermediate value of λ_{sat} (Table 2) and of soil texture (see Fig. S1.1 in Supplement 1). at the Saint-Félix-de-Lauragais (SFL) station on 23 February 2015. The impact of recording temperature with a resolution of 0.1 °C is clearly visible at all depths as this causes a levelling of the curves.

In this study, sub-hourly measurements of soil temperature and soil moisture at a depth of 0.10 m are used, together with soil temperature measurements at 0.05 m and 0.20 m, from 1 January 2008 to 30 September 2015.

2.2. Soil characteristics

In general, the stations are located on formerly cultivated fields and the soil in the enclosure around the stations is covered with grass. Soil properties were measured at each station by an independent laboratory we contracted (INRA-Arras) from soil samples we collected during the installation of the probes. The 21 stations cover a very large range of soil texture characteristics. For example, SBR is located on a sandy soil, PRD on a clay loam, and MNT on a silt loam (Table 1 and Supplement 1). Other properties such as the gravimetric fraction of SOM and of gravels were determined from the soil samples. Table 1 shows that 12 soils present a volumetric gravel content (f_{gravel}) larger than 15 %. Among these, 3 soils (at PRD, BRN, and MJN) have f_{gravel} values larger than 30 %.

In addition, we measured bulk density (ρ_d) using undisturbed oven-dried soil samples we collected using metal cylinders of known volume (about 7×10^{-4} m^3, see Fig. S1.10 in the Supplement).

The porosity values at a depth of 0.10 m are listed in Table 1 together with gravimetric and volumetric fractions of soil particle-size ranges (sand, clay, silt, gravel) and SOM. The porosity, or soil volumetric moisture at saturation (θ_{sat}), is derived from the bulk dry density ρ_d, together with soil texture and soil organic matter observations as:

$$\theta_{sat} = 1 - \rho_d \left[\frac{m_{sand} + m_{clay} + m_{silt} + m_{gravel}}{\rho_{\min}} + \frac{m_{SOM}}{\rho_{SOM}} \right]$$

or

$$\theta_{sat} = 1 - f_{sand} - f_{clay} - f_{silt} - f_{gravel} - f_{SOM} \quad (1)$$

where m_x (f_x) represents the gravimetric (volumetric) fraction of the soil component x. The f_x values are derived from the measured gravimetric fractions, multiplied by the ratio of ρ_d observations to ρ_x, the density of each soil component x. Values of ρ_{SOM} = 1300 kg m^{-3} and ρ_{min} = 2660 kg m^{-3} are used for soil organic matter, and soil minerals, respectively.

2.3. Retrieval of soil thermal diffusivity

The soil thermal diffusivity (D_h) is expressed in m^{2}s^{-1} and is defined as:

$$D_h = \frac{\lambda}{C_h} \quad (2)$$

We used a numerical method ~~In this study, a simple numerical method is used~~ to retrieve instantaneous values of~~-~~ D_h at a depth of 0.10 m using three soil temperature observations at 0.05 m, 0.10 m and 0.20 m, performed every 12 minutes, by solving the Fourier thermal diffusion equation. The latter can be written as:

$$C_h \frac{\partial T}{\partial t} = \frac{\partial}{\partial z}\left(\lambda \frac{\partial T}{\partial z} \right) \quad (3).$$

~~In this study, g~~Given that soil properties are relatively homogeneous on the vertical (Sect. 2.1), values of D_h can be derived from the Fourier one-dimensional law:

$$\frac{\partial T}{\partial t} = D_h \frac{\partial^2 T}{\partial z^2} \qquad (4).$$

However, large differences in soil bulk density, from the top soil layer to deeper soil layers were observed for some soils (see Supplement 1). In order to limit this effect as much as possible, we only used the soil temperature data presenting a relatively low vertical gradient close to the soil surface, where most differences with deeper layers are found. This data sorting procedure is described in Supplement 2.

Given that three soil temperatures T_i (i ranging from 1 to 3) are measured at depths $z_1 = -0.05$ m, $z_2 = -0.10$ m, and $z_3 = -0.20$ m, the soil diffusivity D_{hi} at $z_i = z_2 = -0.10$ m can be obtained by solving the one-dimensional heat equation, using a finite difference method based on the implicit ~~Crank-Nicholson~~ Crank-Nicolson scheme (Crank and Nicolson, 1996). When three soil depths are considered, z_{i-1}, z_i, z_{i+1}, the change in soil temperature T_i at depth z_i, from time t_{n-1} to time t_n, within the time interval ~~-~~ $\Delta t = t_n - t_{n-1}$ can be written as:

$$\frac{T_i^n - T_i^{n-1}}{\Delta t} = D_{hi}\left[\frac{1}{2}\left(\frac{\gamma_{i+1}^n - \gamma_i^n}{\Delta z_m}\right) + \frac{1}{2}\left(\frac{\gamma_{i+1}^{n-1} - \gamma_i^{n-1}}{\Delta z_m}\right)\right] \quad \text{with}$$

$$\gamma_i^n = \frac{T_i^n - T_{i-1}^n}{\Delta z_i}, \; \Delta z_m = \frac{\Delta z_i + \Delta z_{i+1}}{2}, \text{ and } \Delta z_i = z_i - z_{i-1} \qquad (5).$$

In this study, $\Delta z_i = -0.05$ m, $\Delta z_{i+1} = -0.10$ m, and a value of $\Delta t = 2880$ s (48 minutes) is used.

It is important to ensure that D_h retrievals are related to diffusion processes only and not to the transport of heat by water infiltration or evaporation (Parlange et al., 1998 ; Schelde et al., 1998). Therefore, only situations for which changes in soil moisture at all depths do not exceed 0.001 m^3m^{-3} within the Δt time ~~lag~~ interval are considered.

2.4. From soil diffusivity to soil thermal conductivity

The observed soil properties and volumetric soil moisture are used to calculate the soil volumetric heat capacity C_h at a depth of 0.10 m, using the de Vries (1963) mixing model. The C_h values, in units of $Jm^{-3}K^{-1}$, are calculated as:

$$C_h = \theta C_{h\,water} + f_{\min} C_{h\min} + f_{SOM}\, C_{hSOM} \qquad (6)$$

where θ and $f_{\min}$ represent the volumetric soil moisture and the volumetric fraction of soil minerals, respectively. Values of 4.2×10^{6} $Jm^{-3}K^{-1}$, 2.0×10^{6} $Jm^{-3}K^{-1}$, and 2.5×10^{6} $Jm^{-3}K^{-1}$, are used for $C_{h\mathrm{water}}$, $C_{h\mathrm{min}}$, $C_{h\mathrm{SOM}}$, respectively.

The λ values at 0.10 m are then derived from the D_h and C_h estimates (Eq. (2)).

2.5. Soil thermal conductivity model

Various approaches can be used to simulate thermal conductivity of unsaturated soils (Dong et al., 2015). We used an empirical approach based on thermal conductivity values in dry conditions and at saturation.

In dry conditions, soils present low thermal conductivity values (λ_{dry}). Experimental evidence shows that λ_{dry} is negatively correlated with porosity. For example, Lu et al. (2007) give:

$$\lambda_{dry} = 0.51 - 0.56 \times \theta_{sat} \qquad \text{(in } Wm^{-1}K^{-1}\text{)} \qquad (7)$$

When soil pores are gradually filled with water, λ tends to increase towards a maximum value at saturation (λ_{sat}). Between dry and saturation conditions, λ is expressed as:

$$\lambda = \lambda_{dry} + K_e\left(\lambda_{sat} - \lambda_{dry}\right) \qquad (8)$$

where, K_e is the Kersten number (Kersten, 1949). The latter is related to the volumetric soil moisture, θ, i.e. to the degree of saturation (S_d). ~~In this study, the~~We used the formula recommended by Lu et al. (2007) is used:

$$K_e = \exp\left\{\alpha\left(1 - S_d^{(\alpha-1.33)}\right)\right\},$$

with $\alpha = 0.96$ for $Mn_{\text{sand}} \geq 0.4$ kg kg^{-1}, $\alpha = 0.27$ for $Mn_{\text{sand}} < 0.4$ kg kg^{-1}, and

$$S_d = \theta / \theta_{sat} \tag{9}$$

Mn_{sand} represents the sand mass fraction of mineral fine earth (values are given in Supplement 1). ~~Following Peters-Lidard et al. (1998), λ_{other} is taken as 2.0 Wm^{-1}K^{-1} for soils with $Mn_{\text{sand}} > 0.2$ kg kg^{-1}, and 3.0 Wm^{-1}K^{-1} otherwise. In this study $Mn_{\text{sand}} > 0.2$ kg kg^{-1} for all soils, except for URG, PRG, and CDM.~~

The geometric mean equation for λ_{sat} proposed by Johansen (1975) for the mineral components of the soil can be generalized to include the SOM thermal conductivity (Chen et al., 2012) as:

$$\ln(\lambda_{sat}) = f_q \ln(\lambda_q) + f_{other} \ln(\lambda_{other}) + \theta_{sat} \ln(\lambda_{water}) + f_{SOM} \ln(\lambda_{SOM}) \tag{10}$$

where f_q is the volumetric fraction of quartz, and λ_q = 7.7 Wm^{-1}K^{-1}, ~~λ_{other} = 2.0 Wm^{-1}K^{-1},~~ λ_{water} = 0.594 Wm^{-1}K^{-1}, λ_{SOM} = 0.25 Wm^{-1}K^{-1} are the thermal conductivities of quartz, ~~soil minerals other than quartz,~~ water and SOM, respectively. The λ_{other} term corresponds to the thermal conductivity of soil minerals other than quartz. Following Peters-Lidard et al. (1998), λ_{other} is taken as 2.0 Wm^{-1}K^{-1} for soils with $Mn_{\text{sand}} > 0.2$ kg kg^{-1}, and 3.0 Wm^{-1}K^{-1} otherwise. In this study $Mn_{\text{sand}} > 0.2$ kg kg^{-1} for all soils, except for URG, PRG, and CDM. The volumetric fraction of soil minerals other than quartz is defined as:

$$f_{other} = 1 - f_q - \theta_{sat} - f_{SOM}$$

with $f_q = Q \times (1 - \theta_{sat})$ (11)

2.6. Reverse modelling

The λ_{sat} values are retrieved through reverse modelling using the λ model described above (Eqs. (7)-(11)). ~~The λ~~This model is used to produce simulations of λ at the same soil moisture conditions as those encountered for the λ values derived from observations in Sect. 2.4. For a given station, a set of 401 simulations is produced for λ_{sat} ranging from 0 $Wm^{-1}K^{-1}$ to 4 $Wm^{-1}K^{-1}$, with a resolution of 0.01 $Wm^{-1}K^{-1}$. The λ_{sat} retrieval corresponds to the λ simulation presenting the lowest root mean square difference (RMSD) value with respect to the λ observations. Only λ observations for S_d values higher than 0.4 are used because in dry conditions: (1) conduction is not the only mechanism for heat exchange in soils, as the convective water vapour flux may become significant (Schelde et al., 1998;~~,~~ Parlange et al. 1998);~~,~~ (2) the K_e functions found in the literature display more variability; and, (3) the λ_{sat} retrievals are more sensitive to uncertainties in λ observations. The threshold value of S_d = 0.4 results from a compromise between the need of limiting the influence of convection, of the shape of the K_e function on the retrieved values of λ_{sat}, and of using as many observations as possible in the retrieval process. Moreover, the data filtering technique to limit the impact of soil heterogeneities, described in Supplement 2, is used to select valid λ observations.

Finally, the f_q value is derived from the retrieved λ_{sat} solving Eq. (10).

2.7. Scores

Pedotransfer functions for quartz and λ_{sat} are evaluated using the following scores:

- the Pearson correlation coefficient (r), and the squared correlation coefficient (r^2) is used to assess the fraction of explained variance,
- the RMSD,
- the Mean Absolute Error (MAE), i.e. the mean of absolute differences,
- the mean bias, i.e. the mean of differences.

In order to test the predictive and generalization power of the pedotransfer regression equations, a simple bootstrapping resampling technique is used. It consists in calculating a new estimate of f_q for each soil using the pedotransfer function obtained without using this specific soil. Gathering these new f_q estimates, one can calculate new scores with respect to the retrieved f_q values. Also, this method provides a range of possible values of the coefficients of the pedotransfer function and permits assessing the influence of a given f_q retrieval on the final result.

3. Results

3.1. λ_{sat} and f_q retrievals

Retrievals of λ_{sat} and f_q could be obtained for 14 soils. Figure 3 shows retrieved and modelled λ values ~~vs.~~against the observed degree of saturation of the soil, at a depth of 0.10 m, for contrasting retrieved values of λ_{sat}, from high to low ~~λ_{sat}~~ values (2.80, 1.96, 1.52, and 1.26 $Wm^{-1}K^{-1}$) at the SBR, MNT, MTM, and PRD stations, respectively.

All the obtained λ_{sat} and f_q retrievals are listed in Table 2, together with the λ RMSD values and the number of selected λ observations. For three soils (CRD, MZN, and VLV), the reverse modelling technique described in Sect. 2.6 could not be applied as not enough λ observations could be obtained for S_d values higher than 0.4. For four soils (NBN, PZN, BRZ, and MJN), all the λ retrievals were filtered out as the obtained values were influenced by heterogeneities in soil density (see Supplement 2). For the other 14 soils, λ_{sat} and f_q retrievals were obtained using a subset of 20 λ retrievals per soil, at most, corresponding to the soil temperature data presenting the lowest vertical gradient close to the soil surface (Supplement 2).

3.2 Pedotransfer functions for quartz

The f_q retrievals can be used to assess the possibility to estimate f_q using other soil characteristics, which can be easily measured. Another issue is whether volumetric or gravimetric fraction of quartz should be used. Figure 4 presents the fraction of variance (r^2) of Q and f_q explained by various indicators. A key result is that f_q is systematically better correlated to soil characteristics than Q. More than 60 % of the variance of f_q can be explained using indicators based on the sand fraction (either f_{sand} or m_{sand}). The use of other soil mineral fractions does not give good correlations, even when they are associated to the sand fraction as shown by Fig. 4. For example, the f_{gravel} and $f_{gravel}+f_{sand}$ indicators present low r^2 values of 0.04 and 0.24, respectively.

The f_q values cannot be derived directly from the indicators as illustrated by Fig. 5: assuming $f_q = f_{sand}$ tends to markedly underestimate λ_{sat}. Therefore, more elaborate pedotransfer equations are needed. They can be derived from the best indicators, using them as predictors of– f_q. The modelled f_q is written as:

$$f_{qMOD} = a_0 + a_1 \times P$$

$$\text{and} \quad f_{qMOD} \leq 1 - \theta_{sat} - f_{SOM} \qquad (12)$$

where P represents the predictor of f_q.

The a_0 and a_1 coefficients are given in Table 3 for four pedotransfer functions based on the best predictors of f_q. The pedotranfer functions are illustrated in Fig. 6. The scores are displayed in Table 4. The bootstrapping indicates that the SBR sandy soil has the largest individual impact on the obtained regression coefficients. This is why the scores without SBR are also presented in Table 4.

For the m_{sand} predictor, a r^2 value of 0.56 is obtained without SBR, against a value of 0.67 when all the 14 soils are considered. An alternative to this m_{sand} pedotransfer function consists in considering only m_{sand} values smaller than 0.6 kg kg^{-1} in the regression, thus excluding the SBR soil. The corresponding predictor is called m_{sand}*. In this configuration, the sensitivity of f_q to m_{sand} is much increased (with a_1 = 0.944, against a_1 = 0.572 with SBR). For SBR, f_q is overestimated by the m_{sand}* equation but this is corrected by the f_{qMOD} limitation of Eq. (12), and in the end a better r^2 score is obtained when the 14 soils are considered (r^2 = 0.74) .

Values of r^2 larger than 0.7 are obtained for two predictors of f_q: m_{sand}/m_{SOM} and m_{sand}*. A value of r^2 = 0.65 is obtained for 1 − θ_{sat} − f_{sand} (the fraction of soil solids other than sand). The m_{sand}/m_{SOM} predictor presents the best r^2 and RMSD scores in all the configurations (regression, bootstrap, and regression without SBR). Another characteristic of the m_{sand}/m_{SOM} pedotransfer function is that the confidence interval for the a_0 and a_1 coefficients derived from bootstrapping is narrower than for the other pedotransfer functions (Table 3), indicating a more robust relationship of f_q with m_{sand}/m_{SOM} than with other predictors.

An alternative way to evaluate the quartz pedotransfer functions is to compare the simulated λ_{sat} with the retrieved values presented in Table 2. Modelled values of λ_{sat} (λ_{satMOD}) can be derived from f_{qMOD} using Eq. (10) together with θ_{sat} observations. The λ_{satMOD} r^2, RMSD, and mean bias scores are given in Table 5. Again, the best scores are obtained using the m_{sand}/m_{SOM} predictor of f_q, with r^2, RMSD, and mean bias values of 0.86, 0.14 $Wm^{-1}K^{-1}$, and +0.01 $Wm^{-1}K^{-1}$, respectively (Fig. 7).

Finally, we investigated the possibility of estimating θ_{sat} from the soil characteristics listed in Table 1 and of deriving a statistical model for θ_{sat} (θ_{satMOD}). We found the following statistical relationship between θ_{satMOD}, m_{clay}, m_{silt}, and m_{SOM}:

$$\theta_{satMOD} = 0.456 - 0.0735 \frac{m_{clay}}{m_{silt}} + 2.238\, m_{SOM} \quad (13)$$

(r^2 = 0.48, F-test p-value = 0.0027, RMSD=0.036 m^3m^{-3}).

Volumetric fractions of soil components need to be consistent with θ_{satMOD} and can be calculated using the modelled bulk density values derived from θ_{satMOD} using Eq. (1).

Equations (10) to (13) constitute an empirical end-to-end model of λ_{sat}. Table 5 shows that using θ_{satMOD} (Eqs. (13))- instead of the θ_{sat} observations has little impact on the λ_{satMOD} scores.

3.3. Impact of gravels and SOM on λ_{sat}

Gravels and SOM are often neglected in soil thermal conductivity models used in LSMs. The Eqs. (10)-(13) empirical model obtained in Sect. 3.2 permits the assessment of the impact of f_{gravel} and f_{SOM} on λ_{sat}. Table 5 shows the impact on λ_{satMOD} scores of imposing a null value of f_{gravel} and a small value of f_{SOM} to all the soils. The combination of these assumptions is evaluated, also.

Imposing f_{SOM} = 0.013 m^3m^{-3} (the smallest f_{SOM} value, observed for CBR) has a limited impact on the scores, except for the m_{sand}/m_{SOM} pedotransfer function. In this case, λ_{sat} is overestimated by +0.20 $Wm^{-1}K^{-1}$, and r^2 drops to 0.57.

Neglecting gravels (f_{gravel} = 0 m^3m^{-3}) also has a limited impact but triggers the underestimation (overestimation) of λ_{sat} for the m_{sand}/m_{SOM} (m_{sand}*) pedotransfer function, by –0.12 $Wm^{-1}K^{-1}$ (+0.11 $Wm^{-1}K^{-1}$).

On the other hand, it appears that combining these assumptions has a marked impact on all the pedotransfer functions. Neglecting gravels and imposing f_{SOM} = 0.013 m^3m^{-3} has a major impact on λ_{sat}: the modelled λ_{sat} is overestimated by all the pedotransfer functions (with a mean bias ranging from +0.16 $Wm^{-1}K^{-1}$ to +0.24 $Wm^{-1}K^{-1}$) and r^2 is markedly smaller, especially for the m_{sand} and m_{sand}* pedotransfer functions. These results are illustrated in Fig. 8 in the case of the m_{sand}* pedotransfer function. Figure 8 also shows that using the θ_{sat} observations instead of θ_{satMOD} (Eq. (13)) has little impact on λ_{satMOD} (Sect. 3.2) but tends to enhance the impact of neglecting gravels. A similar result is found with the m_{sand} pedotransfer function (not shown).

4. Discussion

4.1. Can uncertainties in heat capacity estimates impact retrievals ?~~Sources of uncertainties in heat capacity estimates~~

In this study, the de Vries (1963) mixing model is applied to estimate soil volumetric heat capacity (Eq. (6)), and a fixed value of 2.0×10^{6} $Jm^{-3}K^{-1}$ is used for soil minerals~~ (Eq. (6))~~. Soil-specific values for C_{hmin} may be more appropriate than using a constant standard value. For example, Tarara and Ham (1997) used a value of 1.92×10^{6} $Jm^{-3}K^{-1}$. However, we did not measure this quantity and we were not able to find such values in the literature.

We investigated the sensitivity of our results to these uncertainties, considering the following minimum and maximum C_{hmin} values: $C_{hmin} = 1.92\times10^{6}$ J m^{-3} K^{-1} and $C_{hmin} = 2.08\times10^{6}$ J m^{-3} K^{-1}. The impact of changes in C_{hmin} on the retrieved values of λ_{sat} and f_q is presented in Supplement 3 (Fig. S3.1)~~9~~. On average, a change of + (–) 0.08×10^{6} J m^{-3} K^{-1} in C_{hmin} triggers a change in λ_{sat} and f_q of + 1.7 % (– 1.8 %) and + 4.8 % (– 7.0 %), respectively.

The impact of changes in C_{hmin} on the regression coefficients of the pedotransfer functions is presented in Table 3 (last column). The impact is very small, except for the a_1 coefficient of the m_{sand}* pedotransfer function. However, even in this case, the impact of C_{hmin} on the a_1 coefficient is much lower than the confidence interval given by the bootstrapping, indicating that the relatively small number of soils we considered ~~in this study~~ (as in other studies, e.g. Lu et al. (2007)) is a larger source of uncertainty.

Moreover, uncertainties in the f_{clay}, f_{silt}, f_{gravel}, or f_{SOM} fractions may be caused by (1) the natural heterogeneity of soil properties, (2) the living root biomass, (3) stones that may not be accounted for in the gravel fraction.

In particular, during the installation of the probes, it was observed that stones are present at some stations. Stones are not evenly distributed in the soil, and it is not possible to investigate whether the soil area where the temperature probes were inserted contains stones as it must be left ~~unperturbed~~undisturbed.

The grasslands considered in this study are not intensively managed. They consist of set-aside fields cut once or twice a year. Calvet et al. (1999) gave an estimate of 0.160 kg m^{-2} for the root dry matter content of such soils for a site in southwestern France, with most roots contained in the 0.25m top soil layer. This represents a gravimetric fraction of organic matter smaller than 0.0005 kg kg^{-1}, i.e. less than 4% of the lowest m_{SOM} values observed in this study (0.013 kg kg^{-1}) or less than 5% of f_{SOM} values. We checked that increasing f_{SOM} values by 5% has negligible impact on heat capacity and on the λ retrievals.

4.2~~3~~. Can the new λ_{sat} model be applied to other soil types ?~~Applicability of the new λ_{sat} model to other soil types~~

The λ_{sat} values ~~found in this study~~we obtained are consistent with values reported by other authors. In this study, λ_{sat} values ranging between 1.26 $Wm^{-1}K^{-1}$ and 2.80 $Wm^{-1}K^{-1}$ are found (Table 2). Tarnawski et al. (2011) gave λ_{sat} values ranging between 2.5 $Wm^{-1}K^{-1}$ ~~–~~and 3.5

$Wm^{-1}K^{-1}$ for standard sands. Lu et al. (2007) gave λ_{sat} values ranging between 1.33 $Wm^{-1}K^{-1}$ and 2.2 $Wm^{-1}K^{-1}$.

A key component of the λ_{sat} model is the pedotransfer function for quartz (Eq. (12)). The f_q pedotranfer functions we propose~~d in this study~~ are based on ~~basic~~ available soil characteristics. The current global soil digital maps provide information about SOM, gravels and bulk density (Nachtergaele et al., 2012). Therefore, using Eq. (1) and Eqs. (6)-(12) at large scale is possible, and porosity can be derived from Eq. (1). On the other hand, the suggested f_q pedotranfer functions are obtained for temperate grassland soils containing a rather large amount of organic matter, and are valid for m_{sand}/m_{SOM} ratio values lower than 40 (Table 2). These equations should be evaluated for other regions. In particular, hematite has to be considered together with quartz for tropical soils (Churchman and Lowe, 2012). Moreover, ~~while~~ the pedotransfer function we get for θ_{sat} (Eq. (13)) and we use to conduct the sensitivity study of Sect. 3.3, is valid for the specific sites we considered. ~~in this study and is used to conduct the sensitivity study of Sect. 3.3~~, Eq. (13) cannot be used to predict porosity in other regions.

In order to assess the applicability of the pedotransfer function for quartz obtained in this study, we used the independent data from Lu et al. (2007) and Tarnawski et al. (2009), for ten Chinese soils (see Supplement 4~~3~~ and Table S4~~3~~.1). These soils consist of reassembled sieved soil samples and contain no gravel, while our data concern undisturbed soils. Moreover, most of these soils contain very little organic matter and the m_{sand}/m_{SOM} ratio can be much larger that the m_{sand}/m_{SOM} values measured at our grassland sites. For the 14 French soils used to determine pedotransfer functions for quartz, the m_{sand}/m_{SOM} ratio ranges from 3.7 to 37.2 (Table 2). Only three soils of Lu et al. (2007) present such low values of m_{sand}/m_{SOM}. The other seven soils of Lu et al. (2007) present m_{sand}/m_{SOM} values ranging from 48 to 1328 (see Table S4~~3~~.1).

We used λ_{sat} experimental values derived from Table 3 in Tarnawski et al. (2009) to calculate Q and f_q for the ten Lu et al. (2007) soils. These data are presented in Supplement 4. Figure ~~10~~ S4.1 shows the statistical relationship between these quantities and m_{sand}. Very good correlations of Q and f_q with m_{sand} are observed, with r^2 values of 0.72 and 0.83, respectively. This is consistent with our finding that f_q is systematically better correlated to soil characteristics than Q (Sect. 3.2). The pedotransfer functions derived from French soils tend to overestimate f_q for the Lu et~~l~~ al. (2007) soils, especially for the seven soils presenting m_{sand}/m_{SOM} values larger than 40. Note that Lu et al. (2007) obtained a similar result for coarse-textured soils with their model, which assumed $Q = m_{sand}$. For the three other soils, presenting m_{sand}/m_{SOM} values smaller than 40, f_q MAE values are given in Table 4. The best MAE score (0.071 m^3m^{-3}) is obtained for the m_{sand}* predictor of f_q.

These results are illustrated by Fig. 9~~11~~ for the m_{sand} predictor of f_q. Figure 9~~11~~ also shows the f_q and λ_{sat} estimates obtained using specific coefficients in Eq. (12), based on the seven Lu et al. (2007) soils presenting m_{sand}/m_{SOM} values larger than 40. These coefficients are given together with the scores in Table 6. Table 6 also present these values for other predictors of f_q. It appears that m_{sand} gives the best scores. The contrasting coefficient values between Table 6 and Table 3 (Chinese and French soils, respectively) illustrate the variability of the coefficients of pedotransfer functions from one soil category to another, and the m_{sand}/m_{SOM} ratio seems to be a good indicator of the validity of a given pedotransfer function.

On the other hand, the m_{sand}/m_{SOM} ratio is not a good predictor of f_q for the Lu et al. (2007) soils presenting m_{sand}/m_{SOM} values larger than 40, and r^2 presents a small value of 0.40 ~~-~~(Table 6). This can be explained by the very large range of m_{sand}/m_{SOM} values for these soils (see Table S4~~3~~.1). Using $ln(m_{sand}/m_{SOM})$ instead of m_{sand}/m_{SOM} is a way to obtain a predictor linearly correlated to f_q.

This is shown by Fig. 12 S4.2 for the ten Lu et al. (2007) soils: the correlation is increased to a large extent (r^2 = 0.60).

4.34. Can m_{sand}-based f_q pedotransfer functions be used across soil types ?

Given the results presented in Tables 3, 4, and 6, it can be concluded that m_{sand} is the best predictor of f_q across mineral soil types. The m_{sand}/m_{SOM} predictor is relevant for the mineral soils containing the largest amount of organic matter.

Although the m_{sand}/m_{SOM} predictor gives the best r^2 scores for the 14 grassland soils considered in this study, it seems more difficult to apply this predictor to other soils, as shown by the high MAE score (MAE = 0.135 m^3m^{-3}) for the corresponding Lu et al. (2007) soils in Table 4. Moreover, the scores are very sensitive to errors in the estimation of m_{SOM} as shown by Table 5. Although the m_{sand}* predictor gives slightly better scores than m_{sand} (Table 4), the a_1 coefficient in more sensitive to errors in C_{hmin} (Table 3), and the bootstrapping reveals large uncertainties in a_0 and a_1 values.

The results presented in this study suggest that the m_{sand}/m_{SOM} ratio can be used to differentiate temperate grassland soils containing a rather large amount of organic matter (3.7 < m_{sand}/m_{SOM} < 40) from soils containing less organic matter (m_{sand}/m_{SOM} > 40). The m_{sand} predictor can be used in both cases to estimate the volumetric fraction of quartz, with the following a_0 and a_1 coefficient values in Eq. (12): 0.15 and 0.572 for m_{sand}/m_{SOM} ranging between 3.7 and 40 (Table 3), and 0.04 and 0.386 for m_{sand}/m_{SOM} > 40 (Table 6), respectively.

~~Although the m_{sand}/m_{SOM} predictor gives the best r^2 scores for the 14 grassland soils considered in this study, it seems more difficult to apply this predictor to other soils, as shown by the high MAE score (MAE = 0.135 $m^3 m^{-3}$) for the corresponding Lu et al. (2007) soils in Table 4. Moreover, the scores are very sensitive to errors in the estimation of m_{SOM} as shown by Table 5. Although the m_{sand}* predictor gives slightly better scores than m_{sand} (Table 4), the a_1 coefficient in more sensitive to errors in C_{hmin} (Table 3), and the bootstrapping reveals large uncertainties in a_0 and a_1 values.~~

4.4~~5~~. Prospects for using soil temperature profiles

Using standard soil moisture and soil temperature observations is a way to investigate soil thermal properties over a large variety of soils, as the access to such data is facilitated by online databases (Dorigo et al., 2013).

A limitation of the data set we used~~ in this study~~, however, is that soil temperature observations (T_i) are recorded with a resolution of ΔT_i = 0.1 °C only (see Sect. 2.1). This low resolution affects the accuracy of the soil thermal diffusivity estimates. In order to limit the impact of this effect, a data filtering technique is used (see Supplement 5~~4~~) and D_h is retrieved with a precision of 18 %. It can be noticed that if T_i data were recorded with a resolution of 0.03 °C (which corresponds to the typical uncertainty of PT100 probes), D_h could be retrieved with a precision of about 5 % in the conditions of Eq. (S54.3). Therefore, one may recommend to revise the current practise of most observation networks consisting in recording soil temperature with a resolution of 0.1 °C only. More precision in the λ estimates would permit investigating other processes of heat transfer in the soil such as those related to water transport (Rutten, 2015).

5. Conclusions

An attempt was made to use routine soil temperature and soil moisture observations of a network of- automatic weather stations to retrieve instantaneous values of the soil thermal conductivity at a depth of 0.10 m. The data from the SMOSMANIA network, in southern France, are used. First, the thermal diffusivity is derived from consecutive measurements of the soil temperature. The λ values are then derived from the thermal diffusivity retrievals and from the volumetric heat capacity calculated using measured soil properties. The relationship between the λ estimates and the measured soil moisture at a depth of 0.10 m permits the retrieval of λ_{sat} for 14 stations. The Lu et al. (2007) empirical λ model is then used to retrieve the quartz volumetric content by reverse modelling. A number of pedotransfer functions is proposed for volumetric fraction of quartz, for the considered region in France. For the grassland soils examined in this study, the ratio of sand to SOM fractions is the best predictor of f_q. A sensitivity study shows that omitting gravels and the SOM information has a major impact on λ_{sat}. Eventually, an error propagation analysis and a comparison with independent λ_{sat} data from Lu et al. (2007) show that the gravimetric fraction of sand within soil solids, including gravels and SOM, is a good predictor of the volumetric fraction of quartz when a larger variety of soil types is considered.

Acknowledgements

We thank Dr. Xinhua Xiao (NC State University Soil Physics, Raleigh, USA), ~~and~~ Dr. Tusheng Ren (China Agricultural University, Beijing, China), and a third anonymous referee, for their review of the manuscript and for their fruitful comments. We thank Dr. Aaron Boone (CNRM, Toulouse, France) for his helpful comments. We thank our Meteo-France colleagues for their support in collecting and archiving the SMOSMANIA data: Catherine Bienaimé, Marc Bailleul, Laurent Brunier, Anna Chaumont, Jacques Couzinier, Mathieu Créau, Philippe Gillodes, Sandrine Girres, Michel Gouverneur, Maryvonne Kerdoncuff, Matthieu Lacan, Pierre Lantuejoul, Dominique Paulais, Fabienne Simon, Dominique Simonpietri, Marie-Hélène Théron, Marie Yardin.

References

Abu-Hamdeh, N. H., and Reeder, R. C.: Soil thermal conductivity: effects of density, moisture, salt concentration, and organic matter, Soil Sci. Soc. Am. J., 64, 1285–1290, 2000.

Albergel, C., Rüdiger, C., Pellarin, T., Calvet, J.-C., Fritz, N., Froissard, F., Suquia, D., Petitpa, A., Piguet, B., and Martin, E.: From near-surface to root-zone soil moisture using an exponential filter: an assessment of the method based on in-situ observations and model simulations, Hydrol. Earth Syst. Sci., 12, 1323–1337, 2008.

Albergel, C., Calvet, J.-C., de Rosnay, P., Balsamo, G., Wagner, W., Hasenauer, S., Naeimi, V., Martin, E., Bazile, E., Bouyssel, F., and Mahfouf, J.-F.: Cross-evaluation of modelled and remotely sensed surface soil moisture with in situ data in southwestern France, Hydrol. Earth Syst. Sci., 14, 2177–2191, doi:10.5194/hess-14-2177-2010, 2010.

Bristow, K. L., Kluitenberg, G. J., and Horton R.: Measurement of soil thermal properties with a dual-probe heat-pulse technique, Soil Sci. Soc. Am. J., 58, 1288–1294, doi:10.2136/sssaj1994.03615995005800050002x, 1994.

Bristow, K. L.: Measurement of thermal properties and water content of unsaturated sandy soil using dual-probe heat-pulse probes, Agr. Forest Meteorol., 89, 75-84, 1998.

Calvet, J.-C., Bessemoulin, P., Noilhan, J., Berne, C., Braud, I., Courault, D., Fritz, N., Gonzalez-Sosa, E., Goutorbe, J.-P., Haverkamp, R., Jaubert, G., Kergoat, L., Lachaud, G., Laurent, J.-P., Mordelet, P., Olioso, A., Péris, P., Roujean, J.-L., Thony, J.-L., Tosca, C., Vauclin, M., Vignes, D.: MUREX: a land-surface field experiment to study the annual cycle of the energy and water budgets, Ann. Geophys., 17, 838-854, 1999.

Calvet, J.-C., Fritz, N., Froissard, F., Suquia, D., Petitpa,A., and Piguet, B.: In situ soil moisture observations for the CAL/VAL of SMOS: the SMOSMANIA network, International

Geoscience and Remote Sensing Symposium, IGARSS, Barcelona, Spain, 23–28 July 2007, 1196–1199, doi:10.1109/IGARSS.2007.4423019, 2007.

Chen, Y. Y., Yang, K., Tang, W., Qin, J., and Zhao, L.: Parameterizing soil organic carbon's impacts on soil porosity and thermal parameters for Eastern Tibet grasslands, Sci. China Earth Sci., 55 (6), 1001–1011, doi:10.1007/s11430-012-4433-0, 2012.

Churchman, G. J. and Lowe, D. J.: Alteration, formation, and occurrence of minerals in soils, in Huang, P. M., Li, C., Summer, M. E. (eds.), Handbook of soil sciences: properties and processes, Chapter 20, 40-42, isbn:978-1-4398-0306-6, CRC Press, Boca Raton (FL), 2012.

Côté, J. and Konrad, J.-M.: A generalized thermal conductivity model for soils and construction materials, Can. Geotech. J., 42, 443:458, doi:10.1139/T04-106, 2005.

Crank J., and Nicolson, P.: A practical method for numerical evaluation of solutions of partial differential equations of the heat-conduction type, Advances in Computational Mathematics, 6, 207-226, doi:10.1007/BF02127704, 1996.

Decharme, B., Brun, E., Boone, A., Delire, C., Le Moigne, P., and Morin, S.: Impacts of snow and organic soils parameterization on northern Eurasian soil temperature profiles simulated by the ISBA land surface model, The Cryosphere, 10, 853–877, doi:10.5194/tc-10-853-2016, 2016.

de Vries, D. A.: Thermal properties of soils, in W.R. Van Wijk (ed.), Physics of plant environment, pp. 210–235, North-Holland Publ. Co., Amsterdam, 1963.

Dong, Y., McCartney, J. S., and Lu, N.: Critical review of thermal conductivity models for unsaturated soils, Geotech. Geol. Eng., 33,2,207-221, doi:10.1007/s10706-015-9843-2, 2015.

Dorigo, W. A., Wagner, W., Hohensinn, R., Hahn, S., Paulik, C., Xaver, A., Gruber, A., Drusch, M, Mecklenburg, S., van Oevelen, P., Robock, A., and Jackson, T.: The International Soil Moisture Network: a data hosting facility for global in situ soil moisture measurements, Hydrol. Earth Syst. Sci., 15, 1675–1698, doi:10.5194/hess-15-1675-2011, 2011.

Draper, C., Mahfouf, J.-F., Calvet, J.-C., Martin, E., and Wagner, W.: Assimilation of ASCAT near-surface soil moisture into the SIM hydrological model over France, Hydrol. Earth Syst. Sci., 15, 3829–3841, doi:10.5194/hess-15-3829-2011, 2011.

Farouki, O. T.: Thermal properties of soils, Series on Rock and Soil Mechanics, 11, Trans. Tech. Pub., Rockport, MA, USA, 136 pp., 1986.

Johansen, O.: Thermal conductivity of soils. Ph.D. thesis, University of Trondheim, 236 pp., Available from Universitetsbiblioteket i Trondheim, Høgskoleringen 1, 7034 Trondheim, Norway, a translation is available at: http://www.dtic.mil/dtic/tr/fulltext/u2/a044002.pdf (last access ~~January~~ November 2016), 1975.

Kersten, M. S.: Thermal properties of soils, University of Minnesota Engineering Experiment Station Bulletin, 28, 227 pp., available at: https://conservancy.umn.edu/handle/11299/124271 (last access November 2016), 1949.

Laanaia, N., Carrer, D., Calvet, J.-C., and Pagé, C.: How will climate change affect the vegetation cycle over France? A generic modeling approach, Climate Risk Management, 13, 31-42, doi:10.1016/j.crm.2016.06.001, 2016.

Lawrence, D. M., and Slater, A. G.: Incorporating organic soil into a global climate model, Clim. Dyn., 30, 145-160, doi:10.1007/s00382-007-0278-1, 2008.

Lu, S., Ren, T., Gong, Y., and Horton, R.: An improved model for predicting soil thermal conductivity from water content at room temperature, Soil Sci. Soc. Am. J., 71, 8-14, doi:10.2136/sssaj2006.0041, 2007.

Nachtergaele, F., van Velthuize, H., Verelst, L., Wiberg, D., Batjes, N., Dijkshoorn, K., van Engelen, V., Fischer, G., Jones, A., Montanarella, L., Petri, M., Prieler, S., Teixeira, E., and Shi, X.: Harmonized World Soil Database, Version 1.2, FAO/IIASA/ISRIC/ISS-CAS/JRC, FAO, Rome, Italy and IIASA, Laxenburg, Austria, available at:

http://webarchive.iiasa.ac.at/Research/LUC/External-World-soil-database/HWSD_Documentation.pdf (last access January November 2016), 2012.

Parlange, M. B., Cahill, A. T., Nielsen, D. R., Hopmans, J. W., and Wendroth, O.: Review of heat and water movement in field soils, Soil Till. Res., 47, 5-10, 1998.

Parrens, M., Zakharova, E., Lafont, S., Calvet, J.-C., Kerr, Y., Wagner, W., and Wigneron, J.-P.: Comparing soil moisture retrievals from SMOS and ASCAT over France, Hydrol. Earth Syst. Sci., 16, 423–440, doi:10.5194/hess-16-423-2012, 2012.

Peters-Lidard, C.D., Blackburn, E., Liang, X., and Wood, E.F.: The effect of soil thermal conductivity parameterization on surface energy fluxes and temperatures, J. Atmos. Sci., 55, 1209–1224, 1998.

Rutten, M. M.: Moisture in the topsoil: From large-scale observations to small-scale process understanding, PhD Thesis, Delft university of Technology,– doi:10.4233/uuid:89e13a16-b456-4692-92f0-7a40ada82451, available at: http://repository.tudelft.nl/view/ir/uuid:89e13a16-b456-4692-92f0-7a40ada82451/ (last access: January November 2016), 2015.

Schelde, K., Thomsen, A., Heidmann, T., Schjonning, P., and Jansson, P.-E.: Diurnal fluctuations of water and heat flows in a bare soil, Water Resour. Res., 34, 11, 2919-2929, 1998.

Schönenberger, J., Momose, T., Wagner, B., Leong, W. H., and Tarnawski, V. R.: Canadian field soils I. Mineral composition by XRD/XRF measurements, Int. J. Thermophys., 33, 342–362, doi:10.1007/s10765-011-1142-4, 2012.

Sourbeer, J. J., and Loheide II, S. P.: Obstacles to long-term soil moisture monitoring with heated distributed temperature sensing, Hydrol. Process., 30, 7, 1017-1035, 2015.

Subin, Z. M., Koven, C. D., Riley, W. J., Torn, M. S., Lawrence, D. M., and Swenson, S. C.: Effects of soil moisture on the responses of soil temperatures to climate change in cold regions, J. Clim., doi:10.1175/JCLI-D-12-00305.1, 26, 3139-3158, 2013.

Tarara, J.M., and J.M. Ham: Measuring soil water content in the laboratory and field with dual-probe heat-capacity sensors, Agron. J., 89, 535–542, 1997.

Tarnawski, V. R., McCombie, M. L., Leong, W. H., Wagner, B., Momose, T., and Schönenberger J.: Canadian field soils II. Modeling of quartz occurrence, Int. J. Thermophys., 33, 843–863, doi:10.1007/s10765-012-1184-2, 2012.

Tarnawski, V. R., Momose, T., and Leong, W. H.: Assessing the impact of quartz content on the prediction of soil thermal conductivity, Géotechnique, 59, 4, 331–338, doi: 10.1680/geot.2009.59.4.331, 2009.

Yang, K., Koike, T., Ye, B., and Bastidas, L.: Inverse analysis of the role of soil vertical heterogeneity in controlling surface soil state and energy partition, J. Geophys. Res., 110, D08101, 15 pp., doi:10.1029/2004JD005500, 2005.

Zakharova, E., Calvet, J.-C., Lafont, S., Albergel, C., Wigneron, J.-P., Pardé, M., Kerr, Y., Zribi, M. : Spatial and temporal variability of biophysical variables in southwestern France from airborne L-band radiometry, Hydrol. Earth Syst. Sci., 16, 1725-1743, doi:10.5194/hess-16-1725-2012, 2012.

Zhang, X., Heitman, J., Horton, R., and Ren, T.: Measuring near-surface soil thermal properties with the heat-pulse method: correction of ambient temperature and soil–air interface effects, Soil Sci. Soc. Am. J., 78, 1575–1583, doi:10.2136/sssaj2014.01.0014, 2014.

Table 1 – –Soil characteristics at 10 cm for the 21 stations of the SMOSMANIA network. Porosity values are derived from Eq. (1). Solid fraction values higher than 0.3 are in bold. The stations are listed from West to East (from top to bottom). ρ_d, θ_{sat}, f, and m, stand for soil bulk density, porosity, volumetric fractions, and gravimetric fractions, respectively. Soil particle fractions larger than 0.3 are in bold. Station full names are given in Supplement 1 (Table S1.1).

~~Soil~~Station	ρ_d (kg m^{-3})	θ_{sat} (m^{3}m^{-3})	f_{sand} (m^{3}m^{-3})	f_{clay} (m^{3}m^{-3})	f_{silt} (m^{3}m^{-3})	f_{gravel} (m^{3}m^{-3})	f_{SOM} (m^{3}m^{-3})	m_{sand} (kg kg^{-1})	m_{clay} (kg kg^{-1})	m_{silt} (kg kg^{-1})	m_{gravel} (kg kg^{-1})	m_{SOM} (kg kg^{-1})
SBR	1680	0.352	**0.576**	0.026	0.013	0.002	0.032	**0.911**	0.041	0.020	0.003	0.024
URG	1365	0.474	0.076	0.078	**0.341**	0.005	0.025	0.149	0.153	**0.665**	0.009	0.024
CRD	1435	0.438	**0.457**	0.027	0.033	0.000	0.045	**0.848**	0.051	0.060	0.000	0.041
PRG	1476	0.431	0.051	0.138	0.138	0.214	0.028	0.092	0.250	0.248	**0.385**	0.025
CDM	1522	0.413	0.073	0.241	0.231	0.012	0.030	0.128	**0.422**	**0.404**	0.020	0.026
LHS	1500	0.416	0.102	0.202	0.189	0.051	0.039	0.181	**0.359**	**0.335**	0.091	0.034
SVN	1453	0.445	0.127	0.073	0.176	0.162	0.017	0.233	0.133	**0.322**	0.296	0.015
MNT	1444	0.447	0.135	0.066	0.230	0.102	0.020	0.248	0.121	**0.424**	0.188	0.018
SFL	1533	0.413	0.127	0.071	0.118	0.250	0.021	0.221	0.123	0.205	**0.434**	0.018
MTM	1540	0.405	0.110	0.081	0.076	0.297	0.032	0.189	0.140	0.131	**0.512**	0.027
LZC	1498	0.429	0.129	0.066	0.068	0.292	0.015	0.229	0.117	0.121	**0.519**	0.013
NBN	1545	0.401	0.063	0.135	0.075	0.290	0.035	0.109	0.232	0.130	**0.499**	0.030
PZN	1311	0.495	0.222	0.074	0.131	0.054	0.023	**0.450**	0.151	0.266	0.111	0.023
PRD	1317	0.494	0.038	0.052	0.069	**0.326**	0.021	0.076	0.105	0.139	**0.659**	0.021
LGC	1496	0.428	0.253	0.044	0.042	0.214	0.019	**0.451**	0.078	0.074	**0.380**	0.017
MZN	1104	0.560	0.212	0.037	0.045	0.097	0.049	**0.510**	0.089	0.109	0.234	0.057
VLV	1274	0.506	0.294	0.054	0.086	0.031	0.029	**0.614**	0.112	0.179	0.064	0.030
BRN	1630	0.379	0.105	0.009	0.016	**0.474**	0.016	0.171	0.015	0.027	**0.774**	0.013
MJN	1276	0.506	0.064	0.029	0.056	**0.317**	0.028	0.133	0.060	0.118	**0.661**	0.029
BRZ	1280	0.508	0.097	0.074	0.109	0.190	0.020	0.202	0.154	0.228	**0.396**	0.021
CBR	1310	0.501	0.120	0.057	0.068	0.241	0.013	0.243	0.116	0.139	**0.489**	0.013

Table 2 – –Thermal properties of 14 grassland soils in southern France: λ_{sat}, f_q and Q retrievals using the λ model (Eqs. (7)-(9) and Eq. (10), respectively) for degree of saturation values higher than 0.4, together with the minimized RMSD between the simulated and observed λ values, and the number of used λ observations (n). The soils are sorted from the largest to the smallest ratio of m_{sand} to m_{SOM}. Station full names are given in Supplement 1 (Table S1.1).

~~Soil~~Station	λ_{sat} ($Wm^{-1}K^{-1}$)	RMSD ($Wm^{-1}K^{-1}$)	n	f_q (m^3m^{-3})	Q (kg kg^{-1})	$\frac{m_{sand}}{m_{SOM}}$
SBR	2.80	0.255	6	0.62	0.96	37.2
LGC	2.07	0.311	20	0.44	0.77	26.6
CBR	1.92	0.156	20	0.44	0.88	18.4
LZC	1.71	0.107	20	0.29	0.51	17.3
SVN	1.78	0.163	20	0.34	0.61	15.4
MNT	1.96	0.058	20	0.42	0.76	13.8
BRN	1.71	0.131	20	0.25	0.40	13.5
SFL	1.57	0.134	20	0.22	0.37	12.5
MTM	1.52	0.095	20	0.21	0.35	7.0
URG	1.37	0.066	20	0.05	0.10	6.2
LHS	1.57	0.136	20	0.26	0.45	5.3
CDM	1.82	0.086	20	0.26	0.44	5.0
PRG	1.65	0.086	20	0.18	0.32	3.7
PRD	1.26	0.176	20	0.14	0.28	3.7

–**Table 3** –– Coefficients of four pedotransfer functions of f_q (Eq. 12) for 14 soils of this study (all with $m_{sand}/m_{SOM} < 40$), together with indicators of the coefficient uncertainty, derived by bootstrapping and by perturbing the volumetric heat capacity of soil minerals (C_{hmin}). The best predictor is in bold.

Predictor of f_q	Coefficients for 14 soils		Confidence interval from bootstrapping		Impact of a change of $\pm 0.08 \times 10^6$ J m^{-3} K^{-1} in C_{hmin}	
	a_0	a_1	a_0	a_1	a_0	a_1
$\boldsymbol{m_{sand} / m_{SOM}}$	0.12	0.0134	[0.10,0.14]	[0.012,0.014]	[0.11,0.13]	[0.013,0.013]
m_{sand}*	0.08	0.944	[0.00,0.11]	[0.85,1.40]	[0.07,0.09]	[0.919,0.966]
m_{sand}	0.15	0.572	[0.08,0.17]	[0.54,0.94]	[0.14,0.17]	[0.55,0.56]
$1 - \theta_{sat} - f_{sand}$	0.73	–1.020	[0.71,0.89]	[–1.38, –0.99]	[0.70,0.73]	[–1.00, –0.99]

(*) only m_{sand} values smaller than 0.6 kg kg^{-1} are used in the regression

Table 4 – Scores of four pedotransfer functions of f_q for 14 soils of this study, together with the scores obtained by bootstrapping, without the sandy SBR soil. The MAE score of these pedotransfer functions for three Chinese soils of Lu et al. (2007) for which m_{sand}/m_{SOM} < 40 is given (within brackets). The best predictor and the best scores are in bold.

Predictor of f_q	Regression scores			Bootstrap scores			Scores without SBR (and MAE for 3 Lu soils)		
	r^2	RMSD (m^3m^{-3})	MAE (m^3m^{-3})	r^2	RMSD (m^3m^{-3})	MAE (m^3m^{-3})	r^2	RMSD (m^3m^{-3})	MAE (m^3m^{-3})
$\boldsymbol{m_{sand} / m_{SOM}}$	**0.77**	**0.067**	0.053	**0.72**	**0.074**	**0.059**	**0.62**	**0.070**	0.057 (*0.135*)
m_{sand}*	0.74	0.072	**0.052**	0.67	0.126	0.100	0.56	0.075	**0.056** (***0.071***)
m_{sand}	0.67	0.081	0.060	0.56	0.121	0.084	0.56	0.075	**0.056** (*0.086*)
$1-\theta_{sat}-f_{sand}$	0.65	0.084	0.064	0.56	0.102	0.079	0.45	0.084	0.061 (*0.158*)

(*) only m_{sand} values smaller than 0.6 kg kg^{-1} are used in the regression

Table 5 – Ability of the Eqs. (10)-(13) empirical model to estimate λ_{sat} values for 14 soils and impact of changes in gravel and SOM volumetric content: f_{gravel} = 0 m^{3}m^{-3} and f_{SOM} = 0.013 m^{3}m^{-3} (the smallest f_{SOM} value, observed for CBR). r^2 values smaller than 0.60, RMSD values higher than 0.20 Wm^{-1}K^{-1}, and mean bias values higher (smaller) than +0.10 (–0.10) are in bold.

Model configuration	Predictor of f_q	r^2	RMSD (Wm^{-1}K^{-1})	Mean bias (Wm^{-1}K^{-1})
Model using θ_{sat} observations	m_{sand} / m_{SOM}	0.86	0.14	+0.01
	m_{sand}*	0.83	0.15	–0.01
	m_{sand}	0.81	0.16	–0.03
	$1 - \theta_{sat} - f_{sand}$	0.82	0.16	–0.03
Full model using θ_{satMOD} (Eqs. (13))	m_{sand} / m_{SOM}	0.85	0.14	+0.03
	m_{sand}*	0.85	0.14	–0.03
	m_{sand}	0.84	0.15	–0.03
	$1 - \theta_{sat} - f_{sand}$	0.82	0.16	–0.02
same with: f_{SOM} = 0.013 m^{3}m^{-3}	m_{sand} / m_{SOM}	**0.57**	**0.35**	**+0.20**
	m_{sand}*	0.83	0.15	+0.00
	m_{sand}	0.81	0.16	–0.02
	$1 - \theta_{sat} - f_{sand}$	0.83	0.15	–0.02
same with: f_{gravel} = 0 m^{3}m^{-3}	m_{sand} / m_{SOM}	0.87	0.19	**–0.12**
	m_{sand}*	0.70	**0.23**	**+0.11**
	m_{sand}	0.79	0.17	+0.04
	$1 - \theta_{sat} - f_{sand}$	0.81	0.17	+0.05
same with: f_{SOM} = 0.013 m^{3}m^{-3} and f_{gravel} = 0 m^{3}m^{-3}	m_{sand} / m_{SOM}	0.63	**0.31**	**+0.16**
	m_{sand}*	**0.52**	**0.36**	**+0.24**
	m_{sand}	**0.59**	**0.29**	**+0.16**
	$1 - \theta_{sat} - f_{sand}$	0.70	**0.25**	**+0.16**

(*) only m_{sand} values smaller than 0.6 kg kg^{-1} are used in the regression

Table 6 – Pedotransfer functions of f_q (Eq. 12) for 7 soils of Lu et al. (2007) with $m_{sand}/m_{SOM} > 40$. The best predictor and the best scores are in bold. The regression p-values are within brackets.

Predictor of f_q	Regression scores for 7 Lu soils with $m_{sand}/m_{SOM} > 40$			Coefficients	
	r^2 (*p-value*)	RMSD (m^3m^{-3})	MAE (m^3m^{-3})	a_0	a_1
m_{sand} / m_{SOM}	0.40 (*0.13*)	0.089	0.075	0.20	0.000148
m_{sand}*	0.82 (*0.005*)	0.073	0.054	0.07	0.425
$\boldsymbol{m_{sand}}$	**0.82 (*0.005*)**	**0.048**	**0.042**	0.04	0.386
$1 - \theta_{sat} - f_{sand}$	0.81 (*0.006*)	0.050	0.043	0.44	−0.814

(*) only m_{sand} values smaller than 0.6 kg kg^{-1} are used in the regression

Deriving pedotransfer functions for soil quartz fraction in southern France from reverse modelling

Jean-Christophe Calvet, Noureddine Fritz,
Christine Berne, Bruno Piguet, William Maurel, and Catherine Meurey

CNRM, UMR 3589 (Météo-France, CNRS), Toulouse, France

27 October 2016

Abstract

The quartz fraction in soils is a key parameter of soil thermal conductivity models. Because it is difficult to measure the quartz fraction in soils, this information is usually unavailable. This source of uncertainty impacts the simulation of sensible heat flux, evapotranspiration, and land surface temperature in numerical simulations of the Earth system. Improving the estimation of soil quartz fraction is needed for practical applications in meteorology, hydrology, and climate modelling. This paper investigates the use of long time series of routine ground observations made in weather stations to retrieve the soil quartz fraction. Profile soil temperature and water content were monitored at 21 weather stations in southern France. Soil thermal diffusivity was derived from the temperature profiles. Using observations of bulk density, soil texture, and fractions of gravel and soil organic matter, soil heat capacity and thermal conductivity were estimated. The quartz fraction was inversely estimated using an empirical geometric mean thermal conductivity model. Several pedotransfer functions for estimating quartz content from gravimetric or volumetric fractions of soil particles (e.g. sand) were analysed. The soil volumetric fraction of quartz (*f_q*) was systematically better correlated to soil characteristics than the gravimetric fraction

of quartz. More than 60 % of the variance of f_q could be explained using indicators based on the sand fraction. It was shown that soil organic matter and (or) gravels may have a marked impact on thermal conductivity values depending on which predictor of f_q is used. For the grassland soils examined in this study, the ratio of sand to soil organic matter fractions was the best predictor of f_q, followed by the gravimetric fraction of sand. An error propagation analysis and a comparison with independent data from other tested models showed that the gravimetric fraction of sand is the best predictor of f_q when a larger variety of soil types is considered.

1. Introduction

Soil moisture is the main driver of temporal changes in values of the soil thermal conductivity (Sourbeer and Loheide, 2015). The latter is a key variable in land surface models (LSMs) used in hydrometeorology or in climate models, for the simulation of the vertical profile of soil temperature in relation to soil moisture (Subin et al., 2013). Shortcomings in soil thermal conductivity models tend to limit the impact of improving the simulation of soil moisture and snowpack in LSMs (Lawrence and Slater, 2008; Decharme et al. 2016). Models of the thermal conductivity of soils are affected by uncertainties, especially in the representation of the impact of soil properties such as the volumetric fraction of quartz (f_q), soil organic matter, and gravels (Farouki, 1986; Chen et al., 2012). As soil organic matter (SOM) and gravels are often neglected in LSMs, the soil thermal conductivity models used in most LSMs represent the mineral fine earth, only. Nowadays, f_q estimates are not given in global digital soil maps and it is often assumed that this quantity is equal to the fraction of sand (Peters-Lidard et al., 1998).

Soil thermal properties are characterized by two key variables: the soil volumetric heat capacity (C_h), and the soil thermal conductivity (λ), in $Jm^{-3}K^{-1}$ and $Wm^{-1}K^{-1}$, respectively. Provided the volumetric fractions of moisture, minerals and organic matter are known, C_h can be calculated easily. The estimation of λ relies on empirical models and is affected by uncertainties (Peters-Lidard et al., 1998; Tarnawski et al., 2012). The construction and the verification of the λ models is not easy. The λ values of undisturbed soils are difficult to directly observe. They are often measured in the lab on perturbed soil samples (Abu-Hamdeh et al., 2000; Lu et al., 2007). Although recent advances in line-source probe and heat pulse methods have made it easier to monitor soil thermal conductivity in the field (Bristow et al., 1994; Zhang et al., 2014), such measurements are currently not made in operational meteorological networks. Moreover, for given soil moisture conditions, λ depends to a large extent on the fraction of soil minerals presenting high thermal conductivities such as quartz, hematite, dolomite or pyrite (Côté and Conrad, 2005). In mid-latitude regions of the world, quartz is the main driver of λ. The information on quartz fraction in a soil is usually unavailable as it can only be measured using X-ray diffraction (XRD) or X-ray fluorescence (XRF) techniques. These techniques are difficult to implement because the sensitivity to quartz is low. In practise, using XRD and XRF together is needed to improve the accuracy of the measurements (Schönenberger et al., 2012). This lack of observations has a major effect on the accuracy of thermal conductivity models and their applications (Bristow, 1998).

Most of the Land Surface Models (LSMs) currently used in meteorology and hydrometeorology simulate λ following the approach proposed by Peters-Lidard et al. (1998). This approach consists of an updated version of the Johansen (1975) model, and assumes that the gravimetric fraction of quartz (Q) is equal to the gravimetric fraction of sand within mineral fine earth. This is a strong assumption, as some sandy soils (e.g. calcareous sands) may contain little quartz, and as quartz may be found in the silt and clay fractions of the soil minerals (Schönenberger et al., 2012). Moreover, the λ models used in most LSMs represent only the mineral fine earth. Yang et al. (2005) and Chen et al. (2012) have shown the importance of accounting for SOM and gravels in λ models for organic top soil layers of grasslands of the Tibetan plateau.

The main goals of this study are to (1) assess the feasibility of using routine automatic soil temperature profile sub-hourly measurements (one observation every 12 minutes) to retrieve instantaneous soil thermal diffusivity values at a depth of 0.10 m; (2) retrieve instantaneous λ values from the soil thermal diffusivity estimates, accounting for the impact of soil vertical heterogeneities; (3) obtain, from reverse modelling, the quartz fraction together with soil thermal conductivity at saturation (λ_{sat}); (4) assess the impact of gravels and SOM on λ_{sat}; (5) derive pedotransfer functions for the soil quartz fraction.

For this purpose, we use the data from 21 weather stations of the Soil Moisture Observing System – Meteorological Automatic Network Integrated Application (SMOSMANIA) network (Calvet et al., 2007) in southern France. The soil temperature and the soil moisture probes are buried in the enclosure around each weather station. Most of these stations are located in agricultural areas. However, the vegetation cover in the enclosure around the stations consists of grass. Along the Atlantic-Mediterranean transect formed by the SMOSMANIA network (Fig. 1), the grass land cover fraction ranges between 10 % and 40 % (Zakharova et al., 2012). Various mineral soil types can be found along this transect, ranging from sand to clay and silt loam (see Supplement 1). During the installation of the probes, we collected soil samples which were used to determine soil characteristics: soil texture, soil gravel content, soil organic matter, and bulk density.

Using this information together with soil moisture, λ values are derived from soil thermal diffusivity and heat capacity. The response of λ to soil moisture is investigated. The feasibility of modelling the λ value at saturation (λ_{sat}) with or without using SOM and gravel fraction observations is assessed using a geometric mean empirical thermal conductivity model based on Lu et al. (2007). The volumetric fraction of quartz, f_q, is retrieved by reverse modelling together with Q. Pedotransfer functions are further proposed for estimating quartz content from soil texture information.

The field data and the method to retrieve λ values are presented in Sect. 2. The λ and f_q retrievals are presented in Sect. 3 together with a sensitivity analysis of λ_{sat} to SOM and gravel fractions. Finally, the results are discussed in Sect. 4, and the main conclusions are summarized in Sect. 5. Technical details are given in Supplements.

2. Data and methods

2.1. The SMOSMANIA data

The SMOSMANIA network was developed by Calvet et al. (2007) in southern France. The main purposes of SMOSMANIA are to (1) validate satellite-derived soil moisture products (Parrens et al., 2012); (2) assess land surface models used in hydrological models (Draper et al., 2011) and in meteorological models (Albergel et al., 2010); and (3) monitor the impact of climate change on water resources and droughts (Laanaia et al., 2016). The station network forms a transect between the Atlantic coast and the Mediterranean sea (Fig. 1). It consists of pre-existing automatic weather stations operated by Meteo-France, upgraded with four soil moisture probes at four depths: 0.05 m, 0.10 m, 0.20 m, and 0.30 m. Twelve SMOSMANIA stations were activated in 2006 in southwestern France. In 2008, nine more stations were installed along the Mediterranean coast, and the whole network (21 stations) was gradually equipped with temperature sensors at the same depths as soil moisture probes. The soil moisture and soil temperature probes consisted of Thetaprobe ML2X and PT100 sensors, respectively. Soil moisture and soil temperature observations were made every 12 minutes at four depths. The soil temperature observations were recorded with a resolution of 0.1 °C.

In this study, the sub-hourly measurements of soil temperature and soil moisture at a depth of 0.10 m were used, together with soil temperature measurements at 0.05 m and 0.20 m, from 1 January 2008 to 30 September 2015.

The ThetaProbe soil moisture sensors provide a voltage signal (V). In order to convert the voltage signal into volumetric soil moisture content ($m^3\ m^{-3}$), site-specific calibration curves were developed using in situ gravimetric soil samples for all stations, and for all depths (Albergel et al., 2008). We revised the calibration in order to avoid spurious high soil moisture values during intense precipitation events. Logistics curves were used (see Supplement 1) instead of exponential curves in the previous version of the data set.

The observations from the soil moisture (48) and from the temperature (48) probes are automatically recorded every 12 minutes. The data are available to the research community through the International Soil Moisture Network web site (https://ismn.geo.tuwien.ac.at/).

Figure 2 shows soil temperature time series in wet conditions at various soil depths, for a station presenting an intermediate value of λ_{sat} (Table 2) and of soil texture (see Fig. S1.1 in Supplement

1). The impact of recording temperature with a resolution of 0.1 °C is clearly visible at all depths as this causes a levelling of the curves.

2.2. Soil characteristics

In general, the stations are located on formerly cultivated fields and the soil in the enclosure around the stations is covered with grass. Soil properties were measured at each station by an independent laboratory we contracted (INRA-Arras) from soil samples we collected during the installation of the probes. The 21 stations cover a very large range of soil texture characteristics. For example, SBR is located on a sandy soil, PRD on a clay loam, and MNT on a silt loam (Table 1 and Supplement 1). Other properties such as the gravimetric fraction of SOM and of gravels were determined from the soil samples. Table 1 shows that 12 soils present a volumetric gravel content (f_{gravel}) larger than 15 %. Among these, 3 soils (at PRD, BRN, and MJN) have f_{gravel} values larger than 30 %.

In addition, we measured bulk density (ρ_{d}) using undisturbed oven-dried soil samples we collected using metal cylinders of known volume (about 7×10^{-4} m^3, see Fig. S1.10 in the Supplement).

The porosity values at a depth of 0.10 m are listed in Table 1 together with gravimetric and volumetric fractions of soil particle-size ranges (sand, clay, silt, gravel) and SOM. The porosity, or soil volumetric moisture at saturation (θ_{sat}), is derived from the bulk dry density ρ_{d}, with soil texture and soil organic matter observations as:

$$\theta_{sat} = 1 - \rho_d \left[\frac{m_{sand} + m_{clay} + m_{silt} + m_{gravel}}{\rho_{\min}} + \frac{m_{SOM}}{\rho_{SOM}} \right]$$

or

$$\theta_{sat} = 1 - f_{sand} - f_{clay} - f_{silt} - f_{gravel} - f_{SOM} \quad (1)$$

where m_x (f_x) represents the gravimetric (volumetric) fraction of the soil component *x*. The f_x values are derived from the measured gravimetric fractions, multiplied by the ratio of ρ_d observations to ρ_x, the density of each soil component *x*. Values of ρ_{SOM} = 1300 kg m^{-3} and ρ_{min} = 2660 kg m^{-3} are used for soil organic matter, and soil minerals, respectively.

2.3. Retrieval of soil thermal diffusivity

The soil thermal diffusivity (D_h) is expressed in m^{2}s^{-1} and is defined as:

$$D_h = \frac{\lambda}{C_h} \quad (2)$$

We used a numerical method to retrieve instantaneous values of D_h at a depth of 0.10 m using three soil temperature observations at 0.05 m, 0.10 m and 0.20 m, performed every 12 minutes, by solving the Fourier thermal diffusion equation. The latter can be written as:

$$C_h \frac{\partial T}{\partial t} = \frac{\partial}{\partial z}\left(\lambda \frac{\partial T}{\partial z}\right) \quad (3).$$

Given that soil properties are relatively homogeneous on the vertical (Sect. 2.1), values of D_h can be derived from the Fourier one-dimensional law:

$$\frac{\partial T}{\partial t} = D_h \frac{\partial^2 T}{\partial z^2} \quad (4).$$

However, large differences in soil bulk density, from the top soil layer to deeper soil layers were observed for some soils (see Supplement 1). In order to limit this effect as much as possible, we only used the soil temperature data presenting a relatively low vertical gradient close to the soil surface, where most differences with deeper layers are found. This data sorting procedure is described in Supplement 2.

Given that three soil temperatures T_i (i ranging from 1 to 3) are measured at depths $z_1 = -0.05$ m, $z_2 = -0.10$ m, and $z_3 = -0.20$ m, the soil diffusivity D_{hi} at $z_i = z_2 = -0.10$ m can be obtained by solving the one-dimensional heat equation, using a finite difference method based on the implicit Crank-Nicolson scheme (Crank and Nicolson, 1996). When three soil depths are considered, z_{i-1}, z_i, z_{i+1}, the change in soil temperature T_i at depth z_i, from time t_{n-1} to time t_n, within the time interval $\Delta t = t_n - t_{n-1}$ can be written as:

$$\frac{T_i^n - T_i^{n-1}}{\Delta t} = D_{hi}\left[\frac{1}{2}\left(\frac{\gamma_{i+1}^n - \gamma_i^n}{\Delta z_m}\right) + \frac{1}{2}\left(\frac{\gamma_{i+1}^{n-1} - \gamma_i^{n-1}}{\Delta z_m}\right)\right] \quad \text{with}$$

$$\gamma_i^n = \frac{T_i^n - T_{i-1}^n}{\Delta z_i}, \; \Delta z_m = \frac{\Delta z_i + \Delta z_{i+1}}{2}, \text{ and } \Delta z_i = z_i - z_{i-1} \qquad (5).$$

In this study, $\Delta z_i = -0.05$ m, $\Delta z_{i+1} = -0.10$ m, and a value of $\Delta t = 2880$ s (48 minutes) is used.

It is important to ensure that D_h retrievals are related to diffusion processes only and not to the transport of heat by water infiltration or evaporation (Parlange et al., 1998 ; Schelde et al., 1998). Therefore, only situations for which changes in soil moisture at all depths do not exceed 0.001 m^3m^{-3} within the Δt time interval are considered.

2.4. From soil diffusivity to soil thermal conductivity

The observed soil properties and volumetric soil moisture are used to calculate the soil volumetric heat capacity C_h at a depth of 0.10 m, using the de Vries (1963) mixing model. The C_h values, in units of $Jm^{-3}K^{-1}$, are calculated as:

$$C_h = \theta C_{h\,water} + f_{\min} C_{h\,\min} + f_{SOM}\, C_{hSOM} \tag{6}$$

where θ and $f_{\min}$ represent the volumetric soil moisture and the volumetric fraction of soil minerals, respectively. Values of 4.2×10^6 $Jm^{-3}K^{-1}$, 2.0×10^6 $Jm^{-3}K^{-1}$, and 2.5×10^6 $Jm^{-3}K^{-1}$, are used for $C_{h\mathrm{water}}$, $C_{h\mathrm{min}}$, $C_{h\mathrm{SOM}}$, respectively.

The λ values at 0.10 m are then derived from the D_h and C_h estimates (Eq. (2)).

2.5. Soil thermal conductivity model

Various approaches can be used to simulate thermal conductivity of unsaturated soils (Dong et al., 2015). We used an empirical approach based on thermal conductivity values in dry conditions and at saturation.

In dry conditions, soils present low thermal conductivity values (λ_{dry}). Experimental evidence shows that λ_{dry} is negatively correlated with porosity. For example, Lu et al. (2007) give:

$$\lambda_{dry} = 0.51 - 0.56 \times \theta_{sat} \qquad \text{(in } Wm^{-1}K^{-1}\text{)} \tag{7}$$

When soil pores are gradually filled with water, λ tends to increase towards a maximum value at saturation (λ_{sat}). Between dry and saturation conditions, λ is expressed as:

$$\lambda = \lambda_{dry} + K_e\left(\lambda_{sat} - \lambda_{dry}\right) \tag{8}$$

where, K_e is the Kersten number (Kersten, 1949). The latter is related to the volumetric soil moisture, θ, i.e. to the degree of saturation (S_d). We used the formula recommended by Lu et al. (2007):

$$K_e = \exp\left\{\alpha\left(1 - S_d^{(\alpha - 1.33)}\right)\right\},$$

with $\alpha = 0.96$ for $Mn_{sand} \geq 0.4$ kg kg^{-1}, $\alpha = 0.27$ for $Mn_{sand} < 0.4$ kg kg^{-1}, and

$$S_d = \theta / \theta_{sat} \quad (9).$$

Mn_{sand} represents the sand mass fraction of mineral fine earth (values are given in Supplement 1). The geometric mean equation for λ_{sat} proposed by Johansen (1975) for the mineral components of the soil can be generalized to include the SOM thermal conductivity (Chen et al., 2012) as:

$$\ln(\lambda_{sat}) = f_q \ln(\lambda_q) + f_{other} \ln(\lambda_{other}) + \theta_{sat} \ln(\lambda_{water}) + f_{SOM} \ln(\lambda_{SOM}) \quad (10)$$

where f_q is the volumetric fraction of quartz, and λ_q = 7.7 Wm^{-1}K^{-1}, λ_{water} = 0.594 Wm^{-1}K^{-1}, λ_{SOM} = 0.25 Wm^{-1}K^{-1} are the thermal conductivities of quartz, water and SOM, respectively. The λ_{other} term corresponds to the thermal conductivity of soil minerals other than quartz. Following Peters-Lidard et al. (1998), λ_{other} is taken as 2.0 Wm^{-1}K^{-1} for soils with $Mn_{sand} > 0.2$ kg kg^{-1}, and 3.0 Wm^{-1}K^{-1} otherwise. In this study $Mn_{sand} > 0.2$ kg kg^{-1} for all soils, except for URG, PRG, and CDM. The volumetric fraction of soil minerals other than quartz is defined as:

$$f_{other} = 1 - f_q - \theta_{sat} - f_{SOM}$$

with $f_q = Q \times (1 - \theta_{sat})$ (11)

2.6. Reverse modelling

The λ_{sat} values are retrieved through reverse modelling using the λ model described above (Eqs. (7)-(11)). This model is used to produce simulations of λ at the same soil moisture conditions as those encountered for the λ values derived from observations in Sect. 2.4. For a given station, a set of 401 simulations is produced for λ_{sat} ranging from 0 $Wm^{-1}K^{-1}$ to 4 $Wm^{-1}K^{-1}$, with a resolution of 0.01 $Wm^{-1}K^{-1}$. The λ_{sat} retrieval corresponds to the λ simulation presenting the lowest root mean square difference (RMSD) value with respect to the λ observations. Only λ observations for S_d values higher than 0.4 are used because in dry conditions: (1) conduction is not the only mechanism for heat exchange in soils, as the convective water vapour flux may become significant (Schelde et al., 1998; Parlange et al. 1998); (2) the K_e functions found in the literature display more variability; and, (3) the λ_{sat} retrievals are more sensitive to uncertainties in λ observations. The threshold value of $S_d = 0.4$ results from a compromise between the need of limiting the influence of convection, of the shape of the K_e function on the retrieved values of λ_{sat}, and of using as many observations as possible in the retrieval process. Moreover, the data filtering technique to limit the impact of soil heterogeneities, described in Supplement 2, is used to select valid λ observations.

Finally, the f_q value is derived from the retrieved λ_{sat} solving Eq. (10).

2.7. Scores

Pedotransfer functions for quartz and λ_{sat} are evaluated using the following scores:

- the Pearson correlation coefficient (r), and the squared correlation coefficient (r^2) is used to assess the fraction of explained variance,

- the RMSD,
- the Mean Absolute Error (MAE), i.e. the mean of absolute differences,
- the mean bias, i.e. the mean of differences.

In order to test the predictive and generalization power of the pedotransfer regression equations, a simple bootstrapping resampling technique is used. It consists in calculating a new estimate of f_q for each soil using the pedotransfer function obtained without using this specific soil. Gathering these new f_q estimates, one can calculate new scores with respect to the retrieved f_q values. Also, this method provides a range of possible values of the coefficients of the pedotransfer function and permits assessing the influence of a given f_q retrieval on the final result.

3. Results

3.1. λ_{sat} and f_q retrievals

Retrievals of λ_{sat} and f_q could be obtained for 14 soils. Figure 3 shows retrieved and modelled λ values against the observed degree of saturation of the soil, at a depth of 0.10 m, for contrasting retrieved values of λ_{sat}, from high to low values (2.80, 1.96, 1.52, and 1.26 $Wm^{-1}K^{-1}$) at the SBR, MNT, MTM, and PRD stations, respectively.

All the obtained λ_{sat} and f_q retrievals are listed in Table 2, together with the λ RMSD values and the number of selected λ observations. For three soils (CRD, MZN, and VLV), the reverse modelling technique described in Sect. 2.6 could not be applied as not enough λ observations could be obtained for S_d values higher than 0.4. For four soils (NBN, PZN, BRZ, and MJN), all the λ retrievals were filtered out as the obtained values were influenced by heterogeneities in soil density (see Supplement 2). For the other 14 soils, λ_{sat} and f_q retrievals were obtained using a subset of 20 λ retrievals per soil, at most, corresponding to the soil temperature data presenting the lowest vertical gradient close to the soil surface (Supplement 2).

3.2 Pedotransfer functions for quartz

The f_q retrievals can be used to assess the possibility to estimate f_q using other soil characteristics, which can be easily measured. Another issue is whether volumetric or gravimetric fraction of quartz should be used. Figure 4 presents the fraction of variance (r^2) of Q and f_q explained by various indicators. A key result is that f_q is systematically better correlated to soil characteristics than Q. More than 60 % of the variance of f_q can be explained using indicators based on the sand fraction (either f_{sand} or m_{sand}). The use of other soil mineral fractions does not give good correlations, even when they are associated to the sand fraction as shown by Fig. 4. For example, the f_{gravel} and $f_{gravel}+f_{sand}$ indicators present low r^2 values of 0.04 and 0.24, respectively.

The f_q values cannot be derived directly from the indicators as illustrated by Fig. 5: assuming $f_q = f_{sand}$ tends to markedly underestimate λ_{sat}. Therefore, more elaborate pedotransfer equations are needed. They can be derived from the best indicators, using them as predictors of f_q. The modelled f_q is written as:

$$f_{qMOD} = a_0 + a_1 \times P$$

and $$f_{qMOD} \leq 1 - \theta_{sat} - f_{SOM} \qquad (12)$$

where P represents the predictor of f_q.

The a_0 and a_1 coefficients are given in Table 3 for four pedotransfer functions based on the best predictors of f_q. The pedotranfer functions are illustrated in Fig. 6. The scores are displayed in Table 4. The bootstrapping indicates that the SBR sandy soil has the largest individual impact on the obtained regression coefficients. This is why the scores without SBR are also presented in Table 4.

For the m_{sand} predictor, a r^2 value of 0.56 is obtained without SBR, against a value of 0.67 when all the 14 soils are considered. An alternative to this m_{sand} pedotransfer function consists in considering only m_{sand} values smaller than 0.6 kg kg^{-1} in the regression, thus excluding the SBR soil. The corresponding predictor is called m_{sand}*. In this configuration, the sensitivity of f_q to m_{sand} is much increased (with a_1 = 0.944, against a_1 = 0.572 with SBR). For SBR, f_q is overestimated by the m_{sand}* equation but this is corrected by the f_{qMOD} limitation of Eq. (12), and in the end a better r^2 score is obtained when the 14 soils are considered (r^2 = 0.74) .

Values of r^2 larger than 0.7 are obtained for two predictors of f_q: m_{sand}/m_{SOM} and m_{sand}*. A value of r^2 = 0.65 is obtained for $1 - \theta_{sat} - f_{sand}$ (the fraction of soil solids other than sand). The m_{sand}/m_{SOM} predictor presents the best r^2 and RMSD scores in all the configurations (regression, bootstrap, and regression without SBR). Another characteristic of the m_{sand}/m_{SOM} pedotransfer function is that the confidence interval for the a_0 and a_1 coefficients derived from bootstrapping is narrower than for the other pedotransfer functions (Table 3), indicating a more robust relationship of f_q with m_{sand}/m_{SOM} than with other predictors.

An alternative way to evaluate the quartz pedotransfer functions is to compare the simulated λ_{sat} with the retrieved values presented in Table 2. Modelled values of λ_{sat} (λ_{satMOD}) can be derived from f_{qMOD} using Eq. (10) together with θ_{sat} observations. The λ_{satMOD} r^2, RMSD, and mean bias scores are given in Table 5. Again, the best scores are obtained using the m_{sand}/m_{SOM} predictor of f_q, with r^2, RMSD, and mean bias values of 0.86, 0.14 $Wm^{-1}K^{-1}$, and +0.01 $Wm^{-1}K^{-1}$, respectively (Fig. 7).

Finally, we investigated the possibility of estimating θ_{sat} from the soil characteristics listed in Table 1 and of deriving a statistical model for θ_{sat} (θ_{satMOD}). We found the following statistical relationship between θ_{satMOD}, m_{clay}, m_{silt}, and m_{SOM}:

$$\theta_{satMOD} = 0.456 - 0.0735 \frac{m_{clay}}{m_{silt}} + 2.238\, m_{SOM} \qquad (13)$$

(r^2 = 0.48, F-test p-value = 0.0027, RMSD=0.036 m^3m^{-3}).

Volumetric fractions of soil components need to be consistent with θ_{satMOD} and can be calculated using the modelled bulk density values derived from θ_{satMOD} using Eq. (1).

Equations (10) to (13) constitute an empirical end-to-end model of λ_{sat}. Table 5 shows that using θ_{satMOD} (Eqs. (13)) instead of the θ_{sat} observations has little impact on the λ_{satMOD} scores.

3.3. Impact of gravels and SOM on λ_{sat}

Gravels and SOM are often neglected in soil thermal conductivity models used in LSMs. The Eqs. (10)-(13) empirical model obtained in Sect. 3.2 permits the assessment of the impact of f_{gravel} and f_{SOM} on λ_{sat}. Table 5 shows the impact on λ_{satMOD} scores of imposing a null value of f_{gravel} and a small value of f_{SOM} to all the soils. The combination of these assumptions is evaluated, also.

Imposing f_{SOM} = 0.013 m^3m^{-3} (the smallest f_{SOM} value, observed for CBR) has a limited impact on the scores, except for the m_{sand}/m_{SOM} pedotransfer function. In this case, λ_{sat} is overestimated by +0.20 $Wm^{-1}K^{-1}$, and r^2 drops to 0.57.

Neglecting gravels (f_{gravel} = 0 m^3m^{-3}) also has a limited impact but triggers the underestimation (overestimation) of λ_{sat} for the m_{sand}/m_{SOM} (m_{sand}*) pedotransfer function, by –0.12 $Wm^{-1}K^{-1}$ (+0.11 $Wm^{-1}K^{-1}$).

On the other hand, it appears that combining these assumptions has a marked impact on all the pedotransfer functions. Neglecting gravels and imposing f_{SOM} = 0.013 m^3m^{-3} has a major impact on λ_{sat}: the modelled λ_{sat} is overestimated by all the pedotransfer functions (with a mean bias ranging from +0.16 $Wm^{-1}K^{-1}$ to +0.24 $Wm^{-1}K^{-1}$) and r^2 is markedly smaller, especially for the m_{sand} and m_{sand}* pedotransfer functions. These results are illustrated in Fig. 8 in the case of the m_{sand}* pedotransfer function. Figure 8 also shows that using the θ_{sat} observations instead of θ_{satMOD} (Eq. (13)) has little impact on λ_{satMOD} (Sect. 3.2) but tends to enhance the impact of neglecting gravels. A similar result is found with the m_{sand} pedotransfer function (not shown).

4. Discussion

4.1. Can uncertainties in heat capacity estimates impact retrievals ?

In this study, the de Vries (1963) mixing model is applied to estimate soil volumetric heat capacity (Eq. (6)), and a fixed value of 2.0×10^{6} $Jm^{-3}K^{-1}$ is used for soil minerals. Soil-specific values for C_{hmin} may be more appropriate than using a constant standard value. For example, Tarara and Ham (1997) used a value of 1.92×10^{6} $Jm^{-3}K^{-1}$. However, we did not measure this quantity and we were not able to find such values in the literature.

We investigated the sensitivity of our results to these uncertainties, considering the following minimum and maximum C_{hmin} values: C_{hmin} = 1.92×10^{6} J m^{-3} K^{-1} and C_{hmin} = 2.08×10^{6} J m^{-3} K^{-1}. The impact of changes in C_{hmin} on the retrieved values of λ_{sat} and f_q is presented in Supplement 3 (Fig. S3.1). On average, a change of + (–) 0.08×10^{6} J m^{-3} K^{-1} in C_{hmin} triggers a change in λ_{sat} and f_q of + 1.7 % (– 1.8 %) and + 4.8 % (– 7.0 %), respectively.

The impact of changes in C_{hmin} on the regression coefficients of the pedotransfer functions is presented in Table 3 (last column). The impact is very small, except for the a_1 coefficient of the m_{sand}* pedotransfer function. However, even in this case, the impact of C_{hmin} on the a_1 coefficient is much lower than the confidence interval given by the bootstrapping, indicating that the relatively small number of soils we considered (as in other studies, e.g. Lu et al. (2007)) is a larger source of uncertainty.

Moreover, uncertainties in the f_{clay}, f_{silt}, f_{gravel}, or f_{SOM} fractions may be caused by (1) the natural heterogeneity of soil properties, (2) the living root biomass, (3) stones that may not be accounted for in the gravel fraction.

In particular, during the installation of the probes, it was observed that stones are present at some stations. Stones are not evenly distributed in the soil, and it is not possible to investigate whether the soil area where the temperature probes were inserted contains stones as it must be left undisturbed.

The grasslands considered in this study are not intensively managed. They consist of set-aside fields cut once or twice a year. Calvet et al. (1999) gave an estimate of 0.160 kg m^{-2} for the root dry matter content of such soils for a site in southwestern France, with most roots contained in the 0.25m top soil layer. This represents a gravimetric fraction of organic matter smaller than 0.0005 kg kg^{-1}, i.e. less than 4% of the lowest m_{SOM} values observed in this study (0.013 kg kg^{-1}) or less than 5% of f_{SOM} values. We checked that increasing f_{SOM} values by 5% has negligible impact on heat capacity and on the λ retrievals.

4.2. Can the new λ_{sat} model be applied to other soil types ?

The λ_{sat} values we obtained are consistent with values reported by other authors. In this study, λ_{sat} values ranging between 1.26 $Wm^{-1}K^{-1}$ and 2.80 $Wm^{-1}K^{-1}$ are found (Table 2). Tarnawski et al. (2011) gave λ_{sat} values ranging between 2.5 $Wm^{-1}K^{-1}$ and 3.5 $Wm^{-1}K^{-1}$ for standard sands. Lu et al. (2007) gave λ_{sat} values ranging between 1.33 $Wm^{-1}K^{-1}$ and 2.2 $Wm^{-1}K^{-1}$.

A key component of the λ_{sat} model is the pedotransfer function for quartz (Eq. (12)). The f_q pedotranfer functions we propose are based on available soil characteristics. The current global soil digital maps provide information about SOM, gravels and bulk density (Nachtergaele et al., 2012). Therefore, using Eq. (1) and Eqs. (6)-(12) at large scale is possible, and porosity can be derived from Eq. (1). On the other hand, the suggested f_q pedotranfer functions are obtained for temperate grassland soils containing a rather large amount of organic matter, and are valid for m_{sand}/m_{SOM} ratio values lower than 40 (Table 2). These equations should be evaluated for other regions. In particular, hematite has to be considered together with quartz for tropical soils (Churchman and Lowe, 2012). Moreover, the pedotransfer function we get for θ_{sat} (Eq. (13)) and we use to conduct the sensitivity study of Sect. 3.3, is valid for the specific sites we considered. Eq. (13) cannot be used to predict porosity in other regions.

In order to assess the applicability of the pedotransfer function for quartz obtained in this study, we used the independent data from Lu et al. (2007) and Tarnawski et al. (2009), for ten Chinese soils (see Supplement 4 and Table S4.1). These soils consist of reassembled sieved soil samples and contain no gravel, while our data concern undisturbed soils. Moreover, most of these soils contain very little organic matter and the m_{sand}/m_{SOM} ratio can be much larger that the m_{sand}/m_{SOM} values measured at our grassland sites. For the 14 French soils used to determine pedotransfer functions for quartz, the m_{sand}/m_{SOM} ratio ranges from 3.7 to 37.2 (Table 2). Only three soils of Lu et al. (2007) present such low values of m_{sand}/m_{SOM}. The other seven soils of Lu et al. (2007) present m_{sand}/m_{SOM} values ranging from 48 to 1328 (see Table S4.1).

We used λ_{sat} experimental values derived from Table 3 in Tarnawski et al. (2009) to calculate Q and f_q for the ten Lu et al. (2007) soils. These data are presented in Supplement 4. Figure S4.1 shows the statistical relationship between these quantities and m_{sand}. Very good correlations of Q and f_q with m_{sand} are observed, with r^2 values of 0.72 and 0.83, respectively. This is consistent with our finding that f_q is systematically better correlated to soil characteristics than Q (Sect. 3.2). The pedotransfer functions derived from French soils tend to overestimate f_q for the Lu et al. (2007) soils, especially for the seven soils presenting m_{sand}/m_{SOM} values larger than 40. Note that Lu et al. (2007) obtained a similar result for coarse-textured soils with their model, which assumed $Q = m_{sand}$. For the three other soils, presenting m_{sand}/m_{SOM} values smaller than 40, f_q MAE values are given in Table 4. The best MAE score (0.071 m^3m^{-3}) is obtained for the m_{sand}* predictor of f_q.

These results are illustrated by Fig. 9 for the m_{sand} predictor of f_q. Figure 9 also shows the f_q and λ_{sat} estimates obtained using specific coefficients in Eq. (12), based on the seven Lu et al. (2007) soils presenting m_{sand}/m_{SOM} values larger than 40. These coefficients are given together with the scores in Table 6. Table 6 also present these values for other predictors of f_q. It appears that m_{sand} gives the best scores. The contrasting coefficient values between Table 6 and Table 3 (Chinese and French soils, respectively) illustrate the variability of the coefficients of pedotransfer functions from one soil category to another, and the m_{sand}/m_{SOM} ratio seems to be a good indicator of the validity of a given pedotransfer function.

On the other hand, the m_{sand}/m_{SOM} ratio is not a good predictor of f_q for the Lu et al. (2007) soils presenting m_{sand}/m_{SOM} values larger than 40, and r^2 presents a small value of 0.40 (Table 6). This can be explained by the very large range of m_{sand}/m_{SOM} values for these soils (see Table S4.1). Using $ln(m_{sand}/m_{SOM})$ instead of m_{sand}/m_{SOM} is a way to obtain a predictor linearly correlated to f_q. This is shown by Fig. S4.2 for the ten Lu et al. (2007) soils: the correlation is increased to a large extent ($r^2 = 0.60$).

4.3. Can m_{sand}-based f_q pedotransfer functions be used across soil types ?

Given the results presented in Tables 3, 4, and 6, it can be concluded that m_{sand} is the best predictor of f_q across mineral soil types. The m_{sand}/m_{SOM} predictor is relevant for the mineral soils containing the largest amount of organic matter.

Although the m_{sand}/m_{SOM} predictor gives the best r^2 scores for the 14 grassland soils considered in this study, it seems more difficult to apply this predictor to other soils, as shown by the high MAE score (MAE = 0.135 m^3m^{-3}) for the corresponding Lu et al. (2007) soils in Table 4. Moreover, the scores are very sensitive to errors in the estimation of m_{SOM} as shown by Table 5. Although the m_{sand}* predictor gives slightly better scores than m_{sand} (Table 4), the a_1 coefficient in more sensitive to errors in C_{hmin} (Table 3), and the bootstrapping reveals large uncertainties in a_0 and a_1 values.

The results presented in this study suggest that the m_{sand}/m_{SOM} ratio can be used to differentiate temperate grassland soils containing a rather large amount of organic matter ($3.7 < m_{sand}/m_{SOM} < 40$) from soils containing less organic matter ($m_{sand}/m_{SOM} > 40$). The m_{sand} predictor can be used in both cases to estimate the volumetric fraction of quartz, with the following a_0 and a_1 coefficient values in Eq. (12): 0.15 and 0.572 for m_{sand}/m_{SOM} ranging between 3.7 and 40 (Table 3), and 0.04 and 0.386 for $m_{sand}/m_{SOM} > 40$ (Table 6), respectively.

4.4. Prospects for using soil temperature profiles

Using standard soil moisture and soil temperature observations is a way to investigate soil thermal properties over a large variety of soils, as the access to such data is facilitated by online databases (Dorigo et al., 2013).

A limitation of the data set we used, however, is that soil temperature observations (T_i) are recorded with a resolution of ΔT_i = 0.1 °C only (see Sect. 2.1). This low resolution affects the accuracy of the soil thermal diffusivity estimates. In order to limit the impact of this effect, a data filtering technique is used (see Supplement 5) and D_h is retrieved with a precision of 18 %.

It can be noticed that if T_i data were recorded with a resolution of 0.03 °C (which corresponds to the typical uncertainty of PT100 probes), D_h could be retrieved with a precision of about 5 % in the conditions of Eq. (S5.3). Therefore, one may recommend to revise the current practise of most observation networks consisting in recording soil temperature with a resolution of 0.1 °C only. More precision in the λ estimates would permit investigating other processes of heat transfer in the soil such as those related to water transport (Rutten, 2015).

5. Conclusions

An attempt was made to use routine soil temperature and soil moisture observations of a network of automatic weather stations to retrieve instantaneous values of the soil thermal conductivity at a depth of 0.10 m. The data from the SMOSMANIA network, in southern France, are used. First, the thermal diffusivity is derived from consecutive measurements of the soil temperature. The λ values are then derived from the thermal diffusivity retrievals and from the volumetric heat capacity calculated using measured soil properties. The relationship between the λ estimates and the measured soil moisture at a depth of 0.10 m permits the retrieval of λ_sat for 14 stations. The Lu et al. (2007) empirical λ model is then used to retrieve the quartz volumetric content by reverse modelling. A number of pedotransfer functions is proposed for volumetric fraction of quartz, for the considered region in France. For the grassland soils examined in this study, the ratio of sand to SOM fractions is the best predictor of f_q. A sensitivity study shows that omitting gravels and the SOM information has a major impact on λ_sat. Eventually, an error propagation analysis and a comparison with independent λ_sat data from Lu et al. (2007) show that the gravimetric fraction of sand within soil solids, including gravels and SOM, is a good predictor of the volumetric fraction of quartz when a larger variety of soil types is considered.

Acknowledgements

We thank Dr. Xinhua Xiao (NC State University Soil Physics, Raleigh, USA), Dr. Tusheng Ren (China Agricultural University, Beijing, China), and a third anonymous referee, for their review of the manuscript and for their fruitful comments. We thank Dr. Aaron Boone (CNRM, Toulouse, France) for his helpful comments. We thank our Meteo-France colleagues for their support in collecting and archiving the SMOSMANIA data: Catherine Bienaimé, Marc Bailleul, Laurent Brunier, Anna Chaumont, Jacques Couzinier, Mathieu Créau, Philippe Gillodes, Sandrine Girres, Michel Gouverneur, Maryvonne Kerdoncuff, Matthieu Lacan, Pierre Lantuejoul, Dominique Paulais, Fabienne Simon, Dominique Simonpietri, Marie-Hélène Théron, Marie Yardin.

References

Abu-Hamdeh, N. H., and Reeder, R. C.: Soil thermal conductivity: effects of density, moisture, salt concentration, and organic matter, Soil Sci. Soc. Am. J., 64, 1285–1290, 2000.

Albergel, C., Rüdiger, C., Pellarin, T., Calvet, J.-C., Fritz, N., Froissard, F., Suquia, D., Petitpa, A., Piguet, B., and Martin, E.: From near-surface to root-zone soil moisture using an exponential filter: an assessment of the method based on in-situ observations and model simulations, Hydrol. Earth Syst. Sci., 12, 1323–1337, 2008.

Albergel, C., Calvet, J.-C., de Rosnay, P., Balsamo, G., Wagner, W., Hasenauer, S., Naeimi, V., Martin, E., Bazile, E., Bouyssel, F., and Mahfouf, J.-F.: Cross-evaluation of modelled and remotely sensed surface soil moisture with in situ data in southwestern France, Hydrol. Earth Syst. Sci., 14, 2177–2191, doi:10.5194/hess-14-2177-2010, 2010.

Bristow, K. L., Kluitenberg, G. J., and Horton R.: Measurement of soil thermal properties with a dual-probe heat-pulse technique, Soil Sci. Soc. Am. J., 58, 1288–1294, doi:10.2136/sssaj1994.03615995005800050002x, 1994.

Bristow, K. L.: Measurement of thermal properties and water content of unsaturated sandy soil using dual-probe heat-pulse probes, Agr. Forest Meteorol., 89, 75-84, 1998.

Calvet, J.-C., Bessemoulin, P., Noilhan, J., Berne, C., Braud, I., Courault, D., Fritz, N., Gonzalez-Sosa, E., Goutorbe, J.-P., Haverkamp, R., Jaubert, G., Kergoat, L., Lachaud, G., Laurent, J.-P., Mordelet, P., Olioso, A., Péris, P., Roujean, J.-L., Thony, J.-L., Tosca, C., Vauclin, M., Vignes, D.: MUREX: a land-surface field experiment to study the annual cycle of the energy and water budgets, Ann. Geophys., 17, 838-854, 1999.

Calvet, J.-C., Fritz, N., Froissard, F., Suquia, D., Petitpa,A., and Piguet, B.: In situ soil moisture observations for the CAL/VAL of SMOS: the SMOSMANIA network, International

Geoscience and Remote Sensing Symposium, IGARSS, Barcelona, Spain, 23–28 July 2007, 1196–1199, doi:10.1109/IGARSS.2007.4423019, 2007.

Chen, Y. Y., Yang, K., Tang, W., Qin, J., and Zhao, L.: Parameterizing soil organic carbon's impacts on soil porosity and thermal parameters for Eastern Tibet grasslands, Sci. China Earth Sci., 55 (6), 1001–1011, doi:10.1007/s11430-012-4433-0, 2012.

Churchman, G. J. and Lowe, D. J.: Alteration, formation, and occurrence of minerals in soils, in Huang, P. M., Li, C., Summer, M. E. (eds.), Handbook of soil sciences: properties and processes, Chapter 20, 40-42, isbn:978-1-4398-0306-6, CRC Press, Boca Raton (FL), 2012.

Côté, J. and Konrad, J.-M.: A generalized thermal conductivity model for soils and construction materials, Can. Geotech. J., 42, 443:458, doi:10.1139/T04-106, 2005.

Crank J., and Nicolson, P.: A practical method for numerical evaluation of solutions of partial differential equations of the heat-conduction type, Advances in Computational Mathematics, 6, 207-226, doi:10.1007/BF02127704, 1996.

Decharme, B., Brun, E., Boone, A., Delire, C., Le Moigne, P., and Morin, S.: Impacts of snow and organic soils parameterization on northern Eurasian soil temperature profiles simulated by the ISBA land surface model, The Cryosphere, 10, 853–877, doi:10.5194/tc-10-853-2016, 2016.

de Vries, D. A.: Thermal properties of soils, in W.R. Van Wijk (ed.), Physics of plant environment, pp. 210–235, North-Holland Publ. Co., Amsterdam, 1963.

Dong, Y., McCartney, J. S., and Lu, N.: Critical review of thermal conductivity models for unsaturated soils, Geotech. Geol. Eng., 33,2,207-221, doi:10.1007/s10706-015-9843-2, 2015.

Dorigo, W. A., Wagner, W., Hohensinn, R., Hahn, S., Paulik, C., Xaver, A., Gruber, A., Drusch, M, Mecklenburg, S., van Oevelen, P., Robock, A., and Jackson, T.: The International Soil Moisture Network: a data hosting facility for global in situ soil moisture measurements, Hydrol. Earth Syst. Sci., 15, 1675–1698, doi:10.5194/hess-15-1675-2011, 2011.

Draper, C., Mahfouf, J.-F., Calvet, J.-C., Martin, E., and Wagner, W.: Assimilation of ASCAT near-surface soil moisture into the SIM hydrological model over France, Hydrol. Earth Syst. Sci., 15, 3829–3841, doi:10.5194/hess-15-3829-2011, 2011.

Farouki, O. T.: Thermal properties of soils, Series on Rock and Soil Mechanics, 11, Trans. Tech. Pub., Rockport, MA, USA, 136 pp., 1986.

Johansen, O.: Thermal conductivity of soils. Ph.D. thesis, University of Trondheim, 236 pp., Available from Universitetsbiblioteket i Trondheim, Høgskoleringen 1, 7034 Trondheim, Norway, a translation is available at: http://www.dtic.mil/dtic/tr/fulltext/u2/a044002.pdf (last access January 2016), 1975.

Kersten, M. S.: Thermal properties of soils, University of Minnesota Engineering Experiment Station Bulletin, 28, 227 pp. [Available from University of Minnesota Agricultural Experiment Station, St. Paul, MN 55108], 1949.

Laanaia, N., Carrer, D., Calvet, J.-C., and Pagé, C.: How will climate change affect the vegetation cycle over France? A generic modeling approach, Climate Risk Management, 13, 31-42, doi:10.1016/j.crm.2016.06.001, 2016.

Lawrence, D. M., and Slater, A. G.: Incorporating organic soil into a global climate model, Clim. Dyn., 30, 145-160, doi:10.1007/s00382-007-0278-1, 2008.

Lu, S., Ren, T., Gong, Y., and Horton, R.: An improved model for predicting soil thermal conductivity from water content at room temperature, Soil Sci. Soc. Am. J., 71, 8-14, doi:10.2136/sssaj2006.0041, 2007.

Nachtergaele, F., van Velthuize, H., Verelst, L., Wiberg, D., Batjes, N., Dijkshoorn, K., van Engelen, V., Fischer, G., Jones, A., Montanarella, L., Petri, M., Prieler, S., Teixeira, E., and Shi, X.: Harmonized World Soil Database, Version 1.2, FAO/IIASA/ISRIC/ISS-CAS/JRC, FAO, Rome, Italy and IIASA, Laxenburg, Austria, available at:

http://webarchive.iiasa.ac.at/Research/LUC/External-World-soil-database/HWSD_Documentation.pdf (last access January 2016), 2012.

Parlange, M. B., Cahill, A. T., Nielsen, D. R., Hopmans, J. W., and Wendroth, O.: Review of heat and water movement in field soils, Soil Till. Res., 47, 5-10, 1998.

Parrens, M., Zakharova, E., Lafont, S., Calvet, J.-C., Kerr, Y., Wagner, W., and Wigneron, J.-P.: Comparing soil moisture retrievals from SMOS and ASCAT over France, Hydrol. Earth Syst. Sci., 16, 423–440, doi:10.5194/hess-16-423-2012, 2012.

Peters-Lidard, C.D., Blackburn, E., Liang, X., and Wood, E.F.: The effect of soil thermal conductivity parameterization on surface energy fluxes and temperatures, J. Atmos. Sci., 55, 1209–1224, 1998.

Rutten, M. M.: Moisture in the topsoil: From large-scale observations to small-scale process understanding, PhD Thesis, Delft university of Technology, doi:10.4233/uuid:89e13a16-b456-4692-92f0-7a40ada82451, available at: http://repository.tudelft.nl/view/ir/uuid:89e13a16-b456-4692-92f0-7a40ada82451/ (last access: January 2016), 2015.

Schelde, K., Thomsen, A., Heidmann, T., Schjonning, P., and Jansson, P.-E.: Diurnal fluctuations of water and heat flows in a bare soil, Water Resour. Res., 34, 11, 2919-2929, 1998.

Schönenberger, J., Momose, T., Wagner, B., Leong, W. H., and Tarnawski, V. R.: Canadian field soils I. Mineral composition by XRD/XRF measurements, Int. J. Thermophys., 33, 342–362, doi:10.1007/s10765-011-1142-4, 2012.

Sourbeer, J. J., and Loheide II, S. P.: Obstacles to long-term soil moisture monitoring with heated distributed temperature sensing, Hydrol. Process., 30, 7, 1017-1035, 2015.

Subin, Z. M., Koven, C. D., Riley, W. J., Torn, M. S., Lawrence, D. M., and Swenson, S. C.: Effects of soil moisture on the responses of soil temperatures to climate change in cold regions, J. Clim., doi:10.1175/JCLI-D-12-00305.1, 26, 3139-3158, 2013.

Tarara, J.M., and J.M. Ham: Measuring soil water content in the laboratory and field with dual-probe heat-capacity sensors, Agron. J., 89, 535–542, 1997.

Tarnawski, V. R., McCombie, M. L., Leong, W. H., Wagner, B., Momose, T., and Schönenberger J.: Canadian field soils II. Modeling of quartz occurrence, Int. J. Thermophys., 33, 843–863, doi:10.1007/s10765-012-1184-2, 2012.

Tarnawski, V. R., Momose, T., and Leong, W. H.: Assessing the impact of quartz content on the prediction of soil thermal conductivity, Géotechnique, 59, 4, 331–338, doi: 10.1680/geot.2009.59.4.331, 2009.

Yang, K., Koike, T., Ye, B., and Bastidas, L.: Inverse analysis of the role of soil vertical heterogeneity in controlling surface soil state and energy partition, J. Geophys. Res., 110, D08101, 15 pp., doi:10.1029/2004JD005500, 2005.

Zakharova, E., Calvet, J.-C., Lafont, S., Albergel, C., Wigneron, J.-P., Pardé, M., Kerr, Y., Zribi, M. : Spatial and temporal variability of biophysical variables in southwestern France from airborne L-band radiometry, Hydrol. Earth Syst. Sci., 16, 1725-1743, doi:10.5194/hess-16-1725-2012, 2012.

Zhang, X., Heitman, J., Horton, R., and Ren, T.: Measuring near-surface soil thermal properties with the heat-pulse method: correction of ambient temperature and soil–air interface effects, Soil Sci. Soc. Am. J., 78, 1575–1583, doi:10.2136/sssaj2014.01.0014, 2014.

Table 1 – Soil characteristics at 10 cm for the 21 stations of the SMOSMANIA network. Porosity values are derived from Eq. (1). Solid fraction values higher than 0.3 are in bold. The stations are listed from West to East (from top to bottom). ρ_d, θ_{sat}, f, and m, stand for soil bulk density, porosity, volumetric fractions, and gravimetric fractions, respectively. Soil particle fractions larger than 0.3 are in bold. Station full names are given in Supplement 1 (Table S1.1).

Station	ρ_d (kg m^{-3})	θ_{sat} (m^{3}m^{-3})	f_{sand} (m^{3}m^{-3})	f_{clay} (m^{3}m^{-3})	f_{silt} (m^{3}m^{-3})	f_{gravel} (m^{3}m^{-3})	f_{SOM} (m^{3}m^{-3})	m_{sand} (kg kg^{-1})	m_{clay} (kg kg^{-1})	m_{silt} (kg kg^{-1})	m_{gravel} (kg kg^{-1})	m_{SOM} (kg kg^{-1})
SBR	1680	0.352	**0.576**	0.026	0.013	0.002	0.032	**0.911**	0.041	0.020	0.003	0.024
URG	1365	0.474	0.076	0.078	**0.341**	0.005	0.025	0.149	0.153	**0.665**	0.009	0.024
CRD	1435	0.438	**0.457**	0.027	0.033	0.000	0.045	**0.848**	0.051	0.060	0.000	0.041
PRG	1476	0.431	0.051	0.138	0.138	0.214	0.028	0.092	0.250	0.248	**0.385**	0.025
CDM	1522	0.413	0.073	0.241	0.231	0.012	0.030	0.128	**0.422**	**0.404**	0.020	0.026
LHS	1500	0.416	0.102	0.202	0.189	0.051	0.039	0.181	**0.359**	**0.335**	0.091	0.034
SVN	1453	0.445	0.127	0.073	0.176	0.162	0.017	0.233	0.133	**0.322**	0.296	0.015
MNT	1444	0.447	0.135	0.066	0.230	0.102	0.020	0.248	0.121	**0.424**	0.188	0.018
SFL	1533	0.413	0.127	0.071	0.118	0.250	0.021	0.221	0.123	0.205	**0.434**	0.018
MTM	1540	0.405	0.110	0.081	0.076	0.297	0.032	0.189	0.140	0.131	**0.512**	0.027
LZC	1498	0.429	0.129	0.066	0.068	0.292	0.015	0.229	0.117	0.121	**0.519**	0.013
NBN	1545	0.401	0.063	0.135	0.075	0.290	0.035	0.109	0.232	0.130	**0.499**	0.030
PZN	1311	0.495	0.222	0.074	0.131	0.054	0.023	**0.450**	0.151	0.266	0.111	0.023
PRD	1317	0.494	0.038	0.052	0.069	**0.326**	0.021	0.076	0.105	0.139	**0.659**	0.021
LGC	1496	0.428	0.253	0.044	0.042	0.214	0.019	**0.451**	0.078	0.074	**0.380**	0.017
MZN	1104	0.560	0.212	0.037	0.045	0.097	0.049	**0.510**	0.089	0.109	0.234	0.057
VLV	1274	0.506	0.294	0.054	0.086	0.031	0.029	**0.614**	0.112	0.179	0.064	0.030
BRN	1630	0.379	0.105	0.009	0.016	**0.474**	0.016	0.171	0.015	0.027	**0.774**	0.013
MJN	1276	0.506	0.064	0.029	0.056	**0.317**	0.028	0.133	0.060	0.118	**0.661**	0.029
BRZ	1280	0.508	0.097	0.074	0.109	0.190	0.020	0.202	0.154	0.228	**0.396**	0.021
CBR	1310	0.501	0.120	0.057	0.068	0.241	0.013	0.243	0.116	0.139	**0.489**	0.013

Table 2 – Thermal properties of 14 grassland soils in southern France: λ_{sat}, f_q and Q retrievals using the λ model (Eqs. (7)-(9) and Eq. (10), respectively) for degree of saturation values higher than 0.4, together with the minimized RMSD between the simulated and observed λ values, and the number of used λ observations (n). The soils are sorted from the largest to the smallest ratio of m_{sand} to m_{SOM}. Station full names are given in Supplement 1 (Table S1.1).

Station	λ_{sat} ($Wm^{-1}K^{-1}$)	RMSD ($Wm^{-1}K^{-1}$)	n	f_q (m^3m^{-3})	Q (kg kg^{-1})	$\frac{m_{sand}}{m_{SOM}}$
SBR	2.80	0.255	6	0.62	0.96	37.2
LGC	2.07	0.311	20	0.44	0.77	26.6
CBR	1.92	0.156	20	0.44	0.88	18.4
LZC	1.71	0.107	20	0.29	0.51	17.3
SVN	1.78	0.163	20	0.34	0.61	15.4
MNT	1.96	0.058	20	0.42	0.76	13.8
BRN	1.71	0.131	20	0.25	0.40	13.5
SFL	1.57	0.134	20	0.22	0.37	12.5
MTM	1.52	0.095	20	0.21	0.35	7.0
URG	1.37	0.066	20	0.05	0.10	6.2
LHS	1.57	0.136	20	0.26	0.45	5.3
CDM	1.82	0.086	20	0.26	0.44	5.0
PRG	1.65	0.086	20	0.18	0.32	3.7
PRD	1.26	0.176	20	0.14	0.28	3.7

Table 3 – Coefficients of four pedotransfer functions of f_q (Eq. 12) for 14 soils of this study (all with $m_{sand}/m_{SOM} < 40$), together with indicators of the coefficient uncertainty, derived by bootstrapping and by perturbing the volumetric heat capacity of soil minerals (C_{hmin}). The best predictor is in bold.

Predictor of f_q	Coefficients for 14 soils		Confidence interval from bootstrapping		Impact of a change of $\pm 0.08\times10^6$ J m^{-3} K^{-1} in C_{hmin}	
	a_0	a_1	a_0	a_1	a_0	a_1
$\boldsymbol{m_{sand} / m_{SOM}}$	0.12	0.0134	[0.10,0.14]	[0.012,0.014]	[0.11,0.13]	[0.013,0.013]
m_{sand}*	0.08	0.944	[0.00,0.11]	[0.85,1.40]	[0.07,0.09]	[0.919,0.966]
m_{sand}	0.15	0.572	[0.08,0.17]	[0.54,0.94]	[0.14,0.17]	[0.55,0.56]
$1- \theta_{sat} - f_{sand}$	0.73	–1.020	[0.71,0.89]	[–1.38, –0.99]	[0.70,0.73]	[–1.00, –0.99]

(*) only m_{sand} values smaller than 0.6 kg kg^{-1} are used in the regression

Table 4 – Scores of four pedotransfer functions of f_q for 14 soils of this study, together with the scores obtained by bootstrapping, without the sandy SBR soil. The MAE score of these pedotransfer functions for three Chinese soils of Lu et al. (2007) for which $m_{sand}/m_{SOM} < 40$ is given (within brackets). The best predictor and the best scores are in bold.

Predictor of f_q	Regression scores			Bootstrap scores			Scores without SBR (and MAE for 3 Lu soils)		
	r^2	RMSD (m^3m^{-3})	MAE (m^3m^{-3})	r^2	RMSD (m^3m^{-3})	MAE (m^3m^{-3})	r^2	RMSD (m^3m^{-3})	MAE (m^3m^{-3})
$\boldsymbol{m_{sand} / m_{SOM}}$	**0.77**	**0.067**	0.053	**0.72**	**0.074**	**0.059**	**0.62**	**0.070**	0.057 (*0.135*)
m_{sand}*	0.74	0.072	**0.052**	0.67	0.126	0.100	0.56	0.075	**0.056** (***0.071***)
m_{sand}	0.67	0.081	0.060	0.56	0.121	0.084	0.56	0.075	**0.056** (*0.086*)
$1-\theta_{sat}-f_{sand}$	0.65	0.084	0.064	0.56	0.102	0.079	0.45	0.084	0.061 (*0.158*)

(*) only m_{sand} values smaller than 0.6 kg kg^{-1} are used in the regression

Table 5 – Ability of the Eqs. (10)-(13) empirical model to estimate λ_{sat} values for 14 soils and impact of changes in gravel and SOM volumetric content: f_{gravel} = 0 m^3m^{-3} and f_{SOM} = 0.013 m^3m^{-3} (the smallest f_{SOM} value, observed for CBR). r^2 values smaller than 0.60, RMSD values higher than 0.20 $Wm^{-1}K^{-1}$, and mean bias values higher (smaller) than +0.10 (–0.10) are in bold.

Model configuration	Predictor of f_q	r^2	RMSD ($Wm^{-1}K^{-1}$)	Mean bias ($Wm^{-1}K^{-1}$)
Model using θ_{sat} observations	m_{sand} / m_{SOM}	0.86	0.14	+0.01
	m_{sand}*	0.83	0.15	–0.01
	m_{sand}	0.81	0.16	–0.03
	$1 - \theta_{sat} - f_{sand}$	0.82	0.16	–0.03
Full model using θ_{satMOD} (Eqs. (13))	m_{sand} / m_{SOM}	0.85	0.14	+0.03
	m_{sand}*	0.85	0.14	–0.03
	m_{sand}	0.84	0.15	–0.03
	$1 - \theta_{sat} - f_{sand}$	0.82	0.16	–0.02
same with: f_{SOM} = 0.013 m^3m^{-3}	m_{sand} / m_{SOM}	**0.57**	**0.35**	**+0.20**
	m_{sand}*	0.83	0.15	+0.00
	m_{sand}	0.81	0.16	–0.02
	$1 - \theta_{sat} - f_{sand}$	0.83	0.15	–0.02
same with: f_{gravel} = 0 m^3m^{-3}	m_{sand} / m_{SOM}	0.87	0.19	**–0.12**
	m_{sand}*	0.70	**0.23**	**+0.11**
	m_{sand}	0.79	0.17	+0.04
	$1 - \theta_{sat} - f_{sand}$	0.81	0.17	+0.05
same with: f_{SOM} = 0.013 m^3m^{-3} and f_{gravel} = 0 m^3m^{-3}	m_{sand} / m_{SOM}	0.63	**0.31**	**+0.16**
	m_{sand}*	**0.52**	**0.36**	**+0.24**
	m_{sand}	**0.59**	**0.29**	**+0.16**
	$1 - \theta_{sat} - f_{sand}$	0.70	**0.25**	**+0.16**

(*) only m_{sand} values smaller than 0.6 kg kg^{-1} are used in the regression

Table 6 – Pedotransfer functions of f_q (Eq. 12) for 7 soils of Lu et al. (2007) with m_{sand}/m_{SOM} > 40. The best predictor and the best scores are in bold. The regression p-values are within brackets.

Predictor of f_q	Regression scores for 7 Lu soils with $m_{sand}/m_{SOM} > 40$			Coefficients	
	r^2 (*p-value*)	RMSD (m^3m^{-3})	MAE (m^3m^{-3})	a_0	a_1
m_{sand} / m_{SOM}	0.40 (*0.13*)	0.089	0.075	0.20	0.000148
m_{sand}*	0.82 (*0.005*)	0.073	0.054	0.07	0.425
$\boldsymbol{m_{sand}}$	**0.82 (*0.005*)**	**0.048**	**0.042**	0.04	0.386
$1 - \theta_{sat} - f_{sand}$	0.81 (*0.006*)	0.050	0.043	0.44	–0.814

(*) only m_{sand} values smaller than 0.6 kg kg^{-1} are used in the regression

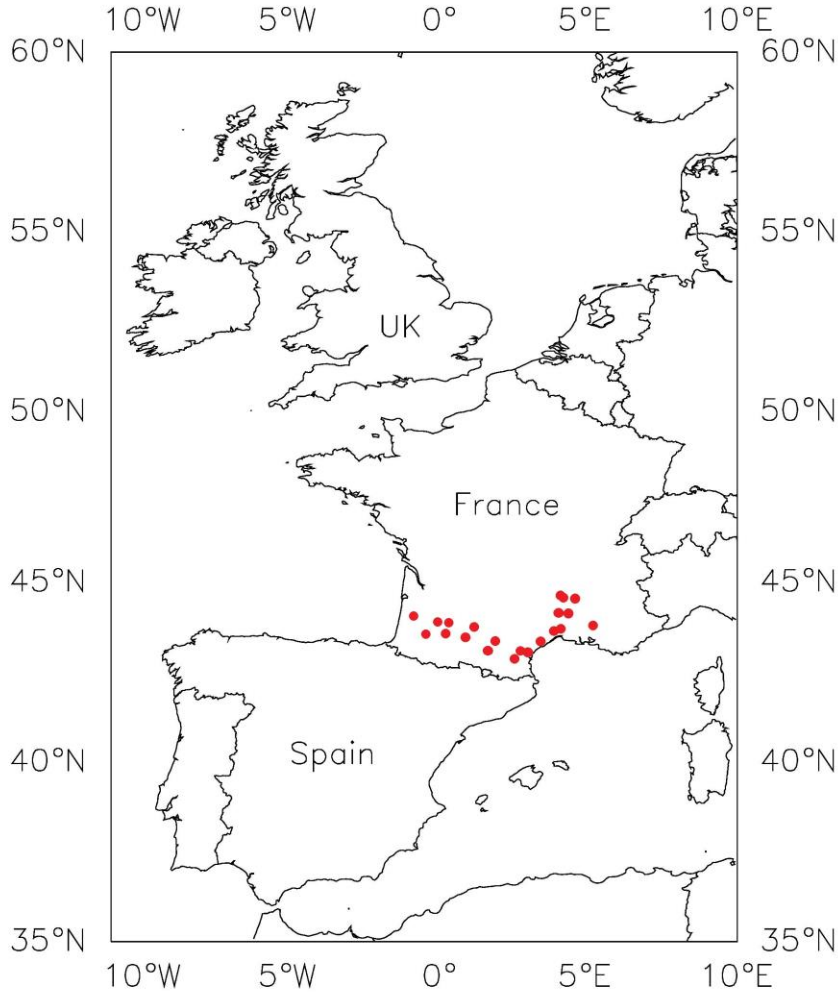

Fig. 1 – Location of the 21 SMOSMANIA stations in southern France (see station names in Supplement 1).

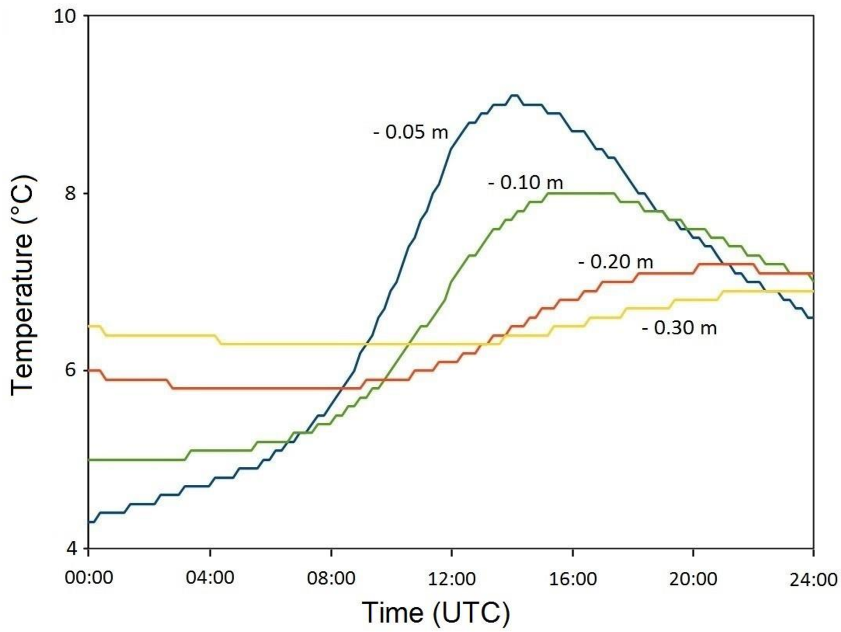

Fig. 2 – Soil temperature measured in wet conditions at the Saint-Félix-de-Lauragais (SFL) station on 23 February 2015, at depths of 0.05, 0.10, 0.20, and 0.30 m. Levelling is due to the low resolution of the temperature records (0.1°C).

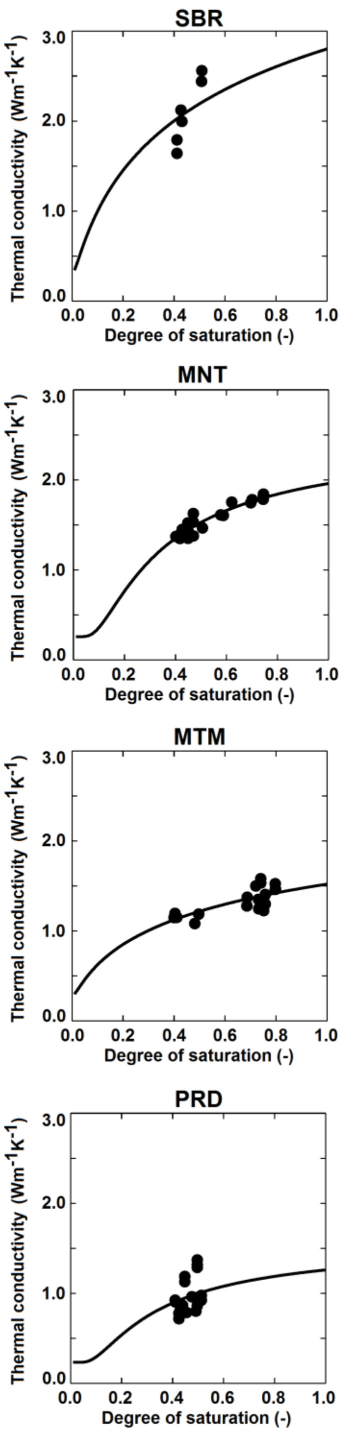

Fig. 3 – Retrieved λ values (dark dots) vs. the observed degree of saturation of the soil, at a depth of 0.10 m, for (from top to bottom) Sabres (SBR), Montaut (MNT), Mouthoumet (MTM), and Prades-le-Lez (PRD), together with simulated λ values from dry to wet conditions (dark lines).

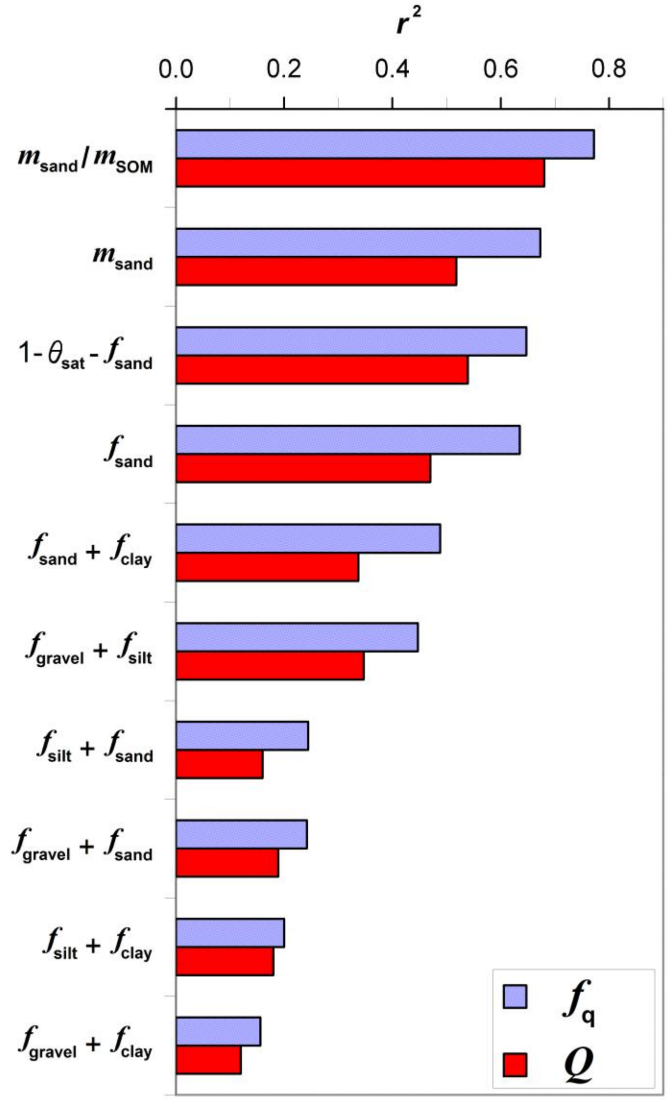

Fig. 4 – Fraction of variance (r^2) of gravimetric and volumetric fraction of quartz (Q and f_q, red and blue bars, respectively) explained by various predictors.

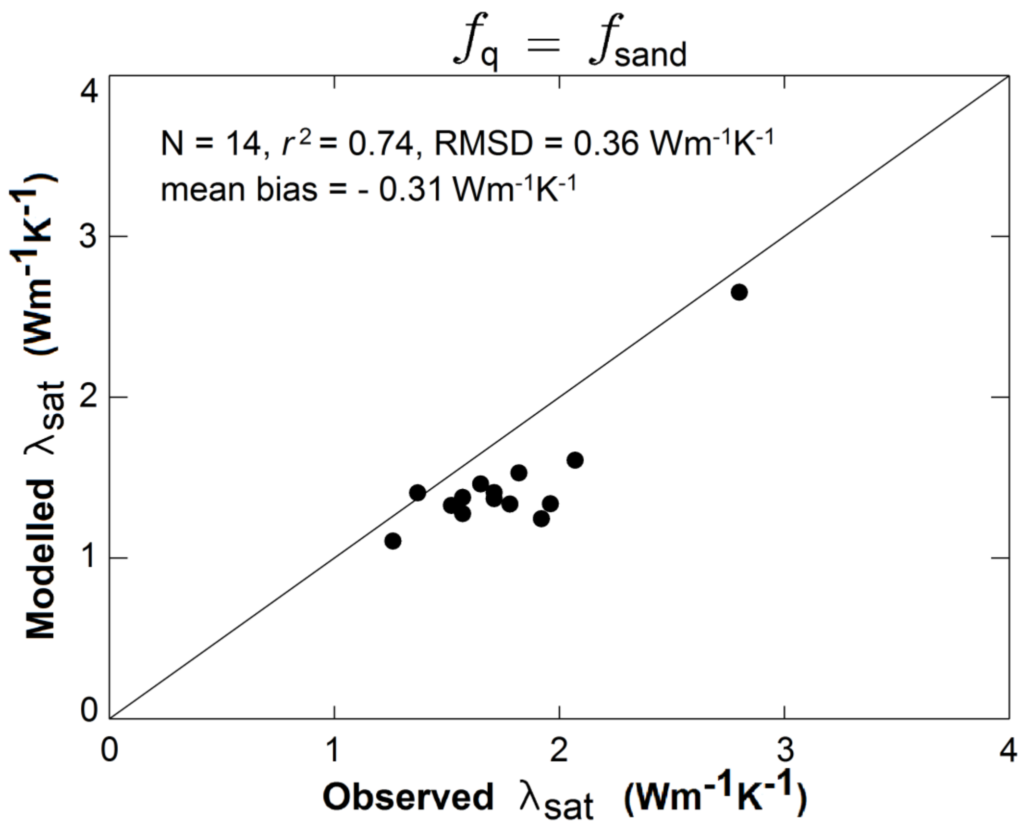

Fig. 5 – λ_{satMOD} values derived from volumetric quartz fractions f_q assumed equal to f_{sand}, using observed θ_{sat} values, vs. λ_{sat} retrievals.

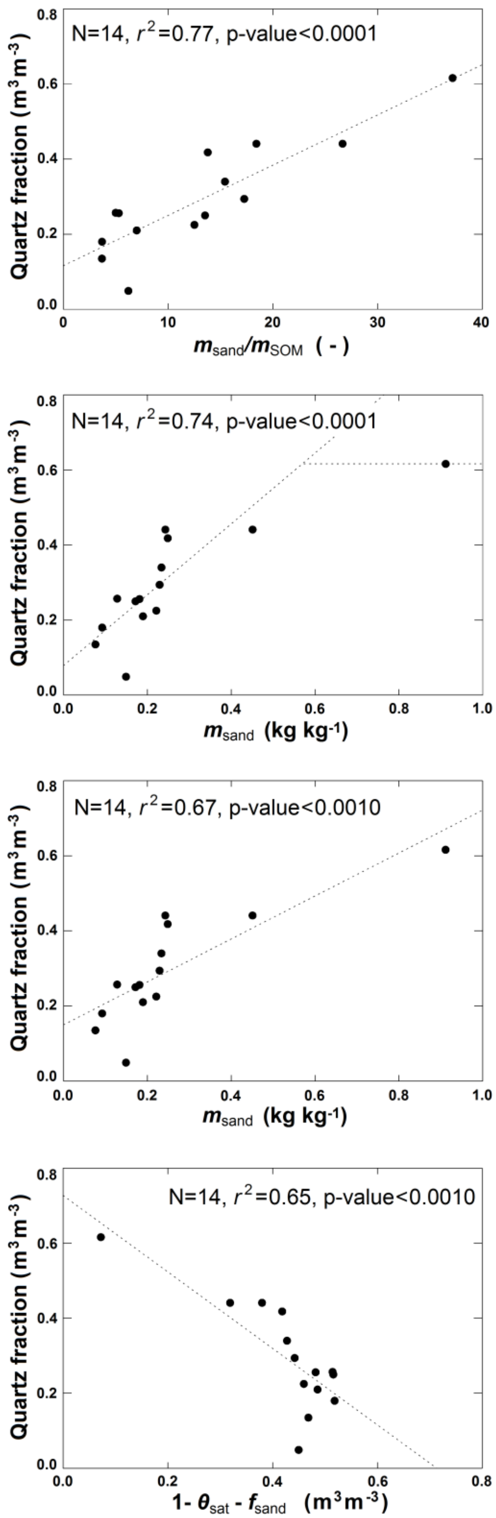

Fig. 6 – Pedotransfer functions for quartz: f_q retrievals (dark dots) vs. the four predictors of f_q given in Table 3. The modelled f_q values are represented by the dashed lines.

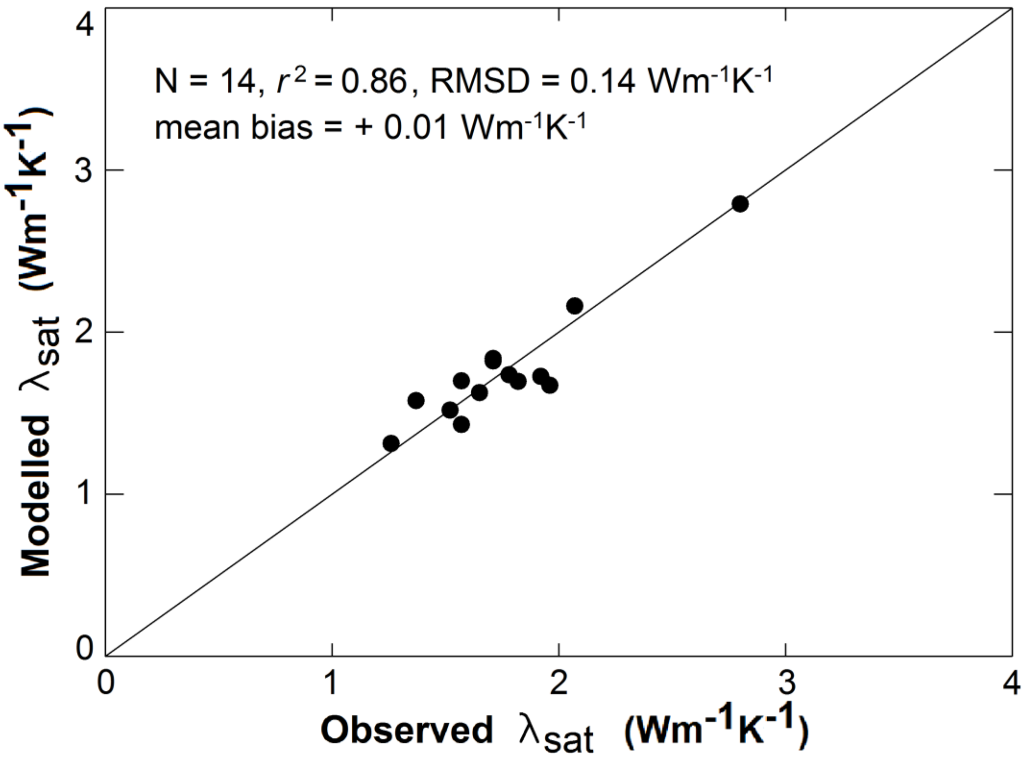

Fig. 7 – λ_{satMOD} values derived from the m_{sand} / m_{SOM} pedotransfer function for the volumetric quartz fractions, using observed θ_{sat} values, vs. λ_{sat} retrievals.

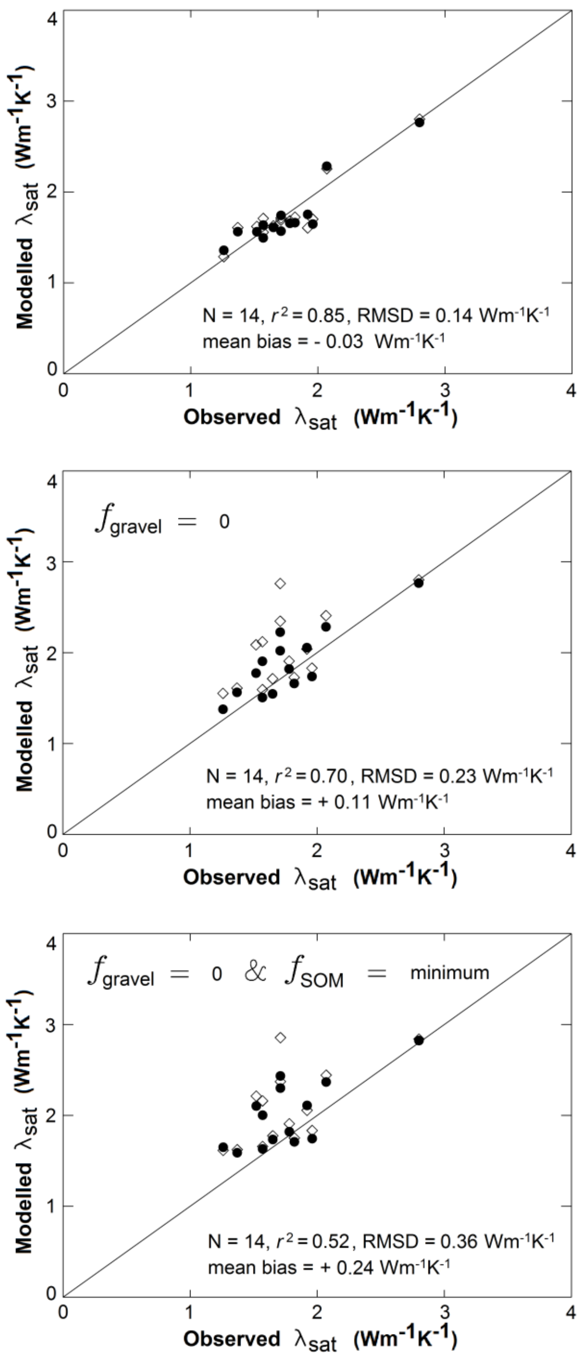

Fig. 8 – λ_{satMOD} values derived from the m_{sand}* pedotransfer function for the volumetric quartz fractions, using θ_{satMOD} (Eqs. (13)) or the observed θ_{sat} (dark dots and opened diamonds, respectively), vs. λ_{sat} retrievals: (top) full model, (middle) f_{SOM} = 0.013 m^3m^{-3}, (bottom) f_{SOM} = 0.013 m^3m^{-3} and f_{gravel} = 0 m^3m^{-3}. Scores are given for the θ_{satMOD} configuration.

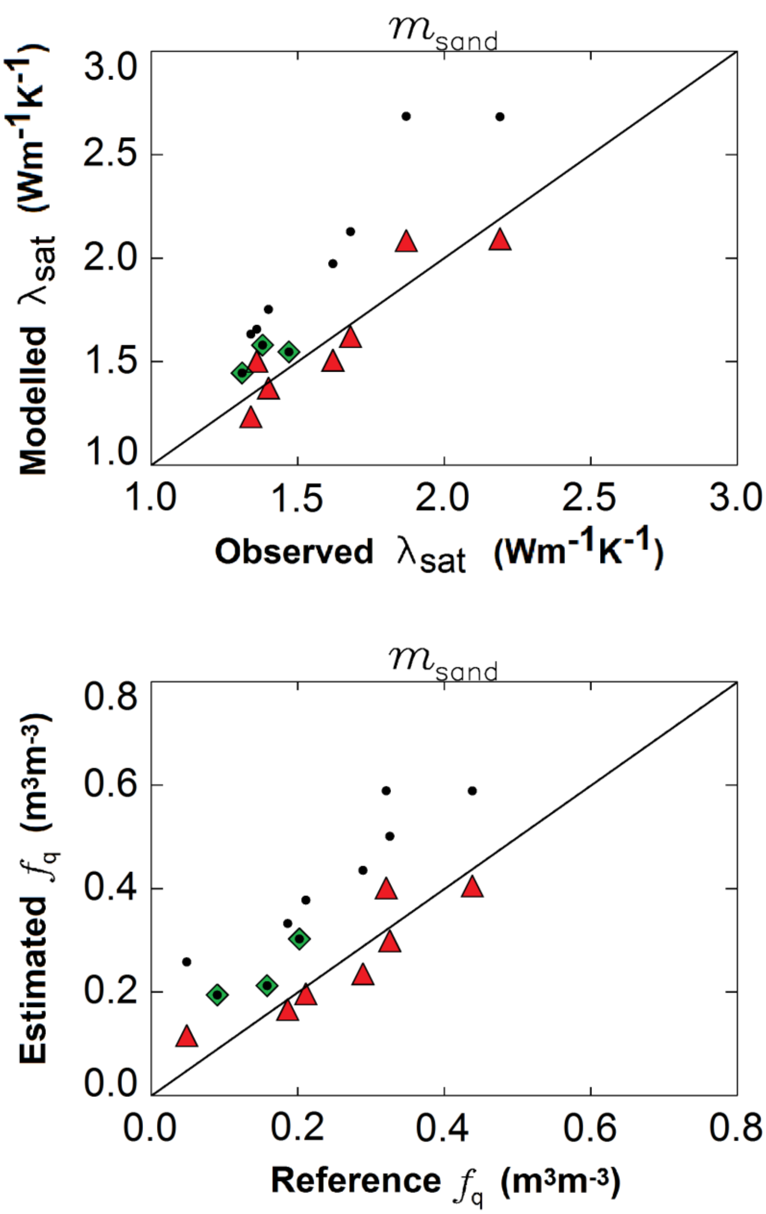

Fig. 9 – Estimated λ_{sat} and volumetric fraction of quartz f_q (top and bottom, respectively) vs. values derived from the λ_{sat} observations of Lu et al. (2007) given by Tarnawski et al. (2009) for 10 Chinese soils, using the gravimetric fraction of sand m_{sand} as a predictor of f_q. Dark dots correspond to the estimations obtained using the m_{sand} pedotransfer function for southern France and the three soils for which $m_{sand}/m_{SOM} < 40$ are indicated by green diamonds. Red triangles correspond to the estimations obtained using the m_{sand} pedotransfer function for the seven soils for which $m_{sand}/m_{SOM} > 40$ (see Table 6).

Supplement # 1

Soil characteristics of the 21 SMOSMANIA stations

Table S1.1 – Soil characteristics at –0.10 m for the 21 stations of the SMOSMANIA network: difference in dry density between soil layers at –0.05 m and –0.10 m ($\Delta\rho_d$), gravimetric fraction of mineral fine earth (*Mn*) of sand, clay, and silt, gravimetric fraction of fine earth (*M*) of soil organic matter (SOM), gravimetric fraction of gravel (m_{gravel}), C/N ratio, and total nitrogen (N_T). The stations are listed from West to East (from top to bottom).

Station (full name)	$\Delta\rho_d$ (kg m^{-3})	Mn_{sand} (%)	Mn_{clay} (%)	Mn_{silt} (%)	M_{SOM} (%)	m_{gravel} (%)	*C/N* (-)	N_T (g kg^{-1})
SBR (Sabres)	–220	93.7	4.2	2.1	2.46	0.27	21.4	0.67
URG (Urgons)	0	15.4	15.8	68.8	2.42	0.93	10.5	1.33
CRD (Créon d'Armagnac)	–130	88.4	5.3	6.3	4.08	0.00	16.0	1.48
PRG (Peyrusse Grande)	–191	15.6	42.3	42.1	4.05	38.51	12.0	1.96
CDM (Condom)	–103	13.4	44.2	42.4	2.61	2.04	11.3	1.34
LHS (Lahas)	18	20.7	41.0	38.3	3.76	9.11	11.5	1.89
SVN (Savenès)	–28	33.9	19.3	46.8	2.15	29.62	11.9	1.04
MNT (Montaut)	–39	31.3	15.3	53.4	2.22	18.81	12.0	1.07
SFL (Saint-Félix-de-Lauragais)	42	40.3	22.4	37.3	3.12	43.36	11.1	1.62
MTM (Mouthoumet)	–102	41.1	30.5	28.4	5.54	51.23	11.0	2.90
LZC (Lézignan- Corbières)	–115	49.0	25.1	25.9	2.76	51.93	10.5	1.53
NBN (Narbonne)	–285	23.2	49.2	27.6	5.97	49.92	12.0	2.89
PZN (Pézenas)	–73	51.9	17.4	39.7	2.56	11.06	13.1	1.13
PRD (Prades-le-Lez)	41	23.7	32.8	43.5	6.04	65.90	13.0	2.69
LGC (La-Grand-Combe)	40	74.8	12.9	12.3	2.73	38.04	22.5	0.70
MZN (Mazan-L'Abbaye)	–143	72.0	12.6	15.4	7.47	23.42	12.2	3.54
VLV (Villevieille)	–158	67.8	12.4	19.8	3.20	6.41	12.2	1.52
BRN (Barnas)	–203	80.4	7.1	12.5	5.61	77.40	16.8	1.93
MJN (Méjannes-le-Clap)	0	42.8	19.3	37.9	8.46	66.11	15.0	3.25
BRZ (Berzème)	–186	34.6	26.4	39.0	3.41	39.59	11.8	1.67
CBR (Cabrières-D'Avignon)	–10	48.8	23.3	27.9	2.58	48.94	10.5	1.42

The gravimetric fractions of sand, clay, and silt (denoted by *x*) are calculated as:

$$m_x = Mn_x \times (1 - M_{SOM}) \times (1 - m_{gravel}) \quad \text{(S1.1)}$$

The gravimetric fraction of SOM is calculated as:

$$m_{SOM} = M_{SOM} \times (1 - m_{gravel}) \quad \text{(S1.2)}$$

Figure S1.1 presents the Mn_x values at –0.10 m together with values at –0.05 m and –0.20 m, and shows that soil texture does not vary much with depth at a given station.

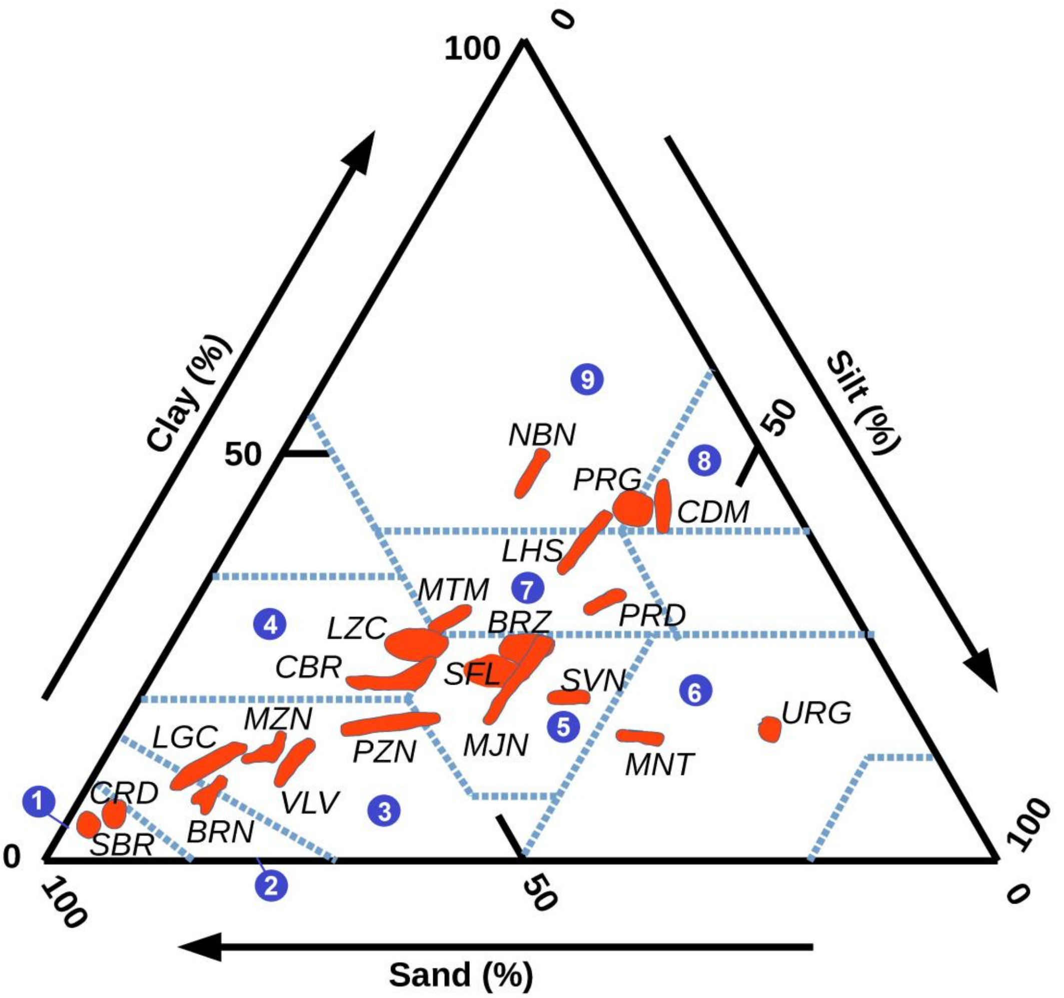

Figure S1.1 – Soil characteristics of the 21 SMOSMANIA stations: mineral fine earth gravimetric fractions of clay, silt and sand. For a given soil, the red mark covers the fraction values measured at 0.05, 0.10 and 0.20 m. Full station names are given in Table S1.1. The dashed blue lines correspond to the USDA textural soil classes:
(1) sand, (2) loamy sand, (3) sandy loam, (4) sandy clay loam, (5) loam, (6) silt loam, (7) clay loam, (8) silty clay, (9) clay.

Table S1.1 shows that some soils present a very high gravimetric fraction of gravels (up to 77 % for BRN). However, we had no difficulty in measuring soil temperature and soil moisture, including at the BRN site, as shown by Fig. S1.2. Note that the sensors we use are designed to work in such difficult conditions. The ThetaProbe and PT100 sensors have very strong rods, 0.06 m and 0.10 m long, respectively.

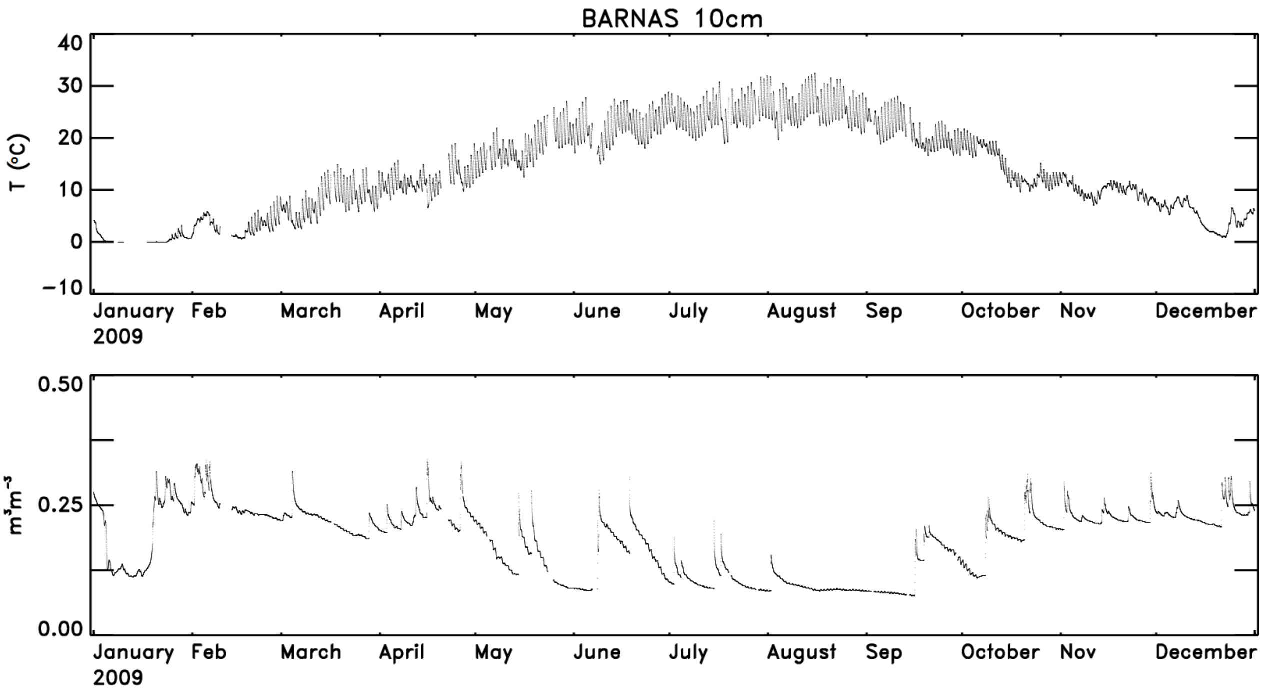

Figure S1.2 - Soil temperature (top) and volumetric soil moisture (bottom) measured in 2009 at the Barnas station (BRN) at a depth of –0.10 m.

The ThetaProbe sensors provide a voltage signal S_V in units of V. In order to convert the voltage signal into volumetric soil moisture content θ (m^3m^{-3}), soil-specific logistic calibration curves were developed using in situ gravimetric soil samples for all stations, and for all depths (z):

$$\theta(z) = K / \left\{ 1 + a(z) e^{-R(z) \times S_V(z)} \right\} \qquad \text{(S1.3)}$$

Values of K, a(z), and R(z) coefficients are given in Table S1.2.

Table S1.2 – Soil-specific coefficients of a logistic calibration curve (Eq. S1.3) for the 21 stations of the SMOSMANIA network. The stations are listed from West to East (from top to bottom).

Station	*K* (m^3m^{-3})	*R*@-5cm (V^{-1})	*R*@-10cm (V^{-1})	*R*@-20cm (V^{-1})	*R*@-30cm (V^{-1})	*a*@-5cm (–)	*a*@-10cm (–)	*a*@-20cm (–)	*a*@-30cm (–)
SBR	0.35	6.546	5.009	6.752	3.052	17.89	15.66	33.02	7.11
URG	0.60	4.558	3.932	4.597	4.234	19.99	19.16	38.44	31.00
CRD	0.44	6.065	3.930	4.620	4.079	13.57	13.36	17.62	18.19
PRG	0.60	3.773	4.530	5.270	4.511	19.89	35.91	70.25	35.52
CDM	0.60	4.198	3.968	8.511	9.628	24.73	18.97	959.10	2713.51
LHS	0.60	4.719	3.766	4.539	7.336	27.61	19.65	35.73	558.92
SVN	0.60	3.627	2.569	2.882	3.019	14.86	11.03	13.53	18.01
MNT	0.60	3.869	3.098	3.605	2.877	11.60	11.02	20.43	12.30
SFL	0.60	3.442	2.926	4.022	4.459	18.54	9.38	24.51	31.41
MTM	0.60	2.377	3.130	2.264	2.888	8.26	10.62	6.01	13.34
LZC	0.60	4.596	4.241	5.030	2.405	35.23	37.83	53.09	19.32
NBN	0.60	3.426	3.702	5.043	7.333	12.58	12.78	37.26	226.11
PZN	0.60	4.410	6.400	3.950	4.758	25.08	58.50	25.89	37.04
PRD	0.60	4.299	4.573	4.449	4.649	26.23	37.11	40.61	47.99
LGC	0.43	5.037	4.723	5.676	7.163	20.37	15.77	38.59	134.96
MZN	0.60	4.770	5.726	4.326	5.394	32.30	72.97	24.58	66.15
VLV	0.60	3.879	3.600	5.236	4.887	23.38	17.06	58.85	48.91
BRN	0.38	7.104	5.585	4.002	6.473	13.89	11.99	9.84	17.12
MJN	0.60	4.547	3.496	3.697	4.136	18.50	14.64	15.94	21.71
BRZ	0.60	3.747	3.355	2.678	3.191	14.38	12.24	11.25	13.65
CBR	0.60	6.239	4.600	3.550	3.598	151.11	26.08	24.48	24.68

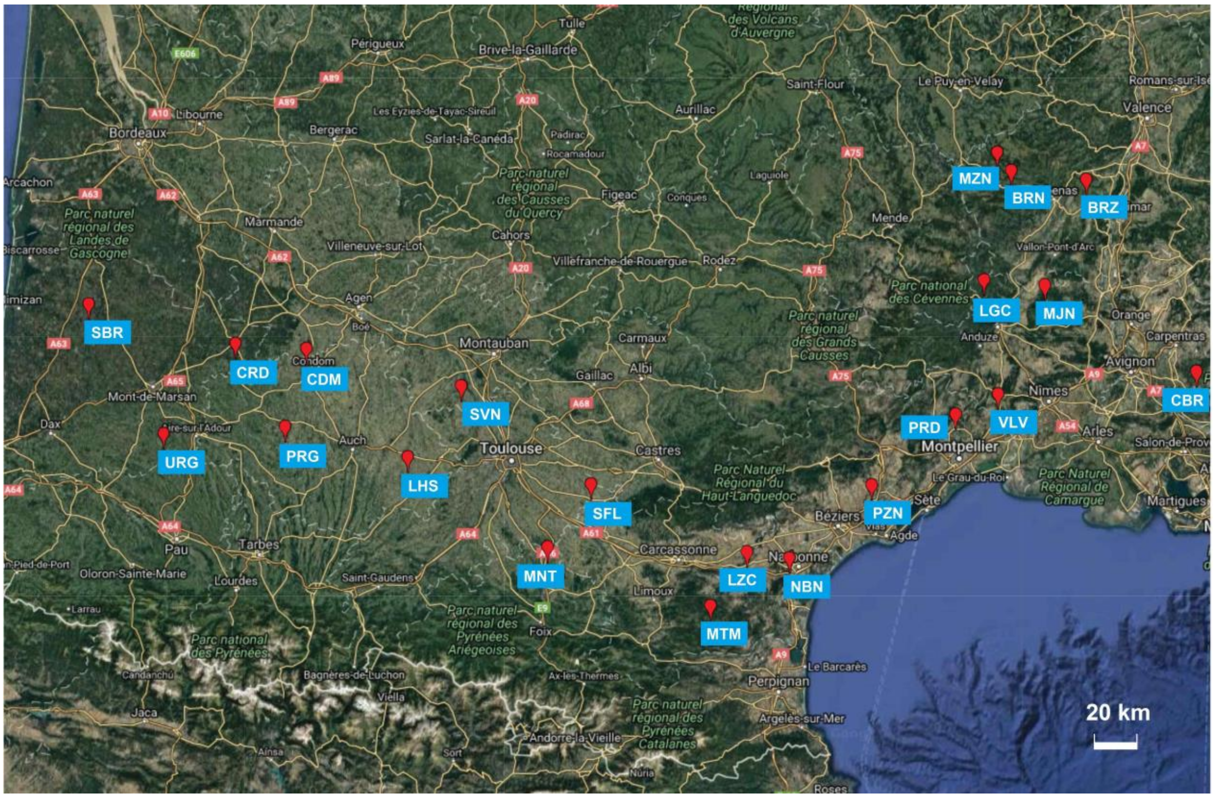

Figure S1.3 - Location of the 21 SMOSMANIA stations in southern France (see station names in Table S1.1). Background geographic information is from Google Maps.

The SMOSMANIA network forms an Atlantic-Mediterranean transect. SBR and CRD are located in agricultural spots in the Les Landes pine forest area, on sandy soils. URG, PRG, CDM, LHS, SVN, MNT and SFL are in the Garonne plain, characterized by croplands and grasslands over undulating terrain. CDM and PRG are on silty clay soil and URG and MNT on silt loams. LZC, NBN, PZN, PRD, VLV, and CBR are in the Mediterranean plain on croplands or mosaics of crops, vineyards, and orchards. Other stations in the Mediterranean area are located in the Corbières, and Cévennes mountainous areas (at altitudes higher than 450 m above sea level) covered by forests or shrubs: MTM, LGC, MZN, BRN, BRZ. MJN is located in a shrub area. The Mediterranean part of the transect is characterized by loamy sands (BRN and LGC), sandy loams (MZN, VLV, PZN), and sandy clay loams (LZC, CBR).

Figure S1.4 - Automatic weather station of Montaut (MNT).

Figure S1.5 - Installation of the probes at Sabres (SBR).

Figure S1.6 - Installation of the probes at Montaut (MNT).

Figure S1.7 - Installation of the probes at Barnas (BRN).

Figure S1.8 - Installation of the probes at Mouthoumet (MTM).

Figure S1.9 - Installation of the probes at Prades-le-Lez (PRD).

Figure S1.10 - Soil sample collection at Prades-le-Lez (PRD).

Supplement # 2

Data filtering technique to limit the impact of soil heterogeneities

The impact of vertical heterogeneities in λ values has to be accounted for in the λ retrieval technique. In order to address this issue, a data analysis procedure aiming at limiting this effect as much as possible was implemented. We used only the soil temperature data presenting a relatively low vertical gradient close to the soil surface, where most differences with deeper layers are found. It must be noted that if this data sorting is omitted, the retrieved λ_{sat} values are lower for all the stations. The procedure is described below.

The 1D Fourier equation in heterogeneous soil conditions can be written as:

$$C_h \frac{\partial T}{\partial t} = \frac{\partial}{\partial z}\left(\lambda \frac{\partial T}{\partial z} \right) \tag{S2.1}$$

and discretized as:

$$\frac{T_i^n - T_i^{n-1}}{\Delta t} = \frac{1}{C_{hi}} \left[\frac{1}{2} \left(\frac{\lambda_{i+1/2} \gamma_{i+1}^n - \lambda_{i-1/2} \gamma_i^n}{\Delta z_m} \right) + \frac{1}{2} \left(\frac{\lambda_{i+1/2} \gamma_{i+1}^{n-1} - \lambda_{i-1/2} \gamma_i^{n-1}}{\Delta z_m} \right) \right] \tag{S2.2}$$

In this study, we assumed that the retrieved λ values, at a depth of –0.10 m, were representative of a bulk soil layer including the three soil temperature probes used to retrieve the thermal diffusivity, and did not differ much from the interfacial λ values along the bottom and top edges of the considered soil layer ($\lambda_{i+1/2}$ and $\lambda_{i-1/2}$, respectively):

$$\lambda \approx \lambda_{i+1/2} \approx \lambda_{i-1/2} \tag{S2.3}$$

and, at a given time *n*,

$$\lambda \gamma_{i+1}^n - \lambda \gamma_i^n \approx \lambda_{i+1/2} \gamma_{i+1}^n - \lambda_{i-1/2} \gamma_i^n \qquad \text{(S2.4).}$$

In reality, differences may occur:

$$\Delta \lambda = \lambda_{i+1/2} - \lambda_{i-1/2} \qquad \text{(S2.5).}$$

Considering the temperature gradient ratio R_{TG} at a given time *n*:

$$R_{TG} = \frac{\gamma_i^n}{\gamma_i^n - \gamma_{i+1}^n} \qquad \text{(S2.6)}$$

and combining Eqs. (S2.4), (S2.5) and (S2.6), the retrieved λ can be written as:

$$\lambda \approx \lambda_{i+1/2} - R_{TG}\ \Delta\lambda \qquad \text{(S2.7).}$$

Since soil temperature gradients were more pronounced close to the soil surface and since, more often than not, soil density presented smaller values close to the soil surface, the $\Delta\lambda$, R_{TG}, and $R_{TG}\Delta\lambda$ values were ≥ 0. Since in the soils considered in this study, differences in soil density were much less pronounced at depth than between the –0.05m and –0.10m soil layers, we considered that $\lambda_{i+1/2}$ was closer to the final value to be retrieved, λ^*, than the initial λ retrieval:

$$\lambda^* \approx \lambda + R_{TG}\ \Delta\lambda \qquad \text{(S2.8).}$$

Eq. (S2.8) shows that the target λ^* value is larger than the initial λ retrieval. The relative error on λ^* can be written as $R_{TG}\Delta\lambda/\lambda^*$ (dimensionless). We used $R_{TG}\Delta\lambda/\lambda^*$ as an indicator of the quality of the λ retrieval, with large values of $R_{TG}\Delta\lambda/\lambda^*$ corresponding to erroneous estimates. In the revised data analysis procedure. The λ retrieval corresponding to high $R_{TG}\Delta\lambda/\lambda^*$ values were excluded from the analysis. The following condition was used:

$$R_{TG}\Delta\lambda/\lambda^* < 10\% \qquad \text{(S2.9).}$$

Finally, a subset of 20 λ retrievals per station was used, at most, corresponding to the lowest $R_{TG}\Delta\lambda/\lambda^*$ values.

The NBN, PZN, BRZ, and MJN observations were completely filtered out as they presented $R_{TG}\Delta\lambda/\lambda^*$ values systematically higher than 10%. The impact of the refined data selection is illustrated in Fig. S2.1 for the MNT and LHS soils.

In practise, the $\Delta\lambda$ term was estimated using the $\Delta\rho_d$ values of Table S1.1 and the sensitivity of λ to changes in dry density, $\Delta\lambda/\Delta\rho_d$. The latter was derived numerically using the Eqs. (7)-(13) model, in soil wetness conditions ranging from S_d = 0.4 to S_d = 1.

Since the derivation of $\Delta\lambda/\Delta\rho_d$ depends on the obtained f_q pedotransfer function, $\Delta\lambda/\Delta\rho_d$ values were recalculated with the new pedotransfer function, and a few iterations permitted refining these estimates.

At saturation (S_d = 1) $\Delta\lambda/\Delta\rho_d$ ranged between 0.64×10^{-3} $Wm^2K^{-1}kg^{-1}$ for PRD to 1.24×10^{-3} $Wm^2K^{-1}kg^{-1}$ for SBR.

At S_d = 0.4, $\Delta\lambda/\Delta\rho_d$ ranged between 0.46×10^{-3} $Wm^2K^{-1}kg^{-1}$ for PRD to 0.81×10^{-3} $Wm^2K^{-1}kg^{-1}$ for SBR.

R_{TG} ranged between 0.5 and 2.4, with a median value of 1.3.

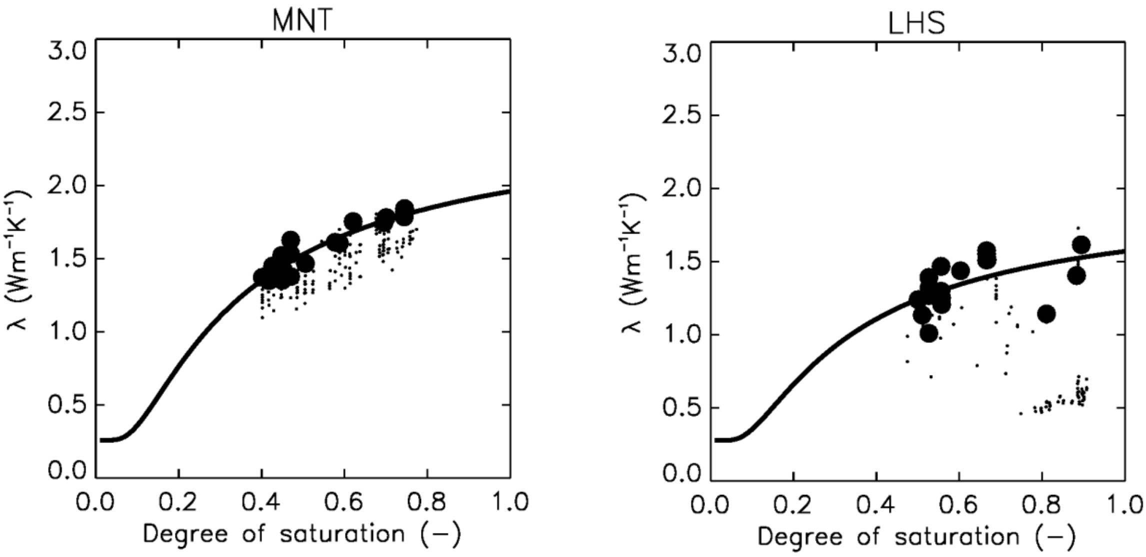

Figure S2.1 - Retrieved and modelled λ values (dots and solid line, respectively) vs. the observed degree of saturation of the soil, at a depth of 0.10 m for the MNT and LHS stations. The 20 λ retrievals used to fit the thermal conductivity model and retrieve λ_{sat} are represented by large dots.

Supplement # 3

Impact of soil volumetric heat capacity of soil solids on the retrieved λ_{sat}

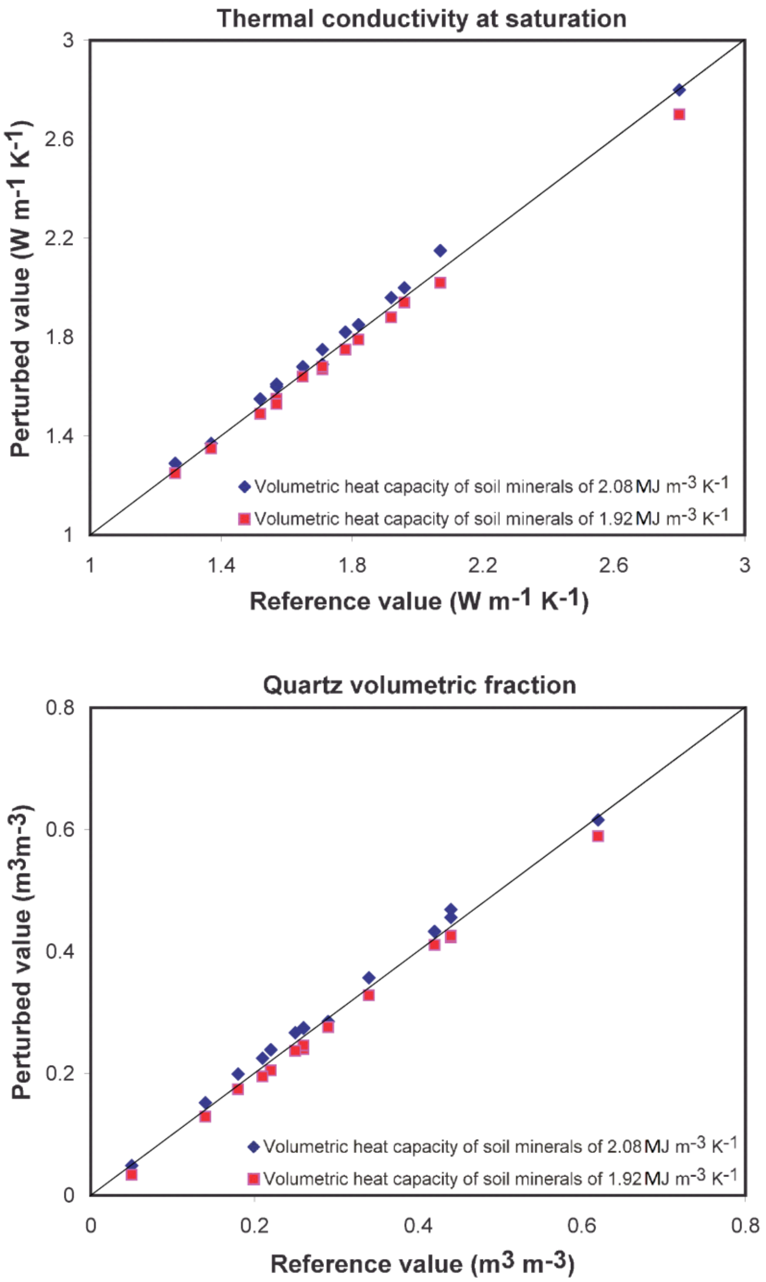

Figure S3.1 – Impact of using values of C_{hmin} = 1.92 MJ m^{-3} K^{-1} and C_{hmin} = 2.08 MJ m^{-3} K^{-1} instead of C_{hmin} = 2.0 MJ m^{-3} K^{-1} on the 14 retrieved values (Table 2) of (top) λ_{sat}, (bottom) volumetric fraction of quartz.

Supplement # 4

Characteristics of 10 Chinese soils

Table S4.1 – Soil characteristics of ten Chinese soils of Lu et al. (2007). ρ_d, θ_{sat}, f, and m, stand for soil bulk density, porosity, volumetric fractions, and gravimetric fractions, respectively. These soils consist of reassembled sieved soil samples and m_{gravel} = 0 kg kg^{-1}. λ_{sat} experimental values are derived from Table 3 in Tarnawski et al. (2009). Soil density is derived from porosity values inverting Eq. (1). The soils are sorted from the largest to the smallest ratio of m_{sand} to m_{SOM}. The ratio values smaller than 40 are in bold.

Lu et al. (2007) soils	λ_{sat} observations (Wm^{-1}K^{-1})	ρ_d (kg m^{-3})	θ_{sat} (m^{3}m^{-3})	f_{sand} (m^{3}m^{-3})	f_{clay} (m^{3}m^{-3})	f_{silt} (m^{3}m^{-3})	f_{SOM} (m^{3}m^{-3})	m_{sand} (kg kg^{-1})	m_{clay} (kg kg^{-1})	m_{silt} (kg kg^{-1})	m_{SOM} (kg kg^{-1})	$\frac{m_{sand}}{m_{SOM}}$
Sand 2	1.87	1567	0.41	0.548	0.035	0.006	0.001	0.929	0.060	0.010	0.001	1327.6
Sand 1	2.19	1567	0.41	0.553	0.029	0.006	0.001	0.939	0.050	0.010	0.001	1043.5
Loam 11	1.62	1350	0.49	0.253	0.046	0.208	0.003	0.499	0.090	0.409	0.003	199.5
Clay loam 9	1.36	1270	0.52	0.152	0.143	0.181	0.003	0.319	0.299	0.379	0.003	118.2
Sandy loam 3	1.68	1333	0.49	0.333	0.060	0.104	0.009	0.664	0.119	0.208	0.009	77.2
Loam 4	1.40	1264	0.52	0.189	0.052	0.232	0.005	0.398	0.109	0.488	0.005	81.2
Silty clay loam 7	1.34	1267	0.52	0.090	0.128	0.256	0.004	0.189	0.269	0.538	0.004	48.5
Silt loam 5	1.38	1272	0.51	0.128	0.104	0.241	0.012	0.267	0.217	0.504	0.012	**22.4**
Silt loam 6	1.47	1255	0.52	0.051	0.089	0.328	0.008	0.109	0.188	0.694	0.008	**13.0**
Silty clay loam 8	1.31	1202	0.52	0.035	0.140	0.263	0.028	0.078	0.310	0.582	0.030	**2.6**

References:

Lu, S., Ren, T., Gong, Y., and Horton, R.: An improved model for predicting soil thermal conductivity from water content at room temperature, Soil Sci. Soc. Am. J., 71, 8–14, doi:10.2136/sssaj2006.0041, 2007.

Tarnawski, V. R., Momose, T., and Leong, W. H.: Assessing the impact of quartz content on the prediction of soil thermal conductivity, Géotechnique, 59, 4, 331–338, doi: 10.1680/geot.2009.59.4.331, 2009.

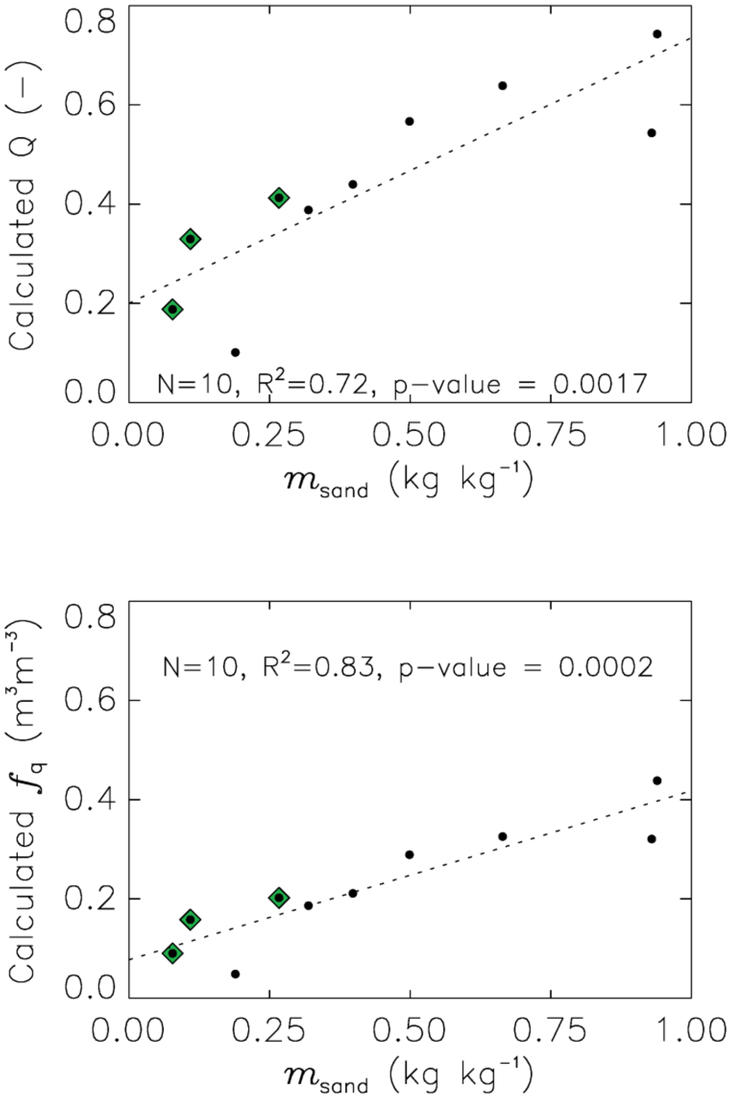

Figure S4.1 – Gravimetric and volumetric fraction of quartz (top and bottom, respectively) derived by Tarnawski et al. (2009) from the λ_{sat} observations of Lu et al. (2007) for 10 soils , vs. the gravimetric fraction of sand m_{sand}. The three soils for which $m_{sand}/m_{SOM} < 40$ are indicated by green diamonds. The dashed lines represent the regression equations based on all soils: $Q = 0.20 + 0.54\ m_{sand}$ and $f_q = 0.08 + 0.34\ m_{sand}$.

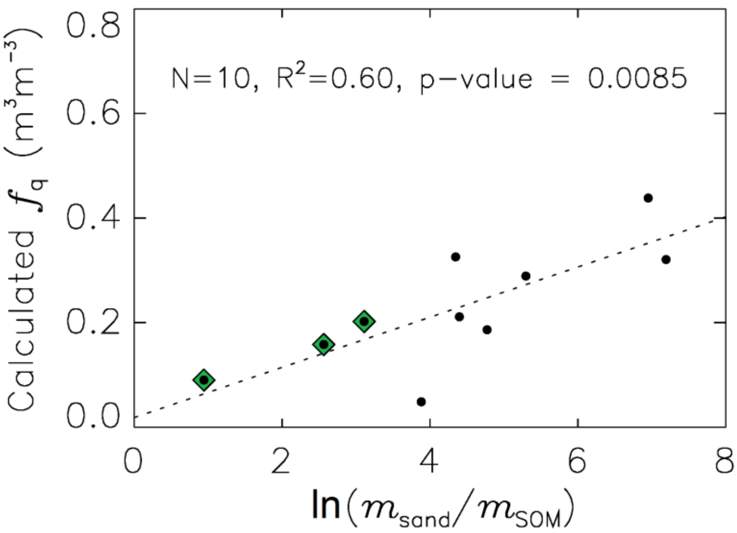

Figure S4.2 – Volumetric fraction of quartz derived by Tarnawski et al. (2009) from the λ_{sat} observations of Lu et al. (2007), vs. the logarithm of the m_{sand} / m_{SOM} ratio. The three soils for which $m_{sand}/m_{SOM} < 40$ are indicated by green diamonds. The dashed line represents the regression equation: $f_q = 0.02 + 0.048 \ln(m_{sand}/m_{SOM})$.

Supplement # 5

Data filtering to limit the impact of low resolution soil temperature

Since T_i is recorded with a resolution of

$$\Delta T_i = \left|\partial\left(T_i^n - T_i^{n-1}\right)\right| = \left|\partial\left(T_{i+1}^n - T_i^n\right)\right| = 0.1°C \qquad \text{(S5.1)},$$

the retrieved D_h values are affected by uncertainties and the relative uncertainty of D_h can be estimated as:

$$\left|\frac{\partial D_{hi}}{D_{hi}}\right| = \Delta T_i \times \left\{\frac{1}{\left|T_i^n - T_i^{n-1}\right|} + \frac{\Delta z_{i+1}^{-1} + \Delta z_i^{-1}}{\left|\gamma_{i+1}^n - \gamma_i^n\right| + \left|\gamma_{i+1}^{n-1} - \gamma_i^{n-1}\right|}\right\} \qquad \text{(S5.2)}.$$

Therefore, D_h retrievals are more accurate in conditions when soil temperature at $z_i = -0.10$ m changes rapidly and when differences in vertical gradients of soil temperature above and below z_i are more pronounced. In general, this occurs around noon (between 0900 LST and 1400 LST), and at dusk to a lesser extent, between 1700 LST and 0000 LST. In this study, we have imposed the following conditions for using the obtained D_h retrievals:

$$\left|T_i^n - T_i^{n-1}\right| > 0.8°C, \quad \left|\gamma_{i+1}^n - \gamma_i^n\right| > 30 K m^{-1}, \text{ and } \left|\gamma_{i+1}^{n-1} - \gamma_i^{n-1}\right| > 30 K m^{-1} \qquad \text{(S5.3)}.$$

According to Eqs. (S4.1)-(S4.2), this ensures that

$$\left|\frac{\partial D_{hi}}{D_{hi}}\right| < 18\% \qquad \text{(S5.4)}.$$